



# Doctoral dissertation

The innovative method of a flow-through lake renovation by a hydrotechnical method supported by biomanipulation.

**University of Warmia and Mazury in Olsztyn**

Faculty of Geoengineering

Scientific discipline: environmental engineering, mining and energy.

Supervision of:

Dr. Renata Tandyrak.

Prof. Robert Czerniawski,

Student:

Eng. Mohammed Z. A. Alhamarna

---

2018-2023



# Rozprawa doktorska

Innowacyjna metoda renowacji jeziora przepływowego metodą hydrotechniczną wspomaganą biomanipulacją.

**Uniwersytet Warmińsko-Mazurski w Olsztynie**

Wydział Geoinżynierii

Dyscyplina naukowa: inżynieria środowiska, górnictwo i energetyka.

Pod nadzorem:

Dr hab. inż. Renata Tandyrak.  
Prof. dr hab. Robert Czerniawski,

Student:

Inż. Mohammed Z. A. Alhamarna

---

2018-2023

## Preface

أبي  
هذا  
من  
أجلك

محمد زياد

# Table of content

## Contents

Table of content.....	4
Abbreviations.....	6
Abstrakt.....	8
Abstract.....	9
1. Introduction .....	10
1.1 Purpose and scope of study.....	14
2. Literature review.....	16
3. Methodology.....	22
3.1 Research Area .....	22
3.2 Plan and description of Święte lake restoration activities.....	25
3.2.1 Details of the installed pipelines system.....	25
3.3 Field measurements.....	33
3.4.1 Sampling date .....	33
3.4.2 Sample's location .....	33
3.4 Sampling procedure.....	34
3.5 Laboratory analysis .....	36
3.6 Statistical Analysis.....	38
4. Results.....	40
4.1 Thermal stratification and circulation pattern of Święte lake.....	40
4.2 Lake hydrology.....	42
4.3 Quality of the lake water .....	45
4.4 Sediment analysis.....	62
4.4.1 Sediments Water content.....	62
4.4.2 Sedimentary interstitial water and water-over-sediment.....	62
4.4.3 Chemical composition of the sediment.....	82
4.4.4 correlation between sediment components .....	88
4.4.5 Sediments nutrients ratios.....	89
4.5 Lake ecosystem .....	91
4.5.1 Phytoplankton.....	91
4.5.2 Zooplankton .....	92
4.5.3 Macrobenthos.....	93
4.5.4 Macrophytes .....	94
4.5.5 Ichthyofauna .....	96

5. Discussion.....	101
6. Conclusion.....	115
Summary .....	117
Streszczenie.....	119
Acknowledgements.....	121
References .....	122
Appendix .....	137

## Abbreviations

‰: percentage.

&: and.

$(\text{NH}_4)_2\text{S}_2\text{O}_8$ : ammonium peroxydisulphate.

Al: aluminum.

ANOVA: analysis of variance.

ASL: above the sea level.

ave. average.

BD-P: phosphorus sensitive to redox potential.

BOD<sub>5</sub>: biological oxygen demand.

C: carbon.

Ca: calcium.

Chl a: chlorophyll a.

CI: confidence interval.

Cm: centimeter.

C°: Celsius degree.

CO<sub>2</sub>: carbon dioxide.

CO<sub>3</sub><sup>-2</sup>: carbonate.

COD-Mn: chemical oxygen demand (oxidizability).

CuSO<sub>4</sub>: copper sulphate.

DO: dissolved oxygen.

EC: electroconductivity.

EtOH: ethyl alcohol (C<sub>2</sub>H<sub>6</sub>O).

Fe (OH)<sub>3</sub>: ferric hydroxide.

Fe: iron.

H: hydrogen.

H<sub>0</sub>: null hypothesis.

H<sub>2</sub>S: hydrogen sulphate.

H<sub>2</sub>SO<sub>4</sub>: Sulfuric acid.

ha: hectare.

HA: Hypolimnion aeration.

HClO<sub>4</sub>: Perchloric acid.

HCl-P: phosphorus bound to calcium.

H<sub>L</sub>: alternative hypothesis.

HNO<sub>3</sub>: Nitric acid.

HW: Hypolimnion withdraw.

Indiv.: individual.

Km<sup>2</sup>: square kilometer.

Km<sup>3</sup>: cubic kilometer.

l: liter.

M: Mole.

M<sup>2</sup>: square meter.

M<sup>3</sup>: cubic meters.

MC: alkalinity.

Mg: magnesium.

mg: milligram.

Mn: manganese.  
Mol: mole.  
mval: milliVal.  
N: nitrogen.  
NaHCO<sub>3</sub>: Sodium bicarbonate.  
NaOH-nrP: phosphorus bound to organic matter.  
NaOH-rP: phosphorus bound to aluminum, iron hydroxides and hydroxides.  
NaOH-TP: phosphorus bound to aluminum and organic matter.  
NH<sub>3</sub>: ammonia.  
NH<sub>4</sub>: Ammonium.  
Nh<sub>4</sub>Cl-P: labile phosphorus.  
Nm: nanometer.  
N<sub>org</sub>: organic nitrogen.  
O.M.: organic matter.  
D. M.: dry matter.  
O<sub>2</sub>: oxygen.  
P: phosphorus.  
pH: power of hydrogen (reaction).  
PO<sub>4</sub><sup>-3</sup>: orthophosphate.  
P<sub>org</sub>: organic phosphorus.  
res P: residual phosphorus.  
rpm: round per minute.  
S: sulphur.  
SD: Secchi disc.  
SiO<sub>2</sub>: Silicon dioxide.  
SO<sub>4</sub><sup>-2</sup>: Sulfate.  
SRP: soluble reactive phosphorus.  
T: temperature.  
TH: total hardness.  
TN: total nitrogen.  
TOC: total organic carbon.  
TP: total phosphorus.  
TSI: trophic state index.  
λ: wavelength.  
μm: micrometer

## Abstrakt

W badaniu tym zbadano zmiany parametrów biofizykochemicznych zbiornika eutroficznego (Jezioro Świąte, N 52°05'06.83"; E 16°02'46.23") w związku z prowadzonym innowacyjnym podejściem renaturyzacyjnym, które łączy w sobie trzy metody renaturyzacji: Napowietrzanie Hypolimnion (HA) , wycofanie hipolimnionu (HW) i zabieg biomanipulacji. Po obu stronach dopływu i odpływu jeziora, gdzie warstwa hipolimnionu jest częściowo przedzielona kurtyną podwodną, zainstalowano grawitacyjny system rurociągów hydrotechnicznych odprowadzający wody hipolimnetyczne. Parametry analizowane w okresie badań poddano statystycznym badaniom w celu sprawdzenia istotnych różnic ( $P \leq 0,05$ ) jakości wody jeziora, wody osadowej, składu chemicznego osadów, osadowych frakcji fosforu, ichtiofauny i zbiorowisk planktonowych. Zadaniem zainstalowanego systemu rurociągów jest wypełnienie i odwodnienie warstwy hipolimnionu poprzez doprowadzenie natlenionego dopływu powierzchniowego do wód dennych jeziora w strefie dopływu oraz odprowadzenie hipolimnetycznej, bogatej w składniki odżywcze wody ze strefy odpływu. Z drugiej strony interwencja biomanipulacji zaczyna korygować piramidę troficzną jeziora. W związku z wymierną poprawą parametrów ekologicznych jeziora nie wykonano ostatniego etapu planu renaturyzacji inaktywacji fosforu przez koagulanty.

**Słowa kluczowe:** Świąte Jezioro, renaturyzacja jeziora, napowietrzanie hypolimnionu, wycofanie się hypolimnionu, rurociąg, analiza biofizykochemiczna, Skład osadów chemiczne, biomanipulacja.



## Abstract

This research study changes in the biophysiochemical parameters of an eutrophic reservoir (Święte lake, N 52°05'06.83"; E 16°02'46.23") before and after the implementation of an innovative approach that combine between a three restoration methods: Hypolimnion aeration (HA), hypolimnion withdraw (HW), and a biomanipulation treatment. A hydrotechnical pipelines system (filling and draining) installed at both sides of the lake inflow and outflow, where the hypolimnion layer partially divided by underwater curtain.

The obtained results of the lake water quality analysis, sedimentary water, chemical composition of the sediment, sedimentary phosphorus fractions, ichthyofauna and planktonic communities during the study period analyzed statistically to investigate the significant difference ( $P \leq 0.05$ ) of the occurred changes. The installed pipelines system at both sides of the lake succeed to enhance the redox potential at the hypolimnion layer by delivering the oxygenated surface inflow to the lake bottom waters, and discharge the nutrients-rich water from it. On the other hand, the biomanipulation intervention starts to correct the trophic pyramid of lake. In view of the tangible improvement of the lake ecological parameters, the last step of the restoration plan to inactivate the phosphorus by coagulants has not been performed.

**Keywords:** Święte Lake, lake restoration, hypolimnion aeration, hypolimnion withdraw, biophysiochemical analysis, sediments chemical composition, biomanipulation.

## 1. Introduction

Lakes are considered an intersection point of our ecosystem, where a wide range of inhabitants depend on it. Limnology defines lake as a lentic water body, which is larger than a pond with a possibility of waves occurrence on its shoreline that induced by wind (Balasubramanian, 2015). According to Global Lakes and Wetlands Database (GLWD), the number of lakes ( $\geq 0.1 \text{ km}^2$ ) may exceed  $1.43 \cdot 10^6$  natural lake with a proximate surface area of  $2.67 \cdot 10^6 \text{ km}^2$ . These lakes occupy 1.8% of global land area (Messenger et. al., 2016).

The regime of water mixing considers the indicator the characterize and determines the limnological type of the lake. Circulation of lakes water commonly termed as "lake turn-over cycle", water mixing is a function of temperature, wind, and water density (Skowron, 2022).

As the surface water heats up due to exposure to sunlight, consequently the surface water becomes lighter and floats over denser water below (MacKay et al., 2009). This stratifies the lake thermally into several water layers "stratification", where it reaches its peak during the summer stagnation (Perks, 2006). Lake morphometries as mean depth, surface area, and volume, strongly affect the stratification of the lake (Skowron, 2022; Butcher et al., 2015).

The water circulation homogenizes oxygen and nutrient concentrations throughout the water column (Hakala 2004). During the turn-over cycle, oxygen ( $\text{O}_2$ ) is introduced from the atmospheric air over the surface water layer and the nutrients are transmitted from sediments and deep water to the surface zone. For a week or more after the overturn, the parameters of the water column, usually lakes don't behave according to a consistent pattern (Nutz, 2018).

The surface water layer "epilimnion" is well lit and oxygenated with a higher water temperature than water below, that promotes lakes productivity and hence supporting the lake inhabitants. The active photosynthesis process by algae, macrophytes, phytoplankton and cyanobacteria, leads to an increase of the dissolved oxygen concentration in this layer.

Below the epilimnion there is a cold and much denser layer called "hypolimnion". The hypolimnion layer can be very large and represents a high percent of the lakes volume in the deep lakes, while this layer often does not occur in shallow lakes as wind or cooling causes regular mixing throughout the year.

Both above-mentioned layers are separated by a transition region called metalimnion or thermocline with a sharp vertical temperature gradient. Thermocline depth is not fixed, but determined by the degree of solar heating, the transparency of the water and the morphometry of the lake (Boehrer and Schultze, 2008, Susann, 2007).

The temperature differences of the lake impact on its inhabitants and plankton communities' composition, distribution, behavior, reproduction, and evolutionary adaptations of organisms, alter fish populations and enhance the dominance of cyanobacteria (Lynch et al., 2015; Rice et al., 2015; Jöhnk et al., 2008; Thomas et al., 2004).

Lakes are subject to natural evolutionary processes because of periodically or permanently acting natural or anthropogenic factors, which leads to significant changes in their aquatic ecosystem (Marszelewski, 2005).

Eutrophication of lakes is a natural aging process resulting from the gradual accumulation of nutrients, mainly nitrogen and phosphorus. This is accompanied by an increase in lake fertility and productivity. Lake productivity refers to the number of plankton that can be produced in lake. Its decomposition contributes to reduce the amount of dissolved oxygen (DO) in the lake and posing risk to aquatic life. An increase in the productivity of lakes can change the trophic state of the lake from oligotrophic to eutrophic and even hypertrophic. Human influences participate in increasing the external load of nutrients and organic matter (OM), which can rapidly accelerate the lake deterioration and its termed as " a cultural eutrophication" (Schindler, 2012).

Eutrophication undesirable consequence are cyanobacteria and algae blooms, which increase the organic matter load into the lake' body. The decomposition of the organic matter depletes dissolved oxygen concentration in the hypolimnetic and sedimentary water. The anoxic/ anaerobic conditions of sediments release phosphorus (P) from it in an internal loading process of the lake (Pettersson, 1998).

The fate of the adsorbed phosphorus by sediments determined the redox potential of the sediments-water interface. Under aerobic conditions the diffused phosphorous from the sediments forms an insoluble complex salt with ferric hydroxide ( $\text{Fe}(\text{OH})_3$ ), but if the hypolimnion layer pass through anoxic conditions, phosphorous remains soluble and accumulates without precipitate (Lean and Nalewajko, 1976).

Many factors influence P releasing process from sediments regarding to a) characteristics of the water-over-sediments, e.g., redox potential, reaction, temperature, iron and calcium contents, or b) factors concern sediments properties, such as: type and amount of its organic matter, microbial bioturbation, resuspension, and diffusion of sediments (Tandyrak et al. 2016).

Under specific conditions, hypolimnion may become extremely anoxic due to the active biological decomposition of the sediments (Kirillin, 2016). Anoxic conditions at the lake's bottom may also lead to a series of chemical and microbial processes like nitrate ammonification, denitrification, desulphurization, and methane formation. That impoverishes water's fauna, e.g., pelagic fish, which release their eggs in the open water that sink to the bottom and cannot continue to reproduce normally in a lake with anoxic sediment surface. Fish kills may also be a result of an advanced eutrophication that initiated by an increase of the pH indicator, because of high photosynthesis rates and total ammonium concentration (Smith and Schindler, 2009).

Lake's ecosystems are distinct from three typical habitats: littoral, limnetic and benthic zones (Lerman et al., 1995). The feeding habits of lake biological communities intersect to form a lake food-web structure (Horn and Goldman, 1994). Autotrophs are the primary producers in the food web followed by the herbivores and planktivorous that feed on plankton. Piscivores feed only on fish -Planktivorous & herbivores-, while detritivores are heterotrophs that obtain nutrients by consuming detritus from the decayed plant and animal material (Jasser et al., 2009; Andersen, 1997).

The lake pelagic zone is where the suspended plankton, neuston and active swimmer's nekton (Brooks and Dodson, 1965). Fish are the most obvious predators of zooplankton. Zooplankton is considered an important planktonic trophic group, where it links between autotrophic and much larger creatures through the food web pyramid and assists to filter the water by feeding on the phytoplankton (Ward and Follows, 2016).

Nutrition, temperature, and dissolved oxygen are the critical factors of the lake ecosystem and its ecological communities. The main nutrients are nitrogen and phosphorous with elements as carbon, hydrogen, oxygen and sulphur support the productivity of high density of algae, fish, and other aquatic organisms.

Eutrophic lakes have much more biomass, due to the existence of high nutrients content in them. The microbial decomposition of the precipitate matters in the sediment's uptake the oxygen from deep water and leave the hypolimnion water in an anoxic condition, especially in summer. In very shallow lakes, the whole lake can become anoxic, which causing a fish kill (Bhagowati and Ahamad, 2020; Imboden,1974). The excessive algal blooms can also significantly reduce oxygen levels and prevent life from functioning at lower depths, that creates dead zones beneath the surface water (Bhateria and Jain, 2016).

Phosphorus considers the critical nutrition element for lake eutrophication, its external load reduction may improve the lake ecological conditions. However, if the reservoir quality deterioration results due to its own internal loading and the bottom sediments become the main source of phosphorus, even a radical reduction of external loads does not bring the expected results and it becomes necessary to reclaim the lake (Jeppesen et al., 2007).

Numerous lake restoration approaches are applicable nowadays (Fig. 1). These techniques consist of technical, chemical, and biological methods with a noticeable progress in the development and improvement of lake restoration with a recognize new treatment techniques and inventions (Alhamarna and Tandyrak, 2021; Łopata et al., 2020). Whereas physical and chemical methods are still the primary reclamation techniques, lake management and the biological control (biomanipulation) are becoming recently more influential (Lewtas et al., 2015). Various factors determine the efficiency of the implemented restoration method, such as: the increase of the water transparency and reduction of [a) nutrients abundance, b) biological oxygen demand (BOD5), c) electrical conductivity, d) suspended solids, e) chlorophyll] with a moderate dissolved oxygen concentration and pH level. It's commonly agreed that perceptible impact could only be achieved by reducing the external nutrient load to a sufficient low level that the lake can handle (Mehner et al., 2002).

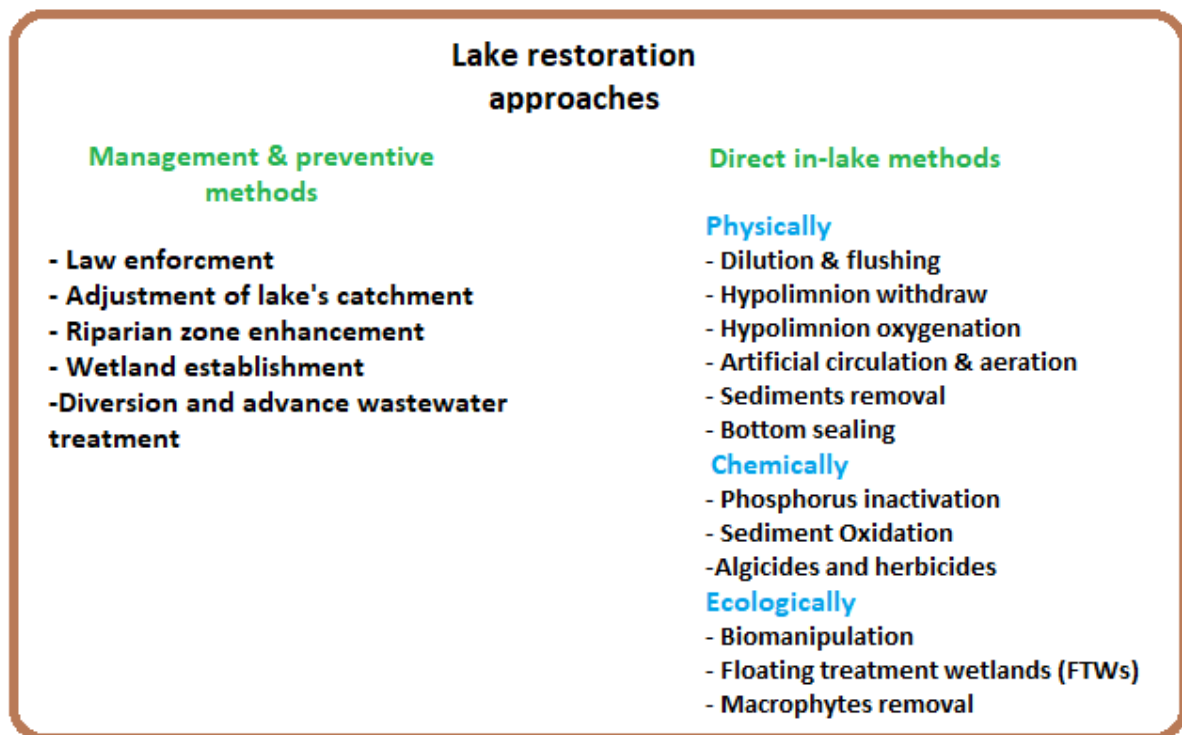


Figure 1. Scheme of approach for restoring Lake.

## 1.1 Purpose and scope of study

Święte lake in Odra is a reservoir used for recreational purposes. In recent years, the quality deterioration of its water has been observed. Consequently, Authorities of the Wolsztyn commune request from Department of water protection engineering and environmental microbiology at University of Warmia and Mazury in Olsztyn to subject Święte lake to a monitoring programme with a purpose to design and implement a procedure for its protection and restoration.

Current work aim is to captures the initial occurred changes of biophysiochemical parameters for an eutrophic reservoir which is thermally and chemically stratified, as a result of an applied restoration activities through a gravitational pipelines system and a biomanipulation treatment process to restore its calm. The operation of the pipelines system started on 27<sup>th</sup> of October 2020.

The conducted restoration plan mainly target the hypolimnion layer of Święte lake, where it has divided into two sections for inflow section (zone) and outflow section by underwater curtain. Each zone pass through a different restoration method and each represent a research site for this study.

The installed pipelines system consist of two restoration methods that targeting the enriched hypolimnetic water: A) hypolimnion aeration (HA) method, at the inflow zone by diverting the incoming flow (Pintus inflow) deep to the hypolimnion layer, and B) hypolimnion withdraw (HW) method from the outflow zone

The research evaluates the combination of three lake restoration techniques that are applied simultaneously on a eutrophic reservoir by observing and analyzing the occurred changes of its limnological parameters (biophysiochemical): water, sediments, and the biological indicators. And as a sub-target, a comparison between the obtained analysis results before the operation of the pipelines system, with the obtained one by the end of the same research period and justify these results.

The scope of the study covers:

- A. A field observation and study.
- B. Technical field measurements.
- C. Series of biophysiochemical analysis during the research period, that included:
  - Chemical and physical analysis of the lake water and its inflow and outflow (Pintus) during restoration.
  - Chemical analysis of lake bottom sediments, and its interstitial waters and water-over- sediment.
  - Observation of ecological status before and after lake's biomanipulation.
  - Statistical processing of the results seeking the occurred changes.
- D. Comparison of research period (2020-2022) results with the obtained ones from previously initiated monitoring program (2017-2018), [Eutrophication of Święte lake in view of the ecological condition, threats, possibilities of protection and reclamation] (Czerniawski et. al., 2018).

## 2. Literature review

Thermally stratified lakes may develop a seasonal anoxic hypolimnion layer, due to the depletion of oxygen during the microbial decomposition of the organic matter alter the redox potential (Siwek et. al., 2018; Schönach et. al., 2017). The anoxic situation at the deeper layer of water leads to release the redox sensitive nutrients from sediments to the hypolimnetic water e.g. carbon, hydrogen, oxygen, nitrogen, phosphorus and sulphur (Wang et. al., 2018; Tandyrak et. al., 2017). There is a direct correlation between these nutrients concentration into hypolimnion and the annual mean of the produced biomass (lake productivity), with a strong dependency of cyanobacterial growth on internal load (Paerl et. al., 2016).

Discharging the enriched hypolimnetic water by the hypolimnion withdraw (HW) method, hinders the mobility of nutrients from reaching to the epilimnion layer and reduce nutrients accessibility of the planktonic communities (Nürnberg, 2020; Jeppesen et al., 2012). Hypolimnion withdraw (HW) is a suitable restoration technique for stratified reservoir because it provides no disruption of its own thermal and chemical regime (Alhamarna and Tandyrak, 2021). This restoration technique is recommended for flow-through lakes (Dunalska, 2020).

HW has been used as a lake restoration technique for more than 65 years in more than 50 times mostly at the northern hemisphere to manage nuisance phytoplankton blooms, where the internal loading is responsible for its trophic statues' deterioration (Nürnberg, 2007). A successful hypolimnetic withdrawal installation has been documented worldwide e.g. Germany, Finland, USA, Canada, Poland, and Australia (Cooke et al. 2005). Kortowskie lake witnessed the first implementation of the hypolimnion withdraw installation based on a technical scale with the longest observing period (Dunalska et al., 2007; Olszewski, 1961)

When it comes to compare HW method with another restoration approaches that target to reduce the lake's internal loading, this method outstands with a low capital and operation costs, together with a long-term effectiveness (Alhamarna and Tandyrak, 2021; Nuremberg, 2019). The efficiency of the HW method depends on minimizing the external load toward the reservoir and maintaining a constant water level in it to avoid its destratification (Lewtas et al., 2015; Mientki and Dunalska, 2002). This in turn, requires lake damming to ensure that the withdrawn water come from hypolimnion zone and to increase the pressure differential



between at both sides of the HW's pipeline. The pipeline's inlet usually laid over the deepest point of the lake (Klapper, 2003).

To achieve a sufficient discharged of hypolimnetic phosphorus concentration, operation of the HW installation should be dovetail with the summer stagnation. That is when the lake is usually stratified and nutrients are accumulated in the hypolimnion layer, and before destratification by autumn turnover (Solivonen et. al., 2021; Bormans et al., 2016; Michael et al., 2014).

During the severe anaerobic condition of the hypolimnion layer and increase of the discharged hypolimnetic water accelerate the removal of the highly bioavailable soluble reactive phosphorus (SRP). The withdrawn outflow water may contain high concentration levels of phosphorous (Łopata et. al., 2019; Jeppesen et. al., 2012).

Besides that, the outflow may contain ammonia ( $\text{NH}_3$ ), hydrogen sulphide ( $\text{H}_2\text{S}$ ) and reduced metals, it has a strong odor with low dissolved oxygen concentration. These drawbacks can cause a water quality issue downstream (Tandyrak et. al., 2016). Various measurements have been applied to minimize the environmental impact downstream, such as: mixing the drawn water with a surface water as Łajskie lake (Łopata and Wisniewski, 2013), treat the outflow in a sewage treatment plant as Leonharder lake (Sampl, 1993), redirect it to wetland as Chain lake (Macdonald et. al., 2004), adding phosphorous precipitants at the outlet as Ulmener Maar lake (Spieker, 2002), aerate it by oxygenation plant or install a fountain at the outlet as Gemündener Maar lake, stripping and adsorption of reduced gases as Meerfelder Maar lake (Kucklentz and Hamm, 1988). In recent HW installations, a movable P elimination device has been used (Nürnberg, 2020).

Several hydraulic calculations are applied to determine the favorable parameters of the HW pipeline system as the pipes diameter, length, flow rate and velocity, hydraulic loss in pipe due to the friction, etc. Using Gauckler–Manning–Strickler, Chézy and Colebrook-White formulas and comprise between them, allows to obtain accurate parameters of HW system (USBR, 2022; Munson, 2016; Jarosz and Wołoszyn, 1966; Manning, 1891).

Another restoration technique that targets the hypolimnion layer is hypolimnetic aeration (HA) (Alhamarna and Tandyrak, 2021). This method was designed to counteract hypolimnetic anoxia and its associated effects on the lake trophic states (Mercier and Perret 1949).

Aeration primarily delivers oxygen and thus enhances the redox potential value, which prevents releasing the redox sensitive sorption of phosphate ( $\text{PO}_4^{3-}$ ) to iron (Fe) and reduces the lake's internal P loading (Katsev, 2006).

Aeration of the hypolimnetic water may also increase diffusion of nutrients into the epilimnion without causing destratification, where phosphorus improvement does not always occur with aeration e.g., the black lake (Ashley, 2011).

This lake's reclamation method is not an efficient option in shallow lakes with a depth less than 12-15 m, or when the hypolimnetic volume is relatively small. Typically, it is desirable to maintain the stratification status of the water body (Cooke and Carlson, 1989). One of the principal reasons for maintaining stratification during aeration is to prevent the recirculation of the released nutrients and to maintain the biota habitats of the cold water at bottom of the lake (Lewtas et. al., 2015). Destratification of the water body may result in a low dissolved oxygen concentration throughout the water column and the introduction of toxic chemicals substances to the epilimnion layer (McQueen and Story, 1986).

Aeration is usually done by special aerators that inject pure oxygen or fine air-bubbles to the hypolimnion layer, without causing a destratification. Some examples of frequently used aerators design at the current time are airlift aerator, Speece Cone and bubble plume diffuser (Singleton and Little, 2006). An experimental multi-point aeration technique consists of eight reactors that are selectively oxygenating only the hypolimnetic waters was successfully used in the strongly eutrophic Lake Łajskie (Masurian Lake District, Poland) (Łopata et. al., 2023).

A groundbreaking aeration technique of the hypolimnion layer without having to install aerators or consume energy involve self-oxygenation of lake waters by delivering the oxygenated surface inflow directly to the deep-water layer of the lake through a gravitational pipeline (Łopata et. al., 2023). HA can maintain oxygen conditions in the hypolimnion throughout the summer stagnation period and reduce the internal supply by improving the hypolimnion redox potential and thus prevents the phosphorus release from sediment without causing destratification (Paul and Klapper, 1985).

This approach is easy to implement without maintenance and operation costs, a weir must construct for damming the incoming water high enough to overcome the internal friction of the pipeline (Łopata and Wisniewski, 2013). The mechanism of the reservoir self-oxygenation

(HA) is the reverse of the hypolimnion withdraw (HW). The first place where its application took place was in Jabeler See (Łopata and Wisniewski, 2013).

The implementation of this kind of hypolimnion aeration will result in a dilution of the hypolimnetic water, that is not achievable under natural conditions especially when lake is thermally stratified. Hypolimnion aeration can be applied as a supporting process of phosphorus inactivation by ferrous coagulants, where efficiency of phosphorus precipitation and immobilization depends on the oxygen content (Dunalska, 2020).

Lake eutrophication enhances the excessive growth of phytoplankton and alters its ecosystem communities' structure and functionality, which leads to loss the biodiversity of the lake (Jeppesen et al., 2000). Phytoplankton abundancy correlates with the lake nutrients content, and it is a principal indicator of the lake's trophic statue, as phytoplankton is related to internal and external loads (Findlay et. al., 2005).

Within the biomanipulation approach, waterbody's aquatic communities are manipulated to maintain phytoplankton biomass at low levels by cascading trophic interactions in aquatic food webs, as; increasing piscivore abundance or reduce the planktivorous (Reynolds, 1994). This in turn will enhance the zooplankton that are grazing on phytoplankton and resulting in an improvement of lake's water visibility (Shapiro and Wright, 1984). For example, large cladocerans (genus of daphnia) are effective grazers on phytoplankton and they play an important role in improving water quality by suppressing the population growth of phytoplankton (Ter Heerdt and Hootsmans, 2007).

The effective biomanipulation procedure consists of an efficient reduction of planktivorous biomass  $\geq 75\%$  and this should be conduct withing 1-3 years. The number of benthic feeding fish must be reduced without stoking juvenile fish. Improve conditions for the submerged macrophytes and reduced the external load as much as possible before the biomanipulation (Hansson et al., 1998). When the removed portion of the non-predatory fish is small, there is a risk that the breeding and growth rates of the remaining stocked fish will rise and thereby reaching rapidly the previous enumeration (Jeppesen and Sammalkorpi, 2002).

Positive biomanipulation effects on the water quality are not only obtained by lowering the predation pressure on the zooplankton by fish stock interventions, but by reducing the density of benthivorous species e.g., bream. Relieving the predation pressure on bottom

invertebrates has great significance to other fish species, for instance perch for whose bottom invertebrates constitute an important food source (Persson and Greenberg, 1990).

One of the issues that are associated with stocking of zooplanktivorous fish fry e.g., pike is that an effect is only obtained during the year of the stocking and lasts for a brief period since stocking event. The sustainable stock of pike depends on the littoral zone extension. Even with a high density of the stocked pike, a small and poor habitat will increase its mortality (Skov et al., 2003b; Grimm and Backx, 1990).

The timing of pike fry stocking is therefore overly critical and to obtain optimum results, stocking should be done immediately after the hatching of the benthivorous fish fry. As the time of hatching varies widely from year to year, optimization may be tricky. Biomanipulation intervention by pike's stocking has yielded very variable results (Grønkjær et al., 2004). Likewise, a massive stocking of pike fry is required to generate adequate effects (Søndergaard et al., 1997b).

The development of dense macrophyte beds, that induced by biomanipulation can stabilize a good water visibility for prolonged period. The Submerged macrophytes strongly affect phytoplankton communities in shallow lakes. Submerged macrophytes create a structure that boosts the abundance of sessile, plant-associated, and pelagic zooplankton species and thereby generate a higher grazing pressure (Lauridsen et al., 1997).

Biomanipulation is expected to decrease the associated improvements water turbidity, chlorophyll-a, total phosphorous (TP), algal biomass and cyanobacterial blooms. As biomanipulation increases transparency of water, this leads to an expansion of submerged macrophytes bed and provides favorable conditions for establishment of rooted plants (Triest et al., 2016).

Various reasons can lead to biomanipulations ineffectiveness, as; insufficient fish removing, immigration of planktivorous from other systems and recolonization, increase in invertebrates-planktivorous, increase the amount of inedible phytoplankton by zooplankton e.g. larger toxic cyanobacteria, resuspension of sediments by wind, low piscivores amount due to fish removing, replacement of fish predation by invertebrates e.g. Chaoborus, long-term instability of the fish population due to overstocking of piscivores (Ofir et al., 2017; Hansson et al., 1998).

Biomanipulation long-term results are rare, and the most successful applications have occurred in shallow and oligotrophic-mesotrophic for the first 1–3 years (Kasprzak et al., 2003). Nevertheless, to establish that biomanipulation is an effective restoration method, there are a need for more examples of biomanipulation applied to lakes with different environments and different aquatic communities (Gulati et. al., 2008; Brouwer et. al., 2002).

### 3. Methodology

#### 3.1 Research Area

Święte lake (52 ° 05'07.6 "N, 16 ° 02'45.8" E), is in central of obra valley mesoregion, which is a part of Pradolina Warciańsko-Odrzańska microregion and it's located at the Nowotomska microregion as a part of Poznań Lakeland, and it was formed during the Poznań phase of Vistula glaciation (Kondracki, 2002).

Święte lake is a flow-through dimictic lake, that shows thermal and chemical stratification during the summer stagnation. The lake's altitude is 60 m (geoportal.gov.pl). The area of its surface is 23.1 ha, with an average depth of 8.9 m, the length of the lake is about 1082 m, the width is about 257 m. The detailed morphometric data of Święte lake are collected at the (Tab. 1).

Table 1. Detailed parameters of Święte lake morphometric (Czerniawski et. al., 2018), that confirmed with the use of google tools.

<b>Parameter</b>	<b>Value</b>
Water mirror surface	23.3 ha
Maximum depth	15.3 m
Medium Depth	8.9 m
Relative depth	0.0317
Depth indicator	0.58
Volume	2.064 x 10 <sup>3</sup> m <sup>3</sup>
Maximum length	1082 m
Maximum width	257 m
Elongation index	4.2
Coastline Length	2660 m
Shoreline Development	1.56

The formation of the lake basin indicates the origin of the basin due to glaciation and deposition; lake has an elongated shape in the north-south direction. The shores are elevated and wooded, which in conjunction with the dominant westly direction of the winds impedes the water mixing process. The inflow and outflow of Pintus are on opposite sides of the lake, on the line of its longer axis in the N - S direction.

Święte lake has a direct catchment area (1.53 km<sup>2</sup>) that surrounds the reservoir evenly from the west and east (Pho. 1). The intermediate catchment area extends north-east and north direction. The total catchment area (about 6 km<sup>2</sup>) covers the area between Niałek Wielki and Powodowo. Due to the connection with Berzyńskie lake through Pintus, the surroundings of

the Wolsztyńskie and Berzyńskie lakes and the areas drained around Dojca River -as a main hydrological axis-, and this surface area can be considered as a total catchment area. However, pollutants that end up in this area are partially transported to the Święte lake. Berzyńskie lake has two surface drains Pintus and Dojca tributaries, both eventually pour into the northern Obra canal. The path of Pintus tributary to reach the north canal goes by Święte lake. The received Pintus-Święte inflow coming as Berzyński-Pintus outflow goes through (Krutla)pumping station, which regulates Święte lake' incoming flow (Pho. 2).

The carried flow through Kiełkowski trench bifurcated at Zimne Kąty into a) Powodowo tributary penetrating Powodowo village continuing its direction to the northwest after, b) while the second fraction of Kiełkowski-flow goes east toward Berzyński lake, where the flow walks alongside the lake reaching the cross-sectional point of the Pintus tributary to the Święte lake.

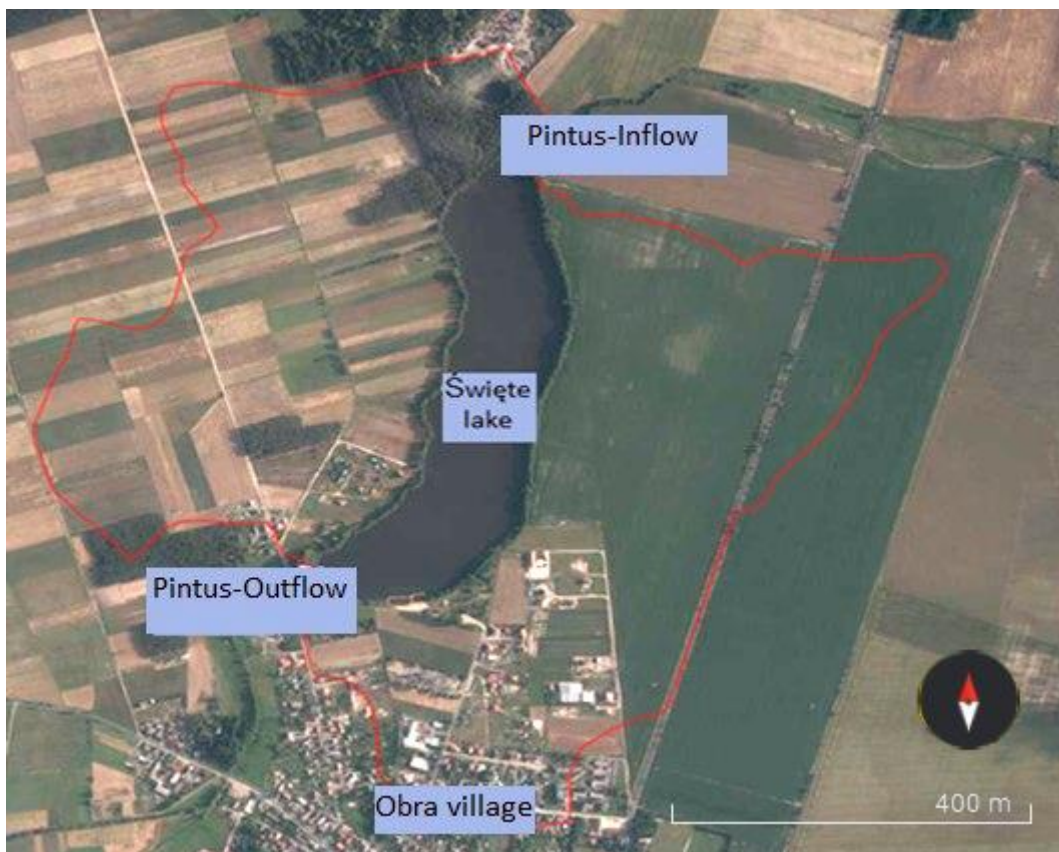


Photo 1. The extent of the direct catchment area of the Święte lake (geoportal.gov.pl).

Due to numerous modifications in the run-off directions in recent years and the functioning drainage systems that are supported by a Krutla drainage pumping station, it is impossible to clearly indicate the area of the current supply of the Święte lake with surface runoff.

Considering the adapted approach to eliminate the outflow from Lake Berzyński toward Święte lake through Pintus tributary, it can be assumed that the recent shaped watershed line determines the real extent of Święte lake water catchment area runs along the western suburb of Berzyńskie lake.



Photo 2. Hydrological network of the research area (earth.google.com).



## 3.2 Plan and description of Święte lake restoration activities

The implemented restoration plan of Święte lake consist of a series of protective and reclamation activities according to the lake and catchment features, which analyzed during the reported one-year monitoring cycle (2017-2018).

Święte lake restoration stages:

- Regulating the directions of water's flow into melioration ditches and cut connection with Berzyńskie lake.
- Construct a pipelines system, one for delivering Pintus surface inflow to water over the bottom of the inflow zone -northern part of the lake -, the second pipe is to discharge the hypolimnetic water over the outflow zone bottom -southern part of the lake-.
- Biomanipulation of Święte lake through regulatory selective catches, that aim to eliminate small cyprinids, and stocking the lake with predatory fish species, as follows:
  - Pike-summer fry: 1500 pcs per ha of open water, which is equivalent to 200 kg per Święte lake of the autumn fry (30,000 pcs per lake).
  - Zander-summer fry: a 750 pcs per ha of open water, which is equivalent to 100 kg per Święte lake of the autumn fry (15,000 pcs per lake).
  - Asp-autumn fry: 15 pcs per ha of open water, which equivalent to 2 kg per Święte lake of the autumn fry (300 pcs per lake).
- Lastly, apply phosphorus inactivation coagulants, PIX 111 iron coagulant and PAX 18 aluminum coagulant, this stage of project does not apply yet.

### 3.2.1 Details of the installed pipelines system

Święte lake has been divided into two sections by underwater curtain. The concept was to deal with the lake as two parts; the northern one where the inflow redirected to lakes bottom (site 2), will work as an oxygen supplier to the deep layer of water in this part, and the outflow will be from the southern section through a pipeline as in normal HW restoration process (Pho. 3).

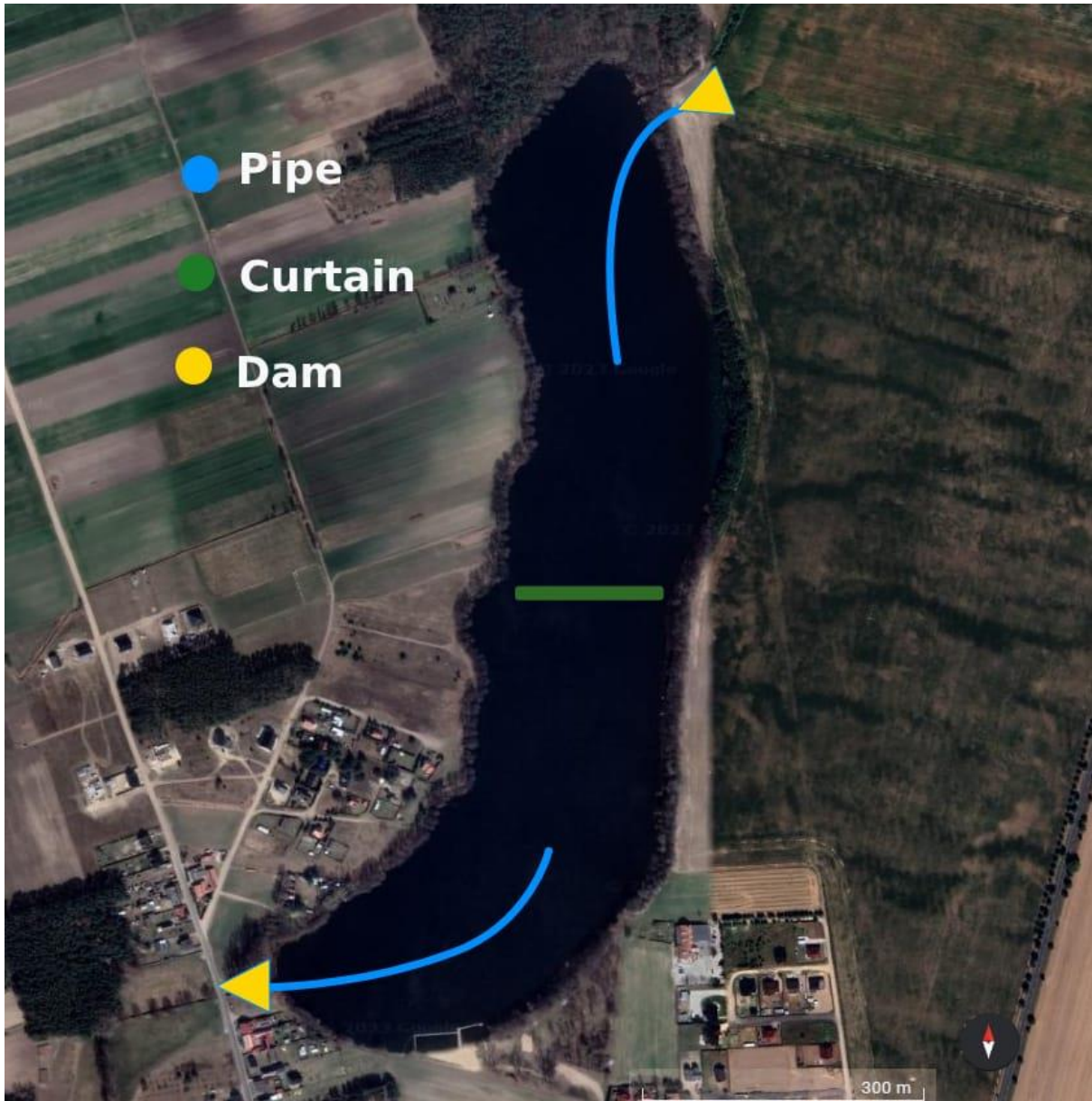


Photo 3. Schema of the pipelines system (earth.google.com)

The installation parts are divided into four parts: underwater curtain, filling pipeline (inflow), discharging pipeline (outflow) and dams -two at the inlet and outlet.

#### **Underwater curtain**

The installed HDPE geomembrane curtain has a length of 95 m with a maximum height of 5 m and 1.5 mm thickness. It reinforced with a displacement rope and an anchor rope to maintain vertical and horizontal stability. Additional stabilization with 10 pieces of metal-rubber weights. The curtain lower edge was adapted to the bottom's shape of the lake, aiming to ensure the curtain-bottom contact along entire length of curtain lower edge. The geodetic

coordinates according to the Polish European Terrestrial Reference Frame 2000 (PL-ETRF2000): West-end (5772929 5571678), East-end (5772917 557177). It was installed on 1-3 October 2020. The curtain leaves 162 m -both sides- of lake in direct contact, and 9-10 m over curtain contact of the water column (Pho.s 4 & 5).



Photo 4. The installed HDPE geomembrane (curtain).



Photo 5. Installation of the underwater curtain.

### North pipeline (filling)

The filling pipeline, which redirects the surface inflow (Pintus), to be discharged over the deepest northern point (site nu. 2). This north pipeline consists of two sections. The beginning section, which is 21 m length from the northern dam with diameter of 400 mm, made of reinforced external sewage pipes, type InCor (SN8). And, then a 211 m bottom section with the same diameter, that is a smooth, thin-walled PVC-U pipes. The outlet of the filling pipeline ends with a 2x3.5 m drop plate with steel angles as a load. The plate prevents the bottom from being washed out by flowing water (Pho. 6).



Photo 6. Filling pipeline and its inlet drop plate.

### South pipeline (outflow)

On the other section of the lake an outflow pipeline has been laid out over the southern deepest point at site nu. 1 (point nu. 1), to discharge the hypolimnion from this lake's section. The inlet of the pipeline -400 mm diameter- directed upwards and supported by a deflector shield to prevent water being sucked in from the upper layers of the lake (Pho. 7). This inlet is set over a 2.5 x 2.5 m stabilizing plate (Pho. 8). The outflow pipeline is similar to the filling pipeline, which consists of two sections. A beginning section with 400 mm diameter and a 33 m length from the southern dam, a reinforced external sewage pipe, type InCor (SN8). And a

bottom section of 309 m length with a diameter of 400 mm made of smooth, thin-walled PVC-U pipes. Both pipelines were installed between 12<sup>th</sup> and 17<sup>th</sup> of October 2020. (Pho. 9), captured during the installation of outflow pipeline.



Photo 7. Deflector shield of the outflow pipeline inlet.



Photo 8. Stabilizing plate of the outflow pipeline.



Photo 9. Outflow pipeline during installation.

**✚ Dams:**

❖ The inlet dam:

Reinforced concrete on a slab, equipped with a grating protecting the inlet of the pipeline, a tight passage, and a bolt with wooden planks to regulate the water level (Pho. 10). Damming ordinate (MAX) 57.5 m above sea level, while the minimum damming ordinate is not defined. Geodetic coordinates of the northern dam according to the PL-ETRF2000 is 5773444 5571791 (pho. 11).

❖ The outlet dam:

Consist of 3 chambers which constructed on a slab from reinforced concrete. a) central chamber with a pipeline inlet and a screw valve adjustment, b) chamber with a fixed threshold defining the upper allowable water level in the ditch, and c) chamber with a fixed threshold that determines the minimum water level in the ditch and with shutter control. The maximum damming ordinate is 57.25 m above sea level (ASL) and the minimum is 57.0 m (ASL) with a geodetic coordinates (PL-ETRF2000): 5772584 5571657 (Pho. 12).



Photo 10. Construction of dam's inlet.



Photo 11. Northern dam (Inlet).



Photo 12. Southern dam (Outlet).



### 3.3 Field measurements

#### 3.4.1 Sampling date

Water samples were collected before the operation of the pipelines system on April 8<sup>th</sup>, May 29<sup>th</sup>, July 4<sup>th</sup>, September 3<sup>rd</sup> and 30<sup>th</sup>, October 28<sup>th</sup> and December 9<sup>th</sup> for year of 2017, on January 18<sup>th</sup>, February 23<sup>rd</sup>, and April 17<sup>th</sup> for year of 2018 and June 22<sup>nd</sup> and August 27<sup>th</sup> in 2020. After functionality of the pipelines system, the water samples were collected on June 21<sup>st</sup> and August 31<sup>st</sup> in 2021, and February 17<sup>th</sup>, April 11<sup>th</sup> and June 13<sup>th</sup>, September 01<sup>st</sup>, October 27<sup>th</sup> and on December 1<sup>st</sup>, 2022.

Sediment samples were collected 4 times during the three consecutive years of the research period, two before the operation of the pipeline system, as follow: on June 22<sup>nd</sup> and August 27<sup>th</sup> during year 2020, and on June 21<sup>st</sup> in 2021, and December 1<sup>st</sup> during year 2022.

During the research period (2020-2022), biological sampling was carried out in May, August, and October 2021, and in May and October 2022. This in addition to the collected data during the monitoring cycle before on April 8<sup>th</sup>, May 29<sup>th</sup>, July 4<sup>th</sup>, September 3<sup>rd</sup> and 30<sup>th</sup>, October 28<sup>th</sup> from year 2018 (Czerniawski et. al., 2018).

#### 3.4.2 Sample's location

##### Water

Water samples were taken from four measurement points. Two of them are located inside (site nu. 1 & 2), and the others are located at the inlet and outlet (site nu. 3 & 4) respectively. Where inflow from the lake inlet (site nu. 3) is directed to the bottom of site nu. 2, and hypolimnetic waters from site nu. 1 are discharged with the outflow (site nu. 4). Both of research sites inside the lake are located over the two deepest bottoms of Święte lake, water samples are collected from the surface water (-1m) and over the bottom (+1m).

##### Sediments and its sedimentary water

The sediments samples and its sedimentary water were collected from four sampling points for each of research sites inside the lake. The southern outflow zone of the lake (site nu. 1) contains: point nu. 1, pt. 2. pt. 3 and pt. 4, and the northern inflow zone of the lake (site nu. 2) contains: pt. 5, pt. 6, pt. 7 and pt. 8. (Pho. 13).

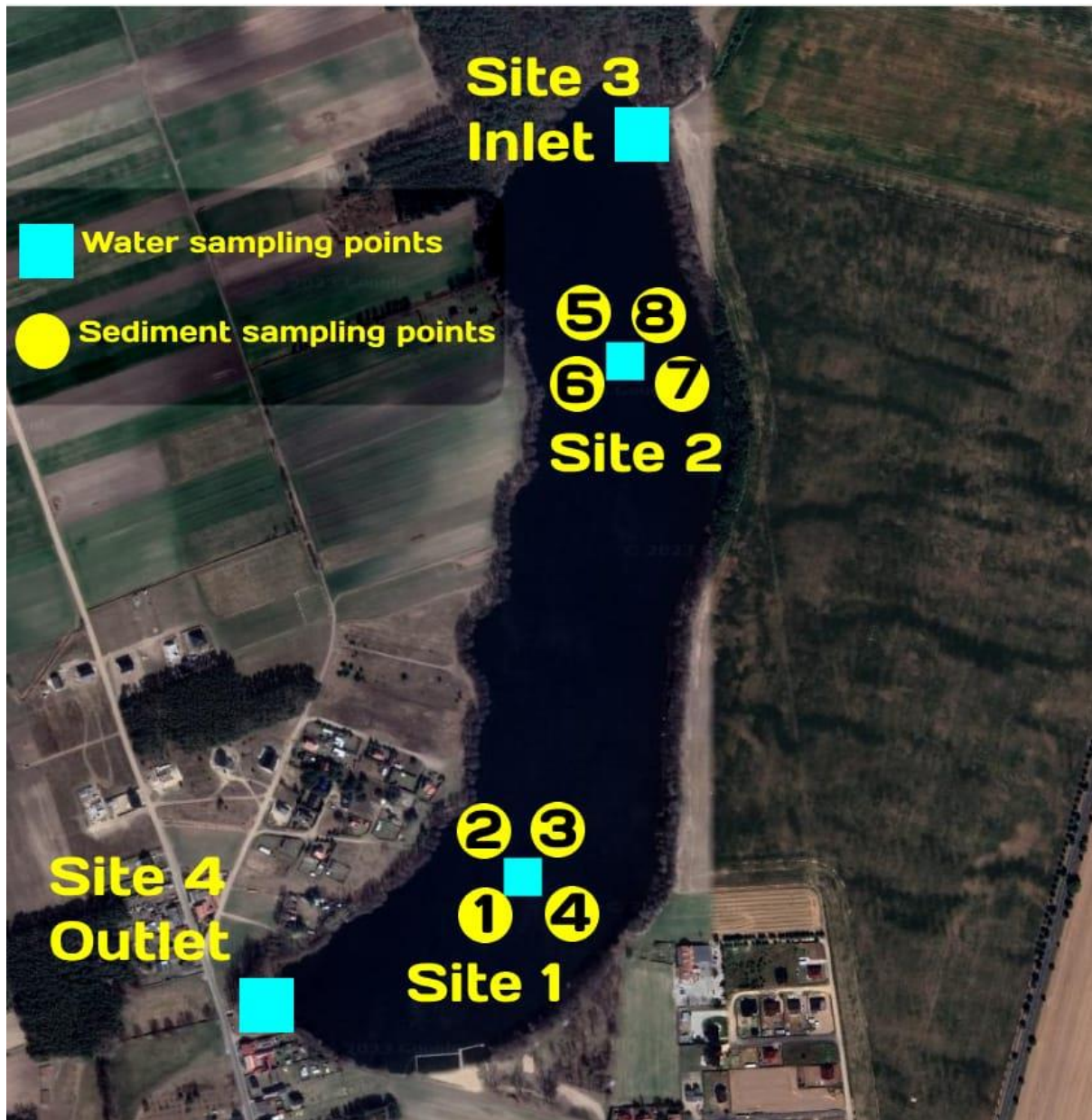


Photo 13. sampling sites and points location (on base of google earth).

### Biological parameters

The biological sampling conducted by the Department of Hydrobiology of University of Szczecin, where phytoplankton and zooplankton were determined from the epilimnion layer during summer from 0.5 m water's depth from both measuring sites inside the lake.

### 3.4 Sampling procedure

#### Water

The quality of Święte lake waters was checked by sampling the water with the use of a 3-liter Ruttner apparatus, samples were collected in containers and transported to the laboratory.

Each time the measurement of water transparency is determined by visible the range of the Secchi disc (SD). Each site, every 1 m deep, thermal-oxygen profiles (T, O<sub>2</sub>, %O<sub>2</sub>), reaction (pH) and conductivity (EC) for the water column were done using a PRO ODO optical oxygen meter by YSI were done. In the absence of oxygen, samples were taken to determine the concentration of hydrogen sulphide (H<sub>2</sub>S).

In addition, in an analogous way, using the Ruttner apparatus, samples were collected at the inflow to the lake (site 3) and at the outflow (site 4). PRO ODO optical oxygen meter by YSI was used to measures the temperature (T), oxygen (O<sub>2</sub>) and its percentage (%O<sub>2</sub>), electroconductivity (EC) and the pH. The velocity of water in the watercourses was measured using the VALEPORT electromagnetic flowmeter (model 801). The instantaneous flow was calculated using Harlacher 's calculation method (Bajkiewicz -Grabowska and Magnuszewski, 2009).

### **Sediments**

Bottom sediments were collected using a Kajak apparatus 52 mm in diameter and 0.5 m long from eight positions. The 10 cm thickness of the undisturbed bottom sediment core were collected from 8 representative sampling points of the lake bottom sediments, divided equally between site 1 and site 2. The sediment's sample from every point has divided to an upper layer of sediments (0-5 cm) and remarked in this research as (Layer 1) and contains [1-8] of sediment samples, and the bottom layer of sediments (5-10 cm) and remarked in research as (Layer 2) and contains [9-16] of sediment samples.

### **Biological parameters**

Samples of zooplankton were taken with a 30 µm plankton mesh, and after preservation with Lugol's solution and formaldehyde, then determined by microscopy. A quantitative sample of zooplankton was taken from each site by straining 50 liters (l) of water through a mill gauze mesh with a mesh size of 20 µm.

Samples of macrobenthos were collected from the littoral zone of the lake using the Kick sampling method (1 minute) from one representative site located in the coastal belt with a mixed form of land cover. The samples were then preserved with ethyl alcohol – EtOH- (C<sub>2</sub>H<sub>6</sub>O) and transported to the laboratory for further analysis.

Periphytons were determined using the transect method, where the samples material was collected from 10 transects distributed evenly along the entire length of the lake's shoreline.

The study of the ichthyofauna of the Świąte lake was carried out using an IUP-12 electric fishing device. The fish were caught from the ten most representative places in the lake. The total length of the caught fish was measured and then weighed. Then, the fish released back to the lake. Stocking procedure were carried out by specialists from the fishing industry, under ichthyologist supervision.

### **3.5 Laboratory analysis**

#### **Water**

All water analyzes were performed according to the methodology that used in hydro-chemical research provided by (Hermanowicz et al. 1999), and the Polish Standard Methods.

Alkalinity (MC) , total hardness (TH), calcium (Ca) and  $H_2S$  (as  $S^{-2}$ ) by titration methods

Magnesium was calculated as the difference between TH and Ca. Dry matter of seston by gravimetry method. Biological oxygen demand ( $BOD_5$ ) by direct method, Chemical oxygen demand (COD-Mn) as oxidizability with 0.0125 mol/L  $KMnO_4$  and 0.0125 mol/L  $Na_2S_2O_4$

Total phosphorus (TP) was determined colorimetrically with a NANOCOLOR spectrophotometer (Macherey-Nagel GmbH&Co. KG, Düren, Germany), after mineralisation with  $H_2SO_4$  and  $K_2S_2O_8$  , with the use of ammonium molybdate and  $SnCl_2$  ( $\lambda = 690$  nm). Total nitrogen (TN) and nonvolatile total organic carbon (TOC) was determined in IL 550 TOC-TN analyser (HACH Inc., Loveland, CO, USA). The concentration of chlorophyll a (Chl a) was determined after filtration through a Whatman GF/C glass fiber filter and extraction with acetone (NANOCOLOR spectrophotometer (Macherey-Nagel GmbH&Co. KG, Düren, Germany)  $\lambda = 650$  and  $750$  nm). Ammonium, nitrate, iron (Fe), manganese (Mn) by spectrophotometric with a MERCK SQ 118 ( Merck KgaA, Darmstadt, Germany).

#### **Sediments analysis**

The overall percentage composition of bottom sediments as a dry matter (% D. M.) was determined according to (Januszkiewicz, 1980), as follows: organic matter was determined as the ignition loss at  $550$  °C. For the determination of silica ( $SiO_2$ ) and other sediment components, the samples were mineralized in a mixture of concentrated acids ( $H_2SO_4$ ,  $HClO_4$ ,  $HNO_3$ ) and then filtered through a hard filter paper. The silica ( $SiO_2$ ) was obtained by calcining the residue on a filter at  $1000$  ° C.

Phosphorus fractions of the bottom sediments were determined by sequential extraction according to the methodology of (Psenner et. al., 1988) quoted by (Hullebusch et al., 2003), while the total phosphorus concentration was according to (Augustyniak, 2018; Golachowska, 1977).

The following phosphorus fractions were determined:

- Labile phosphorus (NH<sub>4</sub>Cl-P) - after 2 h of extraction of sediment in 1 M NH<sub>4</sub>Cl solution.
- Phosphorus sensitive to redox potential changes (BD-P) - after 2 h of extraction in a mixture of 0.11 M NaHCO<sub>3</sub> and 0.11 M Na<sub>2</sub>S<sub>2</sub>O<sub>4</sub>.
- Phosphorus bound to aluminum, iron oxides and hydroxides (NaOH-rP), determined after 16 h of extraction in 0.1 M NaOH solution.
- Phosphorus bound to organic matter (NaOH-nrP), calculated from the difference between total phosphorus determined in the NaOH (NaOH-TP) and NaOH-rP. (NaOH-TP) is extracted after mineralization in a mixture of H<sub>2</sub>SO<sub>4</sub> and HClO<sub>4</sub>.
- Calcium bound phosphorus (HCl-P), determined after 16 h of extraction in 0.5 M HCl solution.
- Residual phosphorus (res-P) - determined after burning the remaining sludge in a mixture of H<sub>2</sub>SO<sub>4</sub> and HClO<sub>4</sub>.
- Total phosphorus (TP) was determined as the sum of all determined phosphorus fractions.

#### **Sedimentary interstitial water and water-over-sediment analysis**

The sedimentary interstitial water obtained by centrifugation sediment samples for 20 minutes at 3000 rpm. The supernatant of interstitial waters, after being filtered through a filter paper, were subjected to chemical analysis in accordance with the methodology used in surface waters. After centrifuged the bottom sediments and separate the supernatant, the residuals sediments where dried and saved for further analysis according to the provided methodology by (Januszkiewicz, 1978) and (Hullebusch et. al., 2003).

The filtered Sedimentary interstitial water and water-over-sediment analyzed to determine the following chemical components:

Ammonium nitrogen (NH<sub>3</sub>-N) by distillation method ( Büchi S-324), Kjeldahl nitrogen (TN) by distillation method after mineralization with sulphuric acid (H<sub>2</sub>SO<sub>4</sub>) and copper (II) sulphate (CuSO<sub>4</sub>), organic nitrogen was calculated as the difference between Kiejdahl nitrogen and ammonium nitrogen, mineral phosphorus (PO<sub>4</sub><sup>3-</sup>) determined colorimetrically

by the molybdenum method ( $\lambda$  - 650 nm ), total phosphorus (TP) by the molybdenum method after mineralization with sulphuric acid ( $\text{H}_2\text{SO}_4$ ) and nitric acid ( $\text{HNO}_3$ ) ( $\lambda$  - 650 nm ), Iron (Fe) by the method from 1, 10 phenanthroline ( $\lambda$ -512 nm), manganese (Mn) by the colorimetric method with ammonium peroxodisulphate ( $(\text{NH}_4)_2\text{S}_2\text{O}_8$ ) ( $\lambda$ -530 nm), calcium (Ca) and aluminum (Al) complexometric titration determination with disodium edetate  $[\text{CH}_2\text{N}(\text{CH}_2\text{CO}_2\text{H})_2]_2$ . While magnesium (Mg) was calculated as the difference between the total hardness (TH) and calcium (Augustyniak, 2018).

The following apparatus were used to determine the abovementioned components:

- Ammoniacal nitrogen - spectrophotometric method Merck Spectroquant Prove 100,
- Kjeldahl nitrogen by Hach IL 550 TOC-TN carbon and nitrogen analyzer,
- Mineral phosphorus -spectrophotometrically- by Merck Spectroquant Prove 100,
- Total phosphorus by Nanocolor spectrophotometer by Macherey Nagel,
- Iron and manganese -spectrophotometric method- by Merck Spectroquant Prove 100.

### **Biological parameters**

The zooplankton qualitative and quantitative evaluation was performed in the laboratory with the use of a zooplankton chamber and a Nikon Eclipse 50i microscope. The samples were concentrated to a volume of 40 ml, then they were preserved in a 4% formaldehyde solution. The organisms of macrobenthos were sorted under a stereoscopic microscope and marked to the lowest possible taxonomic level. And after Periphyton samples were preserved and transported to the laboratory, they were determined under a stereoscopic microscope.

### **Trophic State Index (TSI)**

The trophic state was assessed by the TSI (Trophic State Index) using logarithmic transformation of Secchi disc visibility (SD), concentration of chlorophyll a (Chl a), total phosphorus (TP) (Carlson, 1977) and total nitrogen (TN) (Kratzer i Brezonik 1981) according the equations:  $\text{TSI}(\text{SD}) = 60 - 14.41 \ln(\text{SD})$ ,  $\text{TSI}(\text{Chl}) = 9.81 \ln(\text{Chl}) + 30.6$ ,  $\text{TSI}(\text{TP}) = 14.$

$42 \ln(\text{TP}) + 4.15$ ,  $\text{TSI}(\text{TN}) = 54.45 + 14.43 \ln(\text{TN})$ . The relative value lower than 40 characterizes oligotrophy, in the range 40 to 60 mesotrophy, 60 - 70 eutrophy, above 70–hypertrophy (Carlson, 2007 & 1977).

### **3.6 Statistical Analysis**

The water samples were grouped into 7 datasets; each dataset consider as a one-time measurement interval during the research period (2020-2022). The seventh group of datasets

obtained by finding the average mean results of water from observing period before the operation of the pipelines system (2017-2020) of Święte lake during the observing period (2017-2022) (Czerniawski et. al., 2018).

The sedimentary interstitial water and water-over-sediment samples grouped into 5 datasets, based on its sampling time interval during the research period (2020-2022). The sediment samples were grouped into 4 datasets; each dataset is considered as a one-time measurement interval during the research period (2020-2022).

The statistical analysis is based on a

The null hypothesis ( $H_0$ ) of the performed statistical analysis assumes that there is no changes of Święte lake biophysiochemical parameters regarding to the conducted restoration activities, while the alternative hypothesis ( $H_1$ ) suppose a significant change ( $P \leq 0.05$ ) of the analyzed biophysiochemical parameter during the study period.

In addition to, a Correlation between sediments components and the ratio of TN:TP and O. M.: TN.

The used software were Microsoft Excel 365 and SPSS 26, and the applied statistical tests, as follow:

- Student's t-test, to compare the means of a single variable during different time intervals with 95% of confidence interval (CI) (Von Eye and Wiedermann, 2023; Darryl, 2023),
- ANOVA (Analysis of Variance), to compare the mean difference variances within the group and between two groups or more (Faizi and Alvi, 2023; Pond and Caerano, 2022)
- Pearson correlation, to measure of the strength of a linear relationship between two variables (Dufera et. al., 2023).

## 4. Results

### 4.1 Thermal stratification and circulation pattern of Święte lake

Święte lake shows a thermal stratification during the summer, with a maximum surface temperature of 22.0 °C. The epilimnion layer reaches a depth of 3 m in June and got deeper by 1 m more in August.

At the beginning of April, the thermal stratification begins when the forming epilimnion heated to 10.5-10.6 °C, while in May, June, and July the summer stagnation of the water is confirmed with the stratification typical of this period. This indicates a short-term and incomplete water circulation in the spring. Usually, during May, the epilimnion layer reach to a depth of 2 m of the water column, and in the in the subsequent months until the end of July, it deepened to 4 m with temperature ranged between 20-22 °C, later-on the epilimnion's temperature slightly drop on at the beginning of September.

The gradient of the thermocline layer almost 4 °C/m in June and it took place in depth 3-7 meters with a gradient of 4 °C/m, while in August got one meter deeper (4-8 m) with a gradient of 3.3 °C/m. The hypolimnion layer depth starts below 7 m depth, with a temperature range between 6.7 °C and 5.8 °C at the deep layer of water (Fig. 2). The thermocline layer depth varied, with a maximum thermal gradient in September that occurred between 5 and 6 m deep, and amounted to 4.1 °C/m.

The hypolimnion zone considered some kind thermally stable, temperature in the deepest part of the water amounts to 5.4-5.9 °C. Generally, in October, the epilimnion cooled to approximately 12 °C and deepened to 7-8 m, indicating a cooling circulation. The temperature of the water at the deepest parts of the water column does not change during the summer stagnation.

As an example of the lake water circulation during the spring and autumn turnover, in December 2022, the temperature of the surface water was 6.6 °C for both of the research sites with an oxygen concentration of 5.35 to 4.00 mg O<sub>2</sub>/l for site nu. 1 & 2, respectively. While the temperature stayed constant through the whole water column, a negligible decrease observed regarding the dissolved oxygen concentration at the deep water compared to the surface one (Fig. 3).



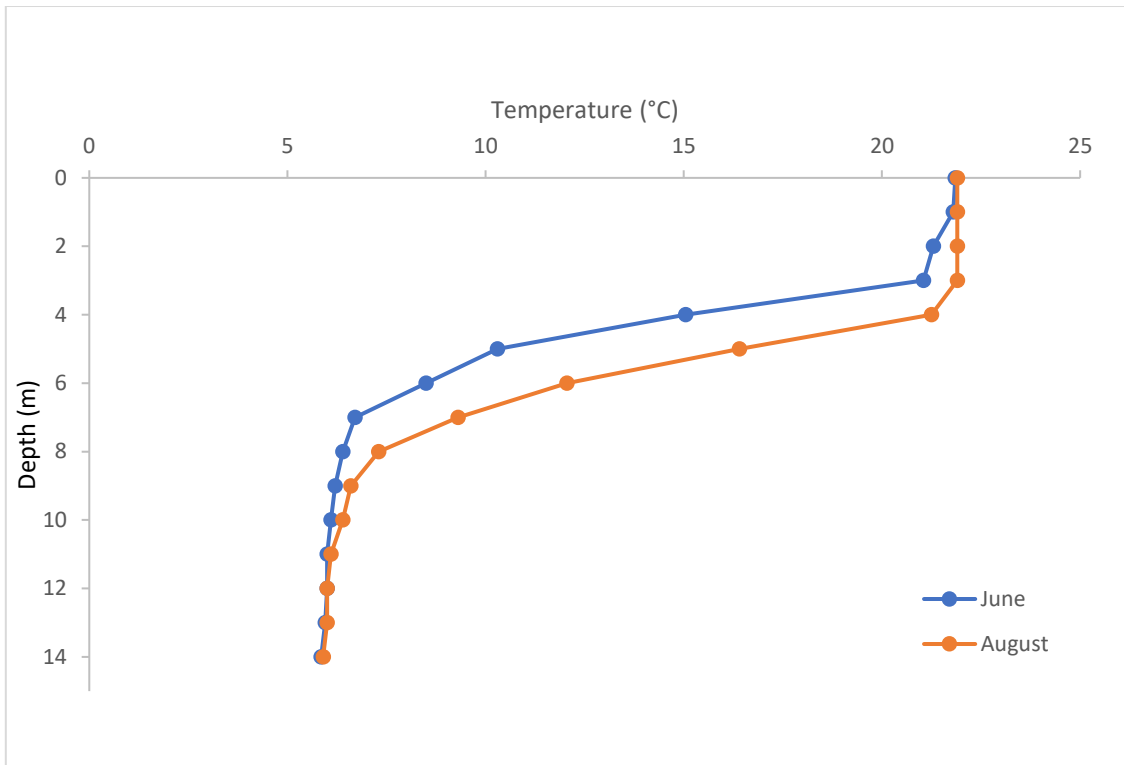


Figure 2. Average temperature for both sites during the summer stagnation, 2020.

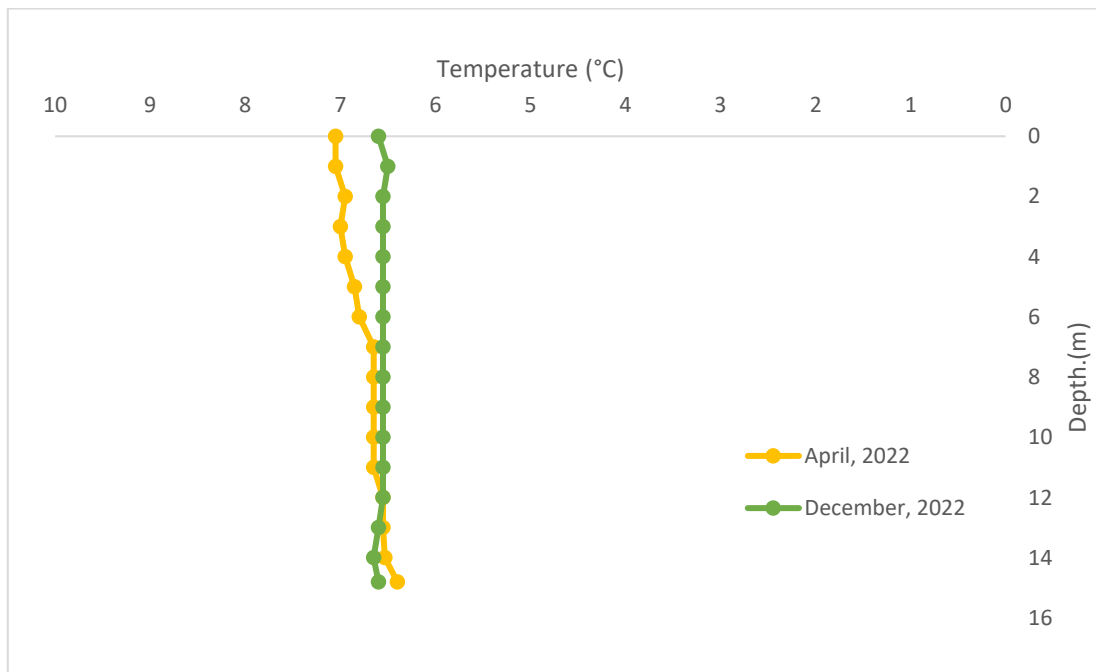


Figure 3. Average temperature for both sites during the late autumn turn-over December 2022.

## 4.2 Lake hydrology

The delivered flow quantity did not follow a systematic pattern with a non-stable outflow, due to failure to apply the operation schedule of Krutla drainage pumping station regarding the meteorological conditions. The average annual number of operating hours of the pumps for the years 2012-2017 was 3955 hours per year with an average flow of 41.7 l/s (Czerniawski et. al., 2018).

The mean value of the inflow pH ranged from 7.17 to 7.34, and for the outflow was 7.94 and slightly rise during spring and summer. The inflow average oxygen concentration was 5.21 mg O<sub>2</sub>/l. The average concentration of seston was over 8.00 mg/l. Sometimes, the inflow electrolytic conductivity exceeded 1000 µS/cm during years 2017 and 2018 with an average of 660.20 and 885.20 µS/cm for the outflow and inflow, respectively. which indicating water contamination by mineral compounds. The outflow conductivity of the lake was characterized by increased values from December 2017 to April 2018.

The inflow is the main supplier of organic matter to lake with mean concentration s of organic nitrogen (N<sub>org</sub>), organic phosphorus (P<sub>org</sub>) and the total organic carbon (TOC) are 5.30 mg N/l, 0.16 mg P/l and 16.74 mg C/l, respectively.

The mineral form of nitrogen (NO<sub>3</sub><sup>-</sup>) reached 9.76 mg N/l in the inflow (mean). While the inflow mean concentration of ammonium nitrogen (NH<sub>4</sub><sup>+</sup>) was 0.24 mg N/l, where its increase in water was correlated with the amount of nitrate.

Phosphate (PO<sub>4</sub><sup>3-</sup>), were found at Zimne Kąty site with an average of 0.162 mg P/l. It was comparable to the organic nitrogen (N<sub>org</sub>) concentration at the same site (Czerniawski et al., 2018). The remaining tributaries water (watercourses) were characterized by twice lower as in Pintus tributary from Krutla pumping station to Święta lake. The flow quality parameters of Święte lake are shown in (Tab. 2)

Table 2. Average parameter values for Pintus flow.

<b>Parameter, (unite)</b>	<b>Pintus - inflow</b>	<b>Pintus - outflow</b>
Flow (l/s)	39.01	52.82
Temperature, (°C)	10.91	12.55
Dissolved oxygen, (mg O <sub>2</sub> /l)	7.16	10.53
Oxygen percentage, (%)	63.41	100.32
pH	7.38	7.94
Conductivity, (µS/cm)	885.20	660.20
Chlorides, (mg /l)	57.66	60.77
BOD <sub>5</sub> , (mg O <sub>2</sub> /l)	4.21	3.58
COD, ([mg O <sub>2</sub> /l)	16.38	13.49
Alkalinity, (mval /l)	6.22	3.61
Hardness, (mval /l)	8.79	11.36
Calcium, (mg /l)	155.21	100.37
Magnesium, (mg /l)	20.80	19.16
Mineral phosphorus, (mg P /l)	0.07	0.03
Organic phosphorus, (mg P /l)	0.13	0.09
Total phosphorus, (mg P /l)	0.13	0.21
Ammonium nitrogen, (mg N /l)	0.14	0.25
Nitrate, (mg N /l)	0.40	1.37
Organic nitrogen, (mg N /l)	0.98	2.10
Total nitrogen, (mg N /l)	1.53	3.73
TOC, (mg /l)	11.70	14.82
Iron, (mg /l)	0.03	0.33
Manganese, (mg /l)	0.26	0.86
Seston, (mg /l)	3.55	7.60
Chlorophyll a, (µg /l)	3.21	4.25

Pintus inflow parameters various during the conduct measurements in 2022. The obtained results in June were the highest in all aspects, almost with the lowest dissolved oxygen concentration (2.60 mg O<sub>2</sub>/ l). The inflow quantity in February was 4.3 l/s, and in December less than 1 l/s. While, during April and June was relatively too small to be considered. The temperature of Pintus tributary increased slightly between February (6.2 °C) and April (8 °C) but rose to more than 20 °C in June and during the summer season. During the last sampling season (December 2022), temperature dropped to 3.5 °C and the pH value was similar during the whole year, approximately 7.7. Summarize of the main inflow parameters for Święte lake (Tab. 3).

Table 3. Summary of Pintus inflow main parameters during year 2022. \*

Parameter, unit	Feb-22	Apr-22	Jun-22	Dec-22
Flow (Q), (l/s)	4.30	no data	no data	0.70
Temperature, (C)	6.20	8.10	20.20	3.50
Oxygen, (mg/l)	8.85	4.06	2.60	5.92
pH	7.60	7.80	7.70	7.70
Seston, (mg/l)	3.00	3.20	3.50	7.60
BOD <sub>5</sub> , (mg O <sub>2</sub> /l)	3.30	3.50	10.60	4.62
COD-Mn, (mg O <sub>2</sub> /l)	13.00	15.06	21.11	10.67
TOC, (mg/l)	14.93	12.94	22.44	11.79
TN, (mg N/l)	14.93	2.40	2.49	2.14
TP, (mg P/l)	0.046	0.108	0.198	0.083
Hardness, (mval/l)	11.60	7.07	9.34	7.03

\* The flow was not stable during the year 2021, to build results on.

In April 2022, the concentration of TP through the outflow was almost three times higher than the inflow, approximately 0.434 mg P/l. For December 2022' measurement, phosphorus (TP) concentration at the inflow (site nu.3) was 0.123 mg P/l, and at the outflow (site nu.4) was 0.125 mg P/l. The organic phosphorus (P<sub>org</sub>) concentration were 0.081 and 0.078 mg P/l for inflow and outflow, respectively.

During April 2022, the inflow Sulphate (SO<sub>4</sub><sup>2-</sup>) concentration was high 185 mg S<sup>2-</sup>/l, while its concentration in the outflow was significantly low and relatively 35 mg S<sup>2-</sup>/l. However, the

registered values for December dropped significantly and none of them exceeded 34.4 mg S<sup>2-</sup>/l. For April 2022' measurements the inflow chloride concentration was 57 mg Cl/l, while in the outflow was 8.7 mg Cl/l.

### 4.3 Quality of the lake water

The oxygen profile during the summer stagnation of year 2020 shows a depletion of oxygen content in the hypolimnion layer (Fig. 4). During the summer stagnation, epilimnion layer was over-oxygenated especially in July up to 11 mg O<sub>2</sub>/l (133.13 %O<sub>2</sub>).

The extent of the deoxygenated layer relay on the summer stagnation, which ranged in depth. It was noticed below 10 m depth in May, below 9 m in July, and deeper than 6 m in September 2020. During the autumn circulation, oxygen deficit in the entire water volume up to a depth of 6 m, around 8 mg O<sub>2</sub>/l was demonstrated. The deeper layers remained deoxygenated.

Spring circulation recompenses for the lost oxygen from the winter period. During the spring, the surface layer was oxygenated to more than 13 mg O<sub>2</sub>/l (157.34 %O<sub>2</sub>). While below 6 m depth the water shows an oxygen deficit. It was initially slight but increased with the lake depth. The presence of oxygen in the water over-the-bottom was less than 1 mg O<sub>2</sub>/l.

The absence of oxygen in the deep-water layer was accompanied by the appearance of hydrogen sulphide (H<sub>2</sub>S). The concentration of this toxic gas was noticeable at 9 meters depth (0.04 mg S<sup>-</sup>/l), to reach its peak at the deep-water layer, with an average concentration of 6.56 mg S<sup>-</sup>/l and 15.12 mg S<sup>-</sup>/l for June and August, respectively. The maximum hydrogen sulphide (H<sub>2</sub>S) value was found in the deeper water of site nu. 2 (17.35 mg S<sup>-</sup>/l).

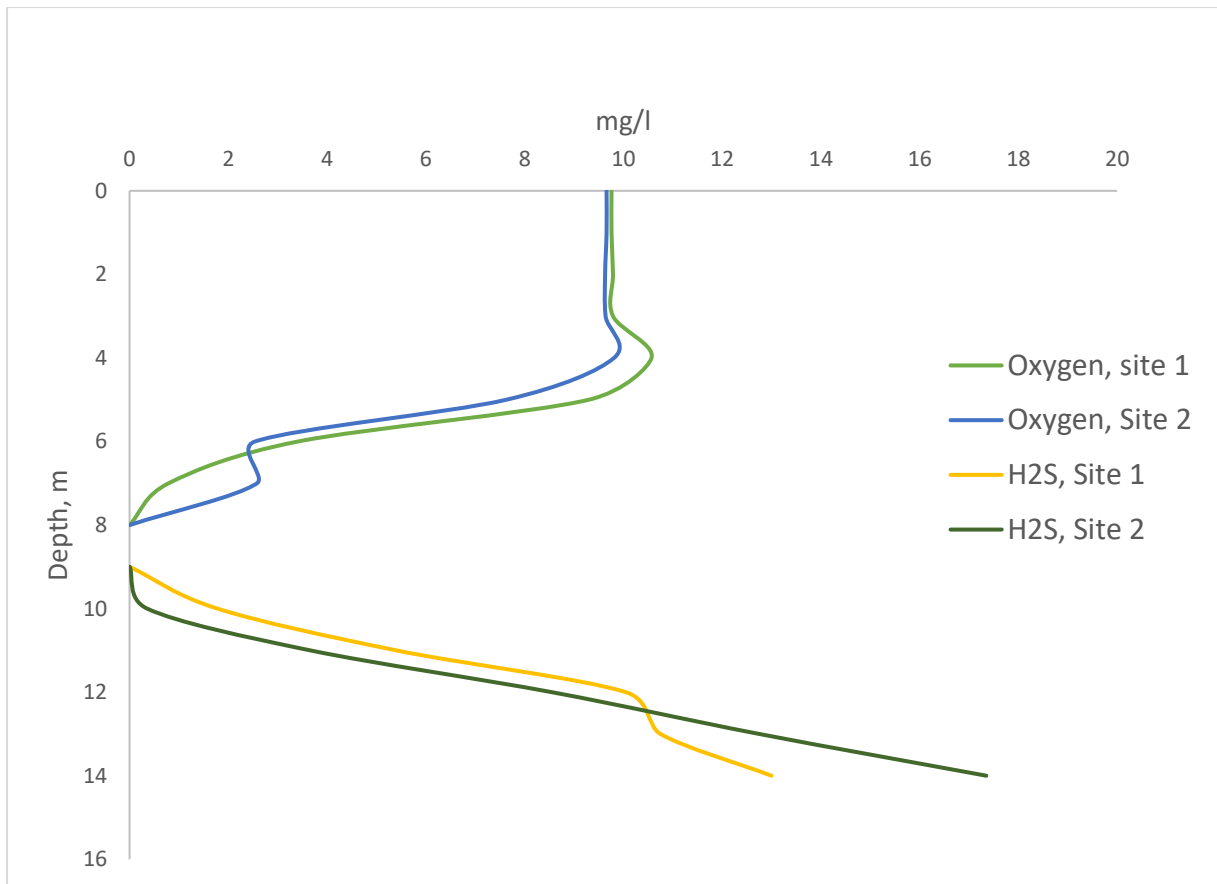


Figure 4. Water column oxygen and hydrogen sulphide concentration, during the summer stagnation, 2020.

Both conducted sampling measurements in year 2022, were conducted during the spring and autumn turnover. Therefore, the temperature and oxygen profiles were uniformed, same the same, the other water parameters through the water column. While the measurements during the summer stagnation of 2021. The lake shows a thermal partitioning, and oxygen deficit at the hypolimnion zone with occurrence of hydrogen sulphide (H<sub>2</sub>S) below 11 m depth (Fig. 5).

During 2022, the dissolved oxygen concentration through the water column during the April measurements were almost twice as much as the observed one in December. For the same year, hydrogen sulphide gas (H<sub>2</sub>S) concentrations ranged from 3.13 to 8.96 mg S<sup>2-</sup>/l at site nu. 1, and from 6.5 to 12.82 mg S<sup>2-</sup>/L at site nu. 2.

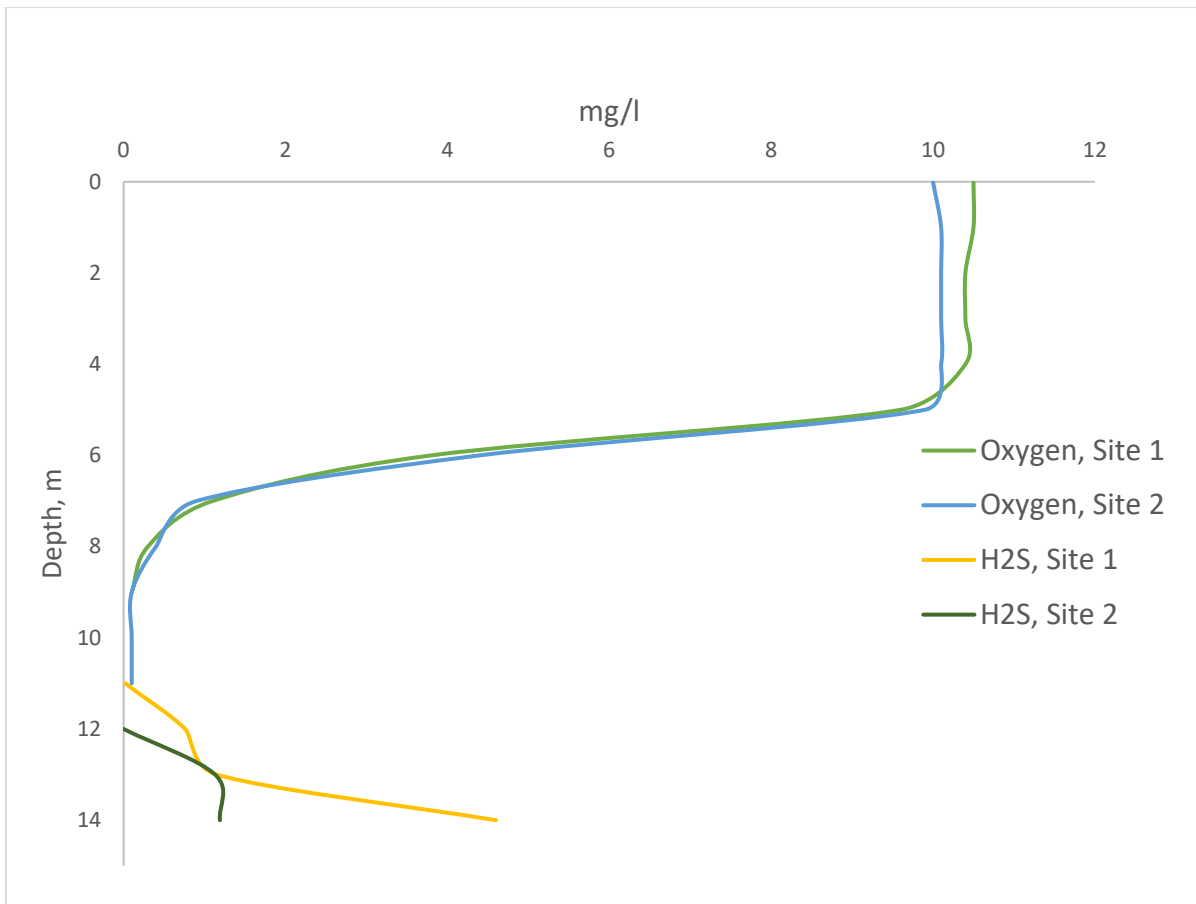


Figure 5. Water column oxygen and hydrogen sulphide concentration, during the summer stagnation, 2021.

One of the symptoms of excessive water fertility is the low visibility of the Secchi disc. Water visibility (SD) of Święte lake for year 2018 ranged from 1.50 m to 3.70 m, while in 2020 the transparency ranged from 1.90 m to 3.20 m for measuring sites nu. 1 & 2, respectively. The visibility range considers quite a good range of visibility, but according to the classification given by (Faraś-Ostrowska and Lange, 1998) it is typical of eutrophic lakes. Transparency of the lake' water in April 2022 were recorded to be 1.75 m and 1.8 m These values rose in December to reach 2.48m at measuring site nu. 1 and 5 m at measuring site nu. 2. Visibility values were slightly higher than observed in the year 2021. Phytoplankton abundance is a critical factor that determines the water' transparency, Chlorophyll a dye concentration in the surface water of site nu. 1 for the April 2022' measuring season found to be 10.6  $\mu\text{g/l}$  deeper than 11 m, while the surface water of site nu. 2 was 8.29  $\mu\text{g/l}$  for the same measuring season. The lowest observed Chlorophyll a concentration was in December 2022 and the found to be 1.79 11.2  $\mu\text{g/l}$  and 3.62 11.2  $\mu\text{g/l}$  for site nu. 1 & 2, respectively.

The transparency showed an improvement after the operation of the pipelines system, the deepest observed depth obtained in December 2022. As chlorophyll a concentration is inversely correlated with waters transparency, and its content in water is an indicator of phytoplankton amount in water. Chlorophyll a founds to be at the lowest level in the same month when the highest depth of SD had been observed (Fig. 6).

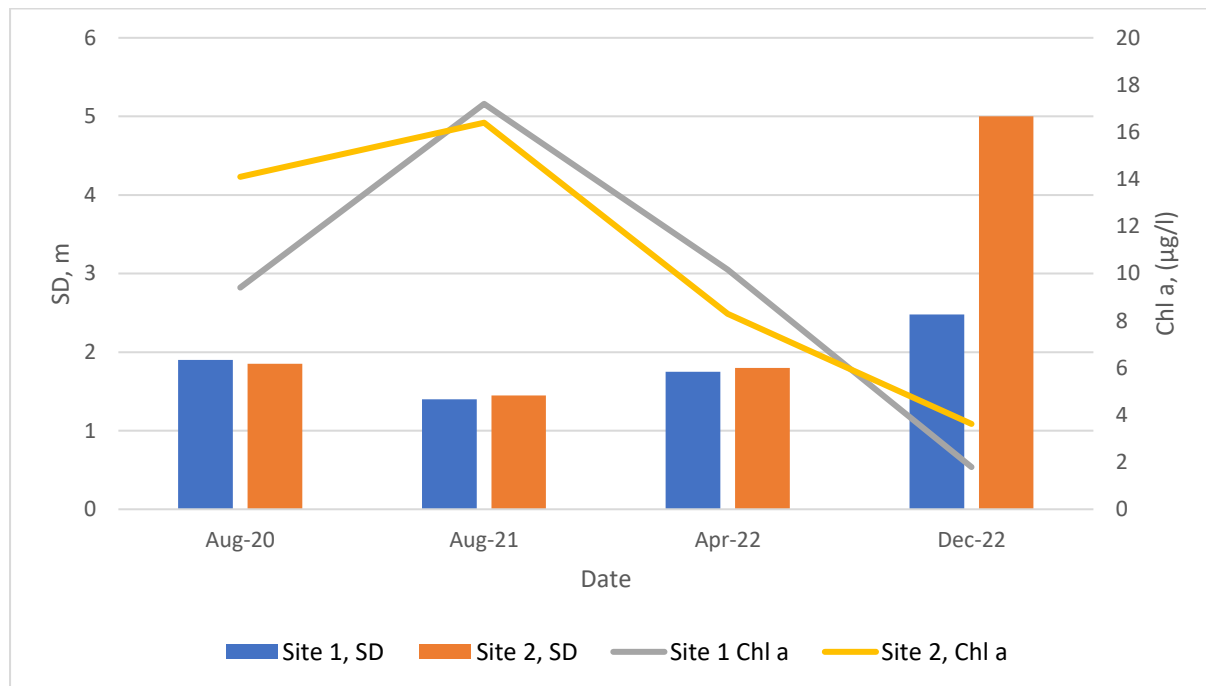


Figure 6. Świąte lake waters transparency and its chlorophyll concentration during the research period (2020-2022).

The obtained results in 2020, showed a deterioration of the lake trophic state regarding phosphorous (P) and nitrogen (N) concentrations for both of the surface water and water-over-sediments in a compare to the recorded values from year 2018. In June 2020, the Hydrogen sulphide concentration was twice as high as in April from the same year. While the dominant form of phosphorus in the deoxygenated hypolimnion for year 2020 was phosphates/ orthophosphate ( $PO_4^{-3}$ ), which indicates that the process of internal loading of this nutrient from bottom sediments was started (Paytan et. al., 2017). Such results indicate the trend of the ecological parameters and justify the implementation of the restoration procedure.



The total phosphorus concentration changed from 0.091 to 0.848 mg P/l, during year 2018. While, varied during year 2020, from 0.054 to 0.139 mg P/l in the surface layer of water and from 0.77 to 1.394 mg P/l above the bottom, usually slightly higher values on the measuring site nu. 2 with an increasing concentration towards the bottom was observed with availability of all forms phosphorus (P). The highest concentrations of phosphorus compounds were recorded at the end of October. The organic fraction, in 2018, was the dominant form of phosphorus in the whole lake. Its percentage share in total phosphorus was 63%. While the dominant form of phosphorus in the deoxygenated hypolimnion for the year 2020, was phosphates/ orthophosphate ( $\text{PO}_4^{3-}$ ). The total phosphorus (TP) concentrations in December 2022 showed a slight increase compared to the one from April, with a predominance of the organic form of phosphorus (P-org) in almost all the measured depths. TP values for both months were bigger in the surface water for site 1 than the deep water, while the deep water of the site 2 showed much higher concentrations than the surface one. Interestingly during the last-mentioned measurement, that all the exist phosphorus in the surface water of site nu. 2 was in organic form with a concentration of 0.125 mg P/l, and for both sites the mineral form of P was equal, 0.042 mg P/l. Maximum values of TP were found during August 2022 to be 0.455 mg P/l and 0.534 mg P/l at site nu. 1 and site nu. 2, respectively. The mineral phosphorus form was found to be 0.14 mg P/L at the southern site nu. 1, while its almost three times more at the northern site nu. 2.

Descriptive statistics of total phosphorus (TP), mineral phosphorus ( $\text{PO}_4$ ) and organic phosphorus ( $\text{P}_{\text{org}}$ ) for both research sites of Świąte lake during the observing period described in (Tab.4). The statistical analysis of variance (ANOVA) reveals that there is not significant difference ( $P>0.05$ ) in any form of the phosphorous concentration between groups of water samples for both of research sites inside the lake, site 1 and site 2 (Tab. 5).

The content of phosphorus (all forms) in surface layer of water was similar for both research sites inside the lake, site nu. 1 & 2. But the surface and deeper waters content of phosphorus varies significantly, where the deeper water has higher phosphorus content level for all the analyzed forms. The deep layer of water at the outflow zone possesses the highest-level phosphorus content level of all analyzed forms (Fig. 7).

Table 4. Descriptives analysis of phosphorus forms at both research sites during the observing period (2017-2022).

		N	Mean	Std. Deviation	Std. Error	95% Confidence Interval for Mean		Min.	Max.
						Lower Bound	Upper Bound		
Mineral Phosphorus (PO <sub>4</sub> ) [mg/l]	Site 1	14	0.17	0.22	0.06	0.04	0.30	0.01	0.56
	Site 2	14	0.17	0.23	0.06	0.04	0.30	0.00	0.55
	Total	28	0.17	0.22	0.04	0.09	0.26	0.00	0.56
Organic Phosphorus (P org) [mg/l]	Site 1	14	0.23	0.20	0.05	0.12	0.35	0.04	0.76
	Site 2	14	0.30	0.28	0.07	0.14	0.46	0.08	1.04
	Total	28	0.27	0.24	0.05	0.17	0.36	0.04	1.04
Total Phosphorus (TP) [mg/l]	Site 1	14	0.33	0.36	0.10	0.12	0.54	0.05	0.97
	Site 2	14	0.42	0.43	0.12	0.17	0.67	0.08	1.18
	Total	28	0.38	0.39	0.07	0.22	0.53	0.05	1.18

Table 5. ANOVA test for phosphorous forms distribution at both research sites during the observing period (2017-2022).

		Sum of Squares	df	Mean Square	F	Sig.
Mineral Phosphorus (PO <sub>4</sub> ) [mg/l]	Between Groups	0.000	1	.000	.000	.992
	Within Groups	1.299	26	.050		
	Total	1.299	27			
Organic Phosphorus (P org) [mg/l]	Between Groups	.031	1	.031	.515	.479
	Within Groups	1.543	26	.059		
	Total	1.573	27			
Total Phosphorus (TP) [mg/l]	Between Groups	.061	1	.061	.383	.541
	Within Groups	4.130	26	.159		
	Total	4.191	27			

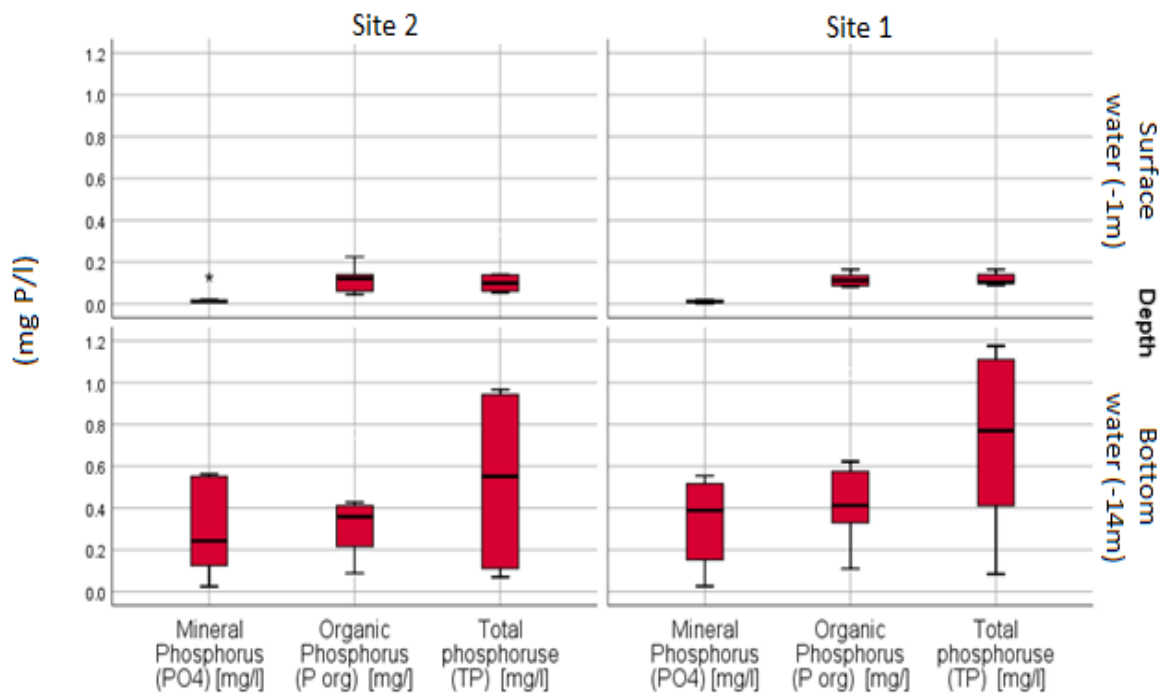


Figure 7. Distribution of the analyzed phosphorus forms [ $\text{PO}_4$  (mg P/l);  $\text{P}_{\text{org}}$  (mg P/l); TP (mg P/l)] at surface and deep water for both of Świąte lake research sites during the observing period (2017-2022).

Nitrogen concentrations were found in 2018, which ranged from 0.91 to 5.71 mg N/l. While for 2020, the registered nitrogen concentrations ranged from 1.0 to 1.26 mg N/l on the surface layer and from 6.33 to 10.68 mg N/l at the deeper layer. These high values of nitrogen concentrations for both years deem the eutrophic nature of Świąte lake, especially that the nitrogen organic form was predominated. The nitrogen amount increases by going deeper into the lake. Mainly, ammonium nitrogen ( $\text{NH}_4^+$ ) clearly dominated among the mineral forms of nitrogen in the deep-water layer, and nitrate nitrogen ( $\text{NO}_3^-$ ) at the surface.

The total nitrogen (TN) concentration for April 2022' measurement for all locations including the inflow and the outflow were similar, around 2.4 mg N/l. These values remain relatively similar, but identical for surface and deep waters of site nu. 2 (2.14 mg N/l) during December 2022' measurement. This is due to that, the site nu. 2 is the receiver of the incoming flow, which was its TN concentration also the same, 2.14 mg N/l. The deep waters of site nu. 1 showed a significant increasing change of TN value to be 12.95 mg N/l, compared to its surface water (2.01 mg N/l). Descriptive analysis of the nitrogen forms in the lake water's column (Tab. 6). The statistical analysis (ANOVA) reveals that there is no significant difference

( $P > 0.05$ ) of the nitrogen concentration in water column, because of the restoration technique at both sides of Świątę lake (Tab. 7). The surface and deep waters have significant different levels of N content at both sites, where the N content in the deeper layer of water is higher compared with surface one, where the N content in the deep layer of water is higher compared with surface one (Fig. 8).

Table 6. Descriptives analysis of nitrogen forms at both research sites during the observing period (2017-2022).

		N	Mean	Std. Deviation	Std. Error	95% Confidence Interval for Mean		Mini.	Max.
						Lower Bound	Upper Bound		
Ammonium nitrate (NH <sub>4</sub> ) [mg/l]	Site 1	14	1.00	1.62	0.43	0.06	1.93	0.00	4.48
	Site 2	14	1.25	1.99	0.53	0.11	2.40	0.00	5.70
	Total	28	1.12	1.78	0.34	0.43	1.82	0.00	5.70
Nitrate (NO <sub>3</sub> ) [mg/l]	Site 1	14	0.07	0.06	0.02	0.04	0.10	0.03	0.25
	Site 2	14	0.10	0.13	0.04	0.03	0.18	0.04	0.55
	Total	28	0.09	0.10	0.02	0.05	0.13	0.03	0.55
Organic Nitrogen [mg/l]	Site 1	14	3.05	3.05	0.82	1.29	4.82	1.03	12.49
	Site 2	14	2.36	1.29	0.35	1.61	3.11	0.18	4.98
	Total	28	2.71	2.33	0.44	1.80	3.61	0.18	12.49
Total nitrogen (TN) [mg/l]	Site 1	14	3.94	3.71	0.99	1.79	6.08	1.03	12.95
	Site 2	14	3.43	2.65	0.71	1.90	4.96	1.22	10.68
	Total	28	3.68	3.17	0.60	2.45	4.91	1.03	12.95

Table 7. ANOVA test for nitrogen forms distribution at research sites during the observing period (2017-2022).

		Sum of Squares	df	Mean Square	F	Sig.
Ammonium nitrate (NH <sub>4</sub> ) [mg/l]	Between Groups	.468	1	.468	.143	.709
	Within Groups	85.33	26	3.282		
	Total	85.79	27			
Nitrate (NO <sub>3</sub> ) [mg/l]	Between Groups	.007	1	.007	.722	.403
	Within Groups	.267	26	.010		
	Total	.275	27			
Organic Nitrogen [mg/l]	Between Groups	3.341	1	3.341	.608	.443
	Within Groups	142.93	26	5.498		
	Total	146.26	27			
Total nitrogen (TN) [mg/l]	Between Groups	1.778	1	1.778	.171	.682
	Within Groups	270.11	26	10.389		
	Total	271.89	27			

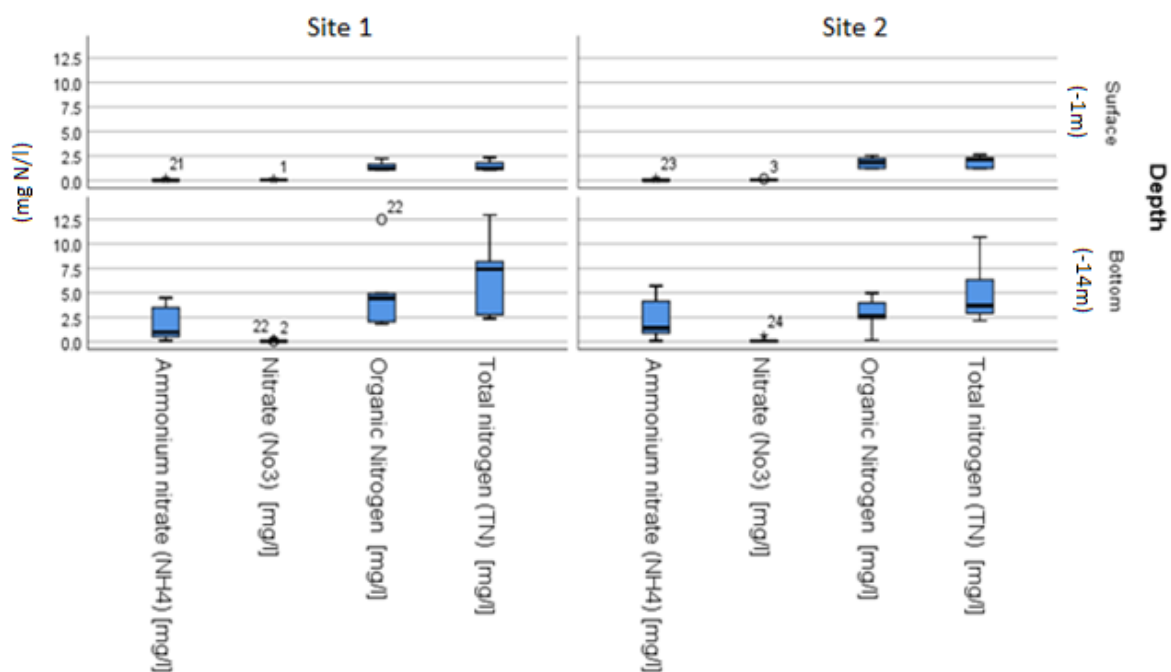


Figure 8. Distribution of analyzed nitrogen forms [TN (mg N/l); N<sub>org</sub> (mg N /l); NO<sub>3</sub> (mg N /l); NH<sub>4</sub> (mg N/l)] at surface and deep layers of water surface and bottom waters for both research sites in Święte lake during the observing period (2017-2022).

The BOD<sub>5</sub> considers as an indicator of the indigenous organic matter. In 2018, its value for the surface water layer ranged from 2.3 to 5.2 mg O<sub>2</sub>/l, and for the deeper water layer from 4.0 to 18.9 mg O<sub>2</sub>/l. For year 2020, the registered BOD<sub>5</sub> values at the measuring site nu. 1 for surface water varied between 1.4 to 2.69 mg O<sub>2</sub> /l and for the water above-bottom ranged between and 13.6 to 25.7 mg O<sub>2</sub>/l . And, for the measuring site nu. 2 the values were between 1.6-3.8 mg O<sub>2</sub>/l and 7.2-27.1 mg O<sub>2</sub>/l, for the surface and deep waters, respectively. The observed results of biological oxygen demand BOD<sub>5</sub> for the surface water during the year 2022, decreased significantly for both measuring stations in December 2022 compared to April. At site nu. 1, BOD<sub>5</sub> dropped from 4.4 mg O<sub>2</sub>/l in April 2022 to 0.28 mg O<sub>2</sub>/l in December, the same for site nu. 2, from 3.9 mg O<sub>2</sub>/l to 0.26 mg O<sub>2</sub>/l. Despite that, BOD<sub>5</sub> value at the deep layer of water increased noticeably at site nu. 1 to be 6.36 mg O<sub>2</sub>/l.

The values of COD-Mn, for 2020, were similar on both test sites and ranged from 5.8 to 12.0 mg O<sub>2</sub>/l in the surface layer and 4.9-29.5 O<sub>2</sub>/l bottom of the water column. The chemical oxygen demand (COD-Mn) for April 2022 for the surface water at site nu. 1 & 2 were 10.75 and 11.03 mg O<sub>2</sub>/l, respectively. While the COD-Mn for the deep water were 8.50 and 9.30 mg O<sub>2</sub>/l for site nu. 1 & 2, respectively. The highest reported BOD<sub>5</sub> values for the surface layer were recorded in June 7.4 and 10.6 mg O<sub>2</sub>/l for sites nu. 1 and nu. 2, respectively. While in the deep layer of water were recorded during September 2022' measurement (COD-Mn) values were 10.9 and 11.5 mg O<sub>2</sub>/l for sites nu. 1 and nu. 2, respectively. And in December 2022, COD-Mn values for the surface water at were 10.14 and 12.58 mg O<sub>2</sub>/l, and for the deeper water were 11.00 and 10.67 mg O<sub>2</sub>/l for site nu. 1 & 2, respectively.

The total organic carbon (TOC) was relatively equal during the April 2022' measurement for the whole water body, around 13 mg C/l, but the out flow registered higher value to be 16.43 mg C/l. For December 2022, TOC values for the surface water varied between both measuring sites 12.2 mg C/l and 9 mg C/l, but similar for the deep layer of water column 11.86 mg C/l and 11.56 mg C/l, site nu. 1 & 2, respectively.

The amount of dry matter of seston during year 2020 ranged between 1.8-2.8 mg/l comparing to the values from year 2018 which ranged among 0.58-5.2 mg/l.

The concentration of seston changed seasonally, site nu. 1 shows slightly higher values than site nu. 2. April 2022' measurement for site nu. 1, seston values ranged from 3.6 mg/l for

surface water and to 3.8 mg/l at the deeper layer of water. While, for site nu. 2 during the same measure seston values were 4.2 mg/l and 1.6 mg/l for surface and deeper water, respectively. In December 2022, seston values at site nu. 1 rose slightly to be 4 mg/l for surface water and 4.4 mg/l at the deep water. While for site nu. 2, these values found to be at the surface layer of water 7.6 mg/l and at the deeper layer of water 7.2 mg/l.

The water quality parameters, as alkalinity, total hardness, total organic carbon, seston, biological oxygen demand and chemical oxygen demand at both research sites of Święte lake are decrepitated at (Tab. 8). There is no significant difference ( $P>0.05$ ) in measurements means of water quality parameters during the observing period (2017-2022) (Tab. 9). The results show a similarity of water parameters at both sites for surface and deep waters, but the deep layer of water has a little higher BOD<sub>5</sub> and COD-Mn values (Fig. 9). This similarity could be explained by the included results from the observing period (2017-2022) before the operation of the pipelines system.

Table 8. Descriptives of water quality parameters (Alkalinity, Total Hardness, Total organic carbon (TOC), Seston, Biological oxygen demand (BOD<sub>5</sub>), Chemical oxygen demand (COD-Mn) at both sites during the observing period (2017-2022).

		N	Mean	Std. Deviation	Std. Error	95% Confidence Interval for Mean		Minimum	Maximum
						Lower Bound	Upper Bound		
Alkalinity [mval/l]	Station 1	14	3.60	1.02	0.27	3.01	4.19	1.90	5.60
	Station 2	14	3.70	0.86	0.23	3.20	4.19	2.35	5.60
	Total	28	3.65	0.93	0.18	3.29	4.01	1.90	5.60
Total Hardness [mval/l]	Station 1	14	12.36	5.91	1.58	8.95	15.78	6.03	19.60
	Station 2	14	12.50	5.76	1.54	9.17	15.83	6.07	19.20
	Total	28	12.43	5.73	1.08	10.21	14.65	6.03	19.60
Total organic carbon (TOC) [mg/l]	Station 1	14	12.11	0.92	0.24	11.58	12.63	10.67	13.48
	Station 2	14	11.64	1.03	0.28	11.05	12.24	9.00	13.14
	Total	28	11.87	0.99	0.19	11.49	12.26	9.00	13.48
Seston [mg/l]	Station 1	14	3.62	1.35	0.36	2.84	4.40	1.80	6.00
	Station 2	14	3.62	1.88	0.50	2.53	4.71	1.20	7.60
	Total	28	3.62	1.61	0.30	3.00	4.24	1.20	7.60
Biological oxygen demand (BOD <sub>5</sub> ) [mg O <sub>2</sub> /l]	Station 1	14	5.79	4.57	1.22	3.15	8.43	0.28	13.60
	Station 2	14	5.11	4.36	1.17	2.59	7.63	0.26	14.10
	Total	28	5.45	4.40	0.83	3.75	7.16	0.26	14.10
Chemical oxygen demand (COD) [mg O <sub>2</sub> /l]	Station 1	14	11.64	5.40	1.44	8.52	14.75	4.87	23.40
	Station 2	14	12.06	5.15	1.38	9.09	15.03	5.87	23.41
	Total	28	11.85	5.18	0.98	9.84	13.86	4.87	23.41



Table 9. ANOVA of water quality parameters (Alkalinity, Total Hardness, Total organic carbon (TOC), Seston, Biological oxygen demand (BOD<sub>5</sub>), Chemical oxygen demand (COD-Mn) at both sites during the observing period (2017-2022).

		Sum of				
		Squares	df	Mean Square	F	Sig.
Alkalinity [mval/l]	Between groups	.070	1	.070	.079	.781
	Within groups	23.165	26	.891		
	Total	23.235	27			
Total Hardness [mval/l]	Between groups	.137	1	.137	.004	.950
	Within groups	886.536	26	34.098		
	Total	886.674	27			
Total organic carbon (TOC) [mg/l]	Between groups	1.500	1	1.500	1.577	.220
	Within groups	24.728	26	.951		
	Total	26.228	27			
Seston [mg/l]	Between groups	.000	1	.000	.000	.995
	Within groups	69.842	26	2.686		
	Total	69.842	27			
Biological oxygen demand (BOD <sub>5</sub> ) [mg o <sub>2</sub> /l]	Between groups	3.244	1	3.244	.162	.690
	Within groups	519.262	26	19.972		
	Total	522.505	27			
Chemical oxygen demand (COD-Mn) [mgC/l]	Between groups	1.252	1	1.252	.045	.834
	Within groups	723.562	26	27.829		
	Total	724.814	27			

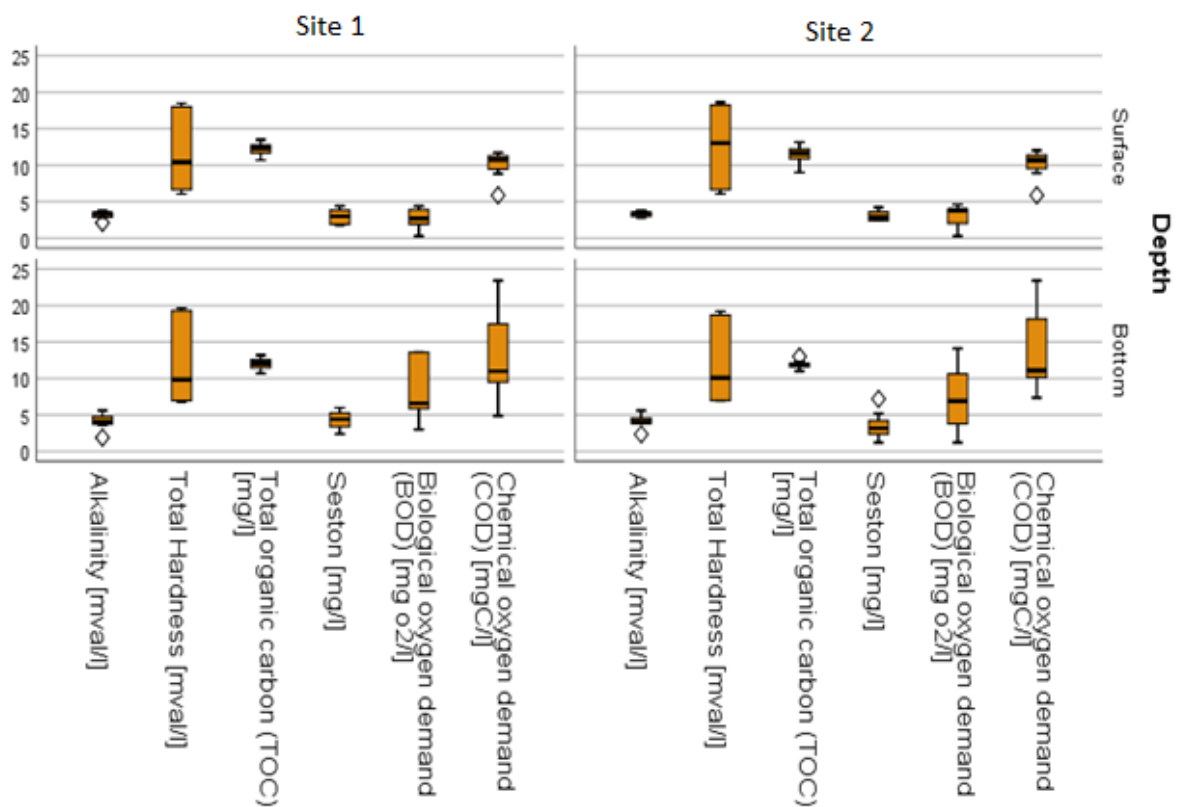


Figure 9. Mean of water quality parameters (Alkalinity, Total Hardness, Total organic carbon (TOC), Seston, Biological oxygen demand (BOD<sub>5</sub>), Chemical oxygen demand (COD-Mn) for both of Świąte lake research sites during the observing period (2017-2022).

The electrolytic conductivity (EC) of the Świąte lake waters in year 2018, varied from 558 to 724  $\mu\text{S}/\text{cm}$ , which over exceeding the parameters for a eutrophic reservoir (200 to 400  $\mu\text{S}/\text{cm}$ ). While in year 2020, the value of conductivity increased to be in range of 720 to 892  $\mu\text{S}/\text{cm}$ , this concerns the increase of the mineral content in the water body. During the spring circulation/turn-over (April 2022), EC values were almost uniform through the water column for whole lake waters and ranged between 777 and 782  $\mu\text{S}/\text{cm}$ .

During year 2018, the water chloride ( $\text{Cl}^-$ ) concentration varied from 43.0 to 115.0 mg Cl/l, the recorded value in year 2020 ranged between 55 and 58 mg Cl/l. Chloride concentration over than 15 mg Cl/l, indicates that the lake receives pollutants from the groundwater and the surface runoff according to the classification of (Mackie et. al., 2022; Olszewski and Paschalski, 1959).

The descriptive analysis of the water mineral content [Iron (Fe), Manganese (Mn), Chloride (Cl<sup>-</sup>), Calcium (Ca<sup>2+</sup>), Magnesium (Mg<sup>2+</sup>) and Sulphate (SO<sub>4</sub><sup>2-</sup>)] at both research sites of the lake demonstrate at (Tab. 10). The statistical analysis (ANOVA) reveals that there is not significant difference (P>0.05) in the water minerals content during the observing period (Tab.11). The surface water at both sites has similar levels of minerals, and the deep water for both the sites has similar mineral content. Deep layer of water has a little higher minerals content compared with the surface water (Fig. 10).

Table 10. Descriptives analysis of water mineral content at both research sites during the observing period (2017-2022).

		N	Mean	Std. Deviation	Std. Error	95% Confidence Interval for Mean		Min.	Max.
						Lower Bound	Upper Bound		
Iron (Fe) [mg/l]	Site 1	14	0.06	0.08	0.02	0.01	0.11	0.01	0.22
	Site 2	14	0.06	0.06	0.02	0.03	0.10	0.01	0.17
	Total	27	0.06	0.07	0.01	0.03	0.09	0.01	0.22
Manganese (Mn) [mg/l]	Site 1	14	0.58	0.69	0.18	0.19	0.98	0.05	1.91
	Site 2	14	0.60	0.65	0.17	0.23	0.98	0.09	1.78
	Total	28	0.59	0.66	0.12	0.34	0.85	0.05	1.91
Chloride (Cl) [mg/l]	Site 1	14	48.78	18.18	4.86	38.28	59.27	5.90	59.00
	Site 2	14	49.11	18.20	4.86	38.60	59.62	6.00	59.00
	Total	28	48.94	17.85	3.37	42.02	55.86	5.90	59.00
Calcium (Ca <sup>2+</sup> ) [mg/l]	Site 1	14	90.26	36.16	9.67	69.38	111.14	7.26	121.89
	Site 2	14	89.82	34.86	9.32	69.70	109.95	7.75	112.20
	Total	28	90.04	34.85	6.59	76.53	103.56	7.26	121.89
Magnesium (Mg <sup>2+</sup> ) [mg/l]	Site 1	14	-1.70	43.41	11.60	-26.76	23.37	-103.73	20.90
	Site 2	14	-2.27	43.25	11.56	-27.24	22.70	-104.02	18.40
	Total	28	-1.98	42.52	8.04	-18.47	14.50	-104.02	20.90
Sulphate (SO <sub>4</sub> <sup>2-</sup> ) [mg/l]	Site 1	12	90.11	68.84	19.87	46.37	133.85	0.00	210.00
	Site 2	12	98.19	71.06	20.51	53.04	143.34	0.00	210.00
	Total	24	94.15	68.54	13.99	65.21	123.09	0.00	210.00

Table 11. ANOVA test for water minerals at both research sites during the observing period (2017-2022).

		Sum of				
		Squares	df	Mean Square	F	Sig.
Iron (Fe) [mg/l]	Between Groups	.000	1	.000	.046	.832
	Within Groups	.127	25	.005		
	Total	.127	26			
Manganese (Mn) [mg/l]	Between Groups	.003	1	.003	.006	.938
	Within Groups	11.629	26	.447		
	Total	11.632	27			
Chloride (Cl) [mg/l]	Between Groups	.756	1	.756	.002	.962
	Within Groups	8601.013	26	330.808		
	Total	8601.769	27			
Calcium (Ca <sup>2+</sup> ) [mg/l]	Between Groups	1.347	1	1.347	.001	.974
	Within Groups	32796.111	26	1261.389		
	Total	32797.459	27			
Magnesium (Mg <sup>2+</sup> ) [mg/l]	Between Groups	2.297	1	2.297	.001	.972
	Within Groups	48808.810	26	1877.262		
	Total	48811.107	27			
Sulphate (SO <sub>4</sub> <sup>2-</sup> ) [mg/l]	Between Groups	392.042	1	392.042	.080	.780
	Within Groups	107666.918	22	4893.951		
	Total	108058.960	23			

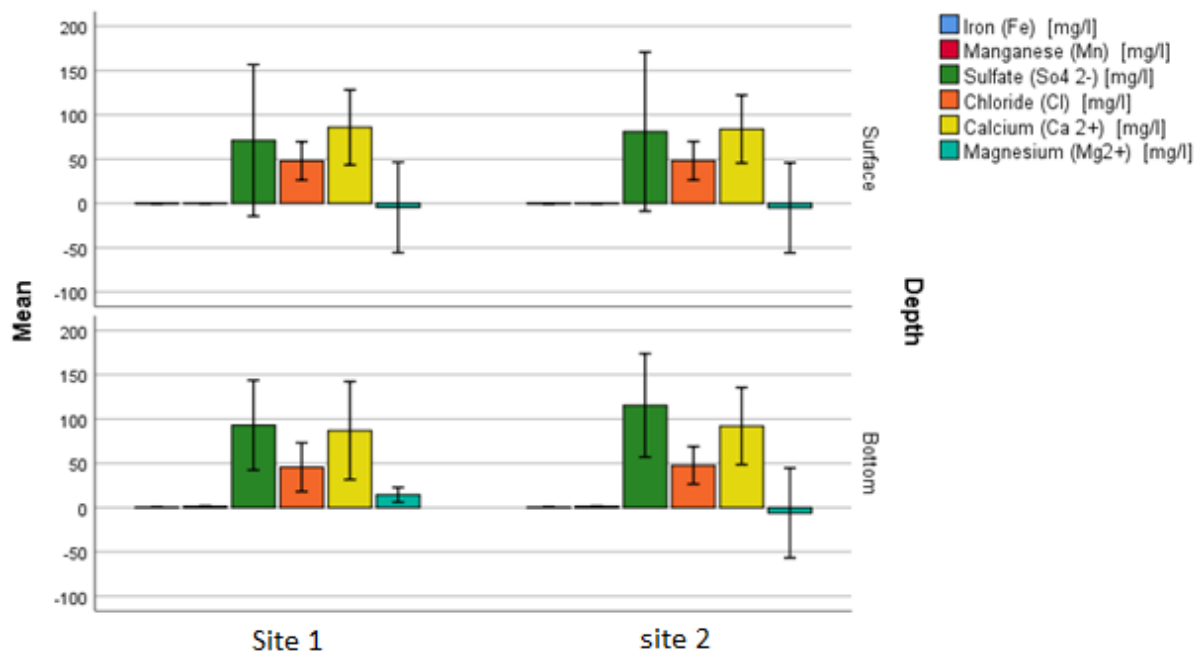


Figure 10. Mean of minerals content of the surface and deep waters for both research sites in Świątę lake during the observing period (2017-2022).

The trophic status index (TSI) Świątę lake before the installation of the pipelines system classify the lake as an eutrophic reservoir (Tab. 12). Phosphorus-TSI (TSI<sub>TP</sub>) for the inflow zone (Site nu.2), showed that the water at this section ranked as hypertrophic one.

Table 12. Trophic State Index (TSI) of Świątę lake for 27<sup>th</sup> August 2020.

TSI Index	Site nu. 1	Site nu. 2
TSI <sub>TP</sub>	68	71
TSI <sub>chl a</sub>	52	56
TSI <sub>SD</sub>	50	51
TSI <sub>TN</sub>	61	61

During summer stagnation of year 2022, an improve of all TSI indexes with a new range that could classify of Świątę lake as an oligotrophic reservoir. Visibility-TSI (TSI<sub>SD</sub>) and chlorophyll a-TSI (TSI<sub>chl a</sub>) indexes of lake waters have been improved from eutrophic to mezotrophic water during the operation of the pipelines system, in case of comparing summer stagnation of 2020 to the same period from year 2022. TSI<sub>TN</sub> stayed almost stable before and after the restoration installations (Tab.13).

Table 13. Trophic State Index (TSI) of Świątę lake for 01<sup>st</sup> September 2022.

<b>TSI Index</b>	<b>Site nu. 1</b>	<b>Site nu. 2</b>
<b>TSI<sub>TP</sub></b>	61	66
<b>TSI<sub>chl a</sub></b>	40	39
<b>TSI<sub>SD</sub></b>	47	46
<b>TSI<sub>TN</sub></b>	62	62

#### 4.4 Sediment analysis

##### 4.4.1 Sediments Water content

Slightly higher water content found in the upper layer (0-5 cm) of the sediment than the bottom one. The median percentage of the sedimentary interstitial water before the operation of the pipelines system in sediment samples for was 86.6 %, with a standard division (SD) of 1.14. The median percentage of the water content in sediment samples for the years 2021 & 2022 after the operation of the pipelines system was 83.5 %, with a standard division (SD) of 5.92. This is for the whole 10 cm depth of the sample.

##### 4.4.2 Sedimentary interstitial water and water-over-sediment

The average total nitrogen (TN) concentration in the sediments interstitial waters for all sampling points during the summer stagnation of 2020, was around 20 mg N/l and the maximum was 29.68 mg N/l. The difference between its concentration in the upper layer of sediments (0-5 cm), and the bottom one (6-10 cm), was relatively small with 2 mg N/l variance, except for two sampling points. The ammoniacal nitrogen (N-NH<sub>4</sub>) was the dominant form with an average of 16.9 mg N/l, while the organic form average value was 4.57 mg N/l.

It was noticed that, in contrast to interstitial waters, concentrations in water over the sediments decreased along with the summer stagnation, which may result from the uneven supply of organic matter under the conditions of its anaerobic decomposition.

During 2020 summer stagnation -June to August-, the organic form of phosphorus was the predominant one among sedimentary interstitial water total phosphorus (TN). Its average concentration was approximately 4.5 mg P/l, forming a shear percentage over than 60% of the TP. The concentrations of total phosphorus in the water-over-sediments was much lower than the interstitial water. The two deepest bottoms of the lake -sites 1 and 2-, were distinguished clearly by a higher concentrations.

By the end of the research period the average contents of TP, TN and TOC were 0.56 mg P/l, 3.68 mg N/l and 15.53 mg C/l, respectively. The organic form of nitrogen ( $N_{org}$ ) dominant the TN percentage, while both forms of phosphorus; mineral ( $PO_4^{3-}$ ) and organic ( $P_{org}$ ) were relatively equal. The sedimentary interstitial water average content of phosphorus (TP) was 4.62 mg P/l with more existence of the mineral form ( $PO_4^{3-}$ ), whereas its average nitrogen content (TN) was 19.05 mg N/l. The ammoniacal nitrogen form ( $NH_4$ ) was more than organic form ( $N_{org}$ ), differ than the situation in water-over-sediment. Both TP and TN concentrations increase with the depth of sediment, this could be concluded by an existence of more TP and TN content in the bottom layer than the upper one.

The average of the total organic carbon (TOC) in the sedimentary interstitial water was 102.69 mg C/l, and in contrary to TP and TN, the upper layer showed higher content than the bottom one.

#### **4.4.2.1 Phosphorous**

During the summer stagnation (June – August 2021), the organic form of phosphorus was the predominant one among sedimentary interstitial water total phosphorus. Its average concentration was approximately 4.5 mg P/l, forming a shear percentage over than 60% of the TP. The concentrations of total phosphorus in the water-over-sediments were much lower than the interstitial water. The two deepest bottoms of the lake sites nu. 1 & 2 were distinguished clearly by a higher concentration.

The descriptive analysis indicates a mean change of TP concentration of the sedimentary water between the measurement intervals, where it reaches its lowest value in April 2022, and return to increase by the end of the year but stills lower than value before the pipelines system operation (Tab. 14). Besides its clearly shown that mean of TP variable decreased slightly prior to the operation of the pipelines system and in the last sampling season, statistically the means varied significantly ( $p < 0.05$ ) for all five intervals -sampling seasons-, even if the change was not big (Tab. 15).

The TP concentration in water-over-sediment at sampling point nu. 5 -close to inflow pipes outlet-, was the highest value during December 2022' measurement, followed by point nu. 3, which is in the outflow zone (Fig. 11). Until April 2022, the trend and efficiency to reduce the overall TP concentration in sediment water is noticeable. Besides that, the TP concentration

in water-over-sediment increased in December 2022, its concentration in the interstitial water for both layers declined. As can be seen in the (Fig.s 12 & 13) the concentration of phosphorus in individual research points, especially in site nu. 1, decreased during the research period. The same applies to points 1-3 of the 0-5 cm layer, in other points this tendency is not clearly visible.

The TP concentration in the water-over-sediment is considered low compared to the existing content of it, at the sediment layer below. The direction of P intensity through the sedimentary water indicates that the sediment retains P.

Table 14. Descriptive statistics of Total Phosphorus TP (mg/l) from 8 points for five-time intervals.

	N	Mean	Std. Deviation	Std. Error Mean
June 2020	24	4.65	3.08	.62
August 2020	24	4.99	3.27	.66
June 2021	24	3.14	2.27	.46
April 2022	24	.95	1.39	.28
December 2022	24	3.26	2.03	.41

Table 15. T-test statistics of Total Phosphorus TP (mg/l) from 8 points for five-time intervals.

	t	df	Sig. (2-tailed)	Mean Difference	95% CI	
					Lower	Upper
June 2020	7.400	23	.000	4.65	3.35	5.96
August 2020	7.480	23	.000	4.99	3.61	6.38
June 2021	6.774	23	.000	3.14	2.18	4.11
April 2022	3.361	23	.003	.95	.36	1.55
December 2022	7.882	23	.000	3.26	2.41	4.12



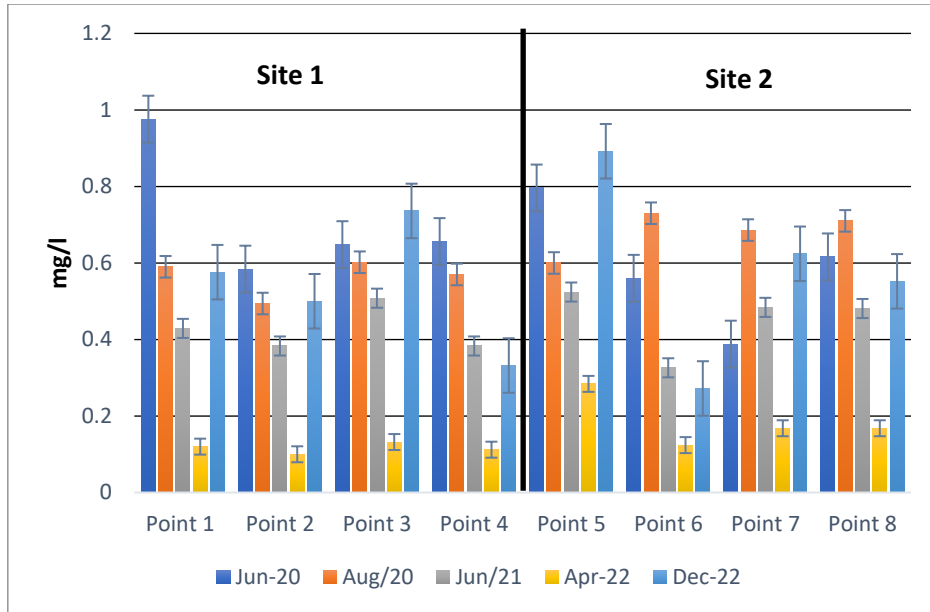


Figure 11. Total phosphorous concentration (mg/l) in water-over-sediments (0-10 cm), for five-time intervals during the research period (2020-2022).

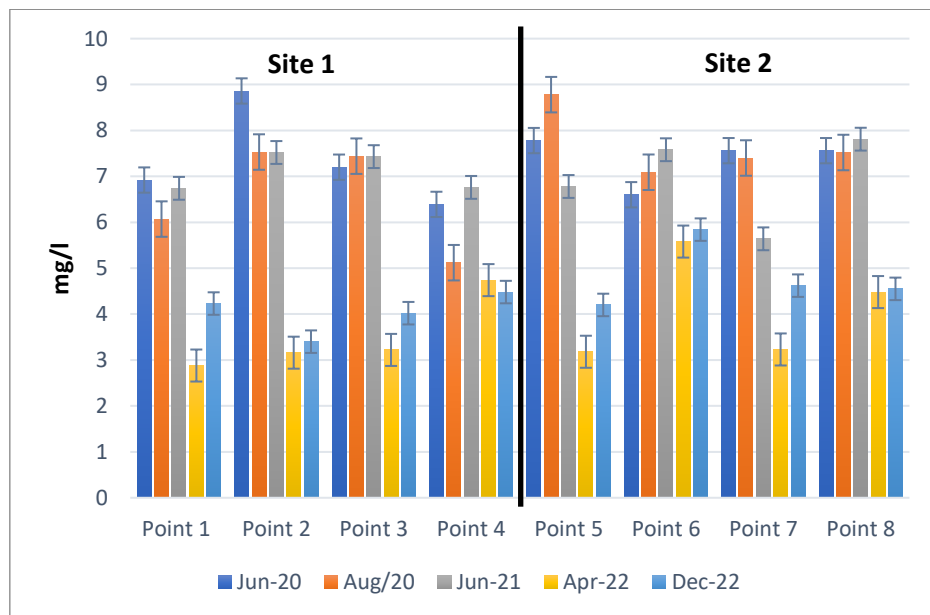


Figure 12. Sedimentary interstitial water total phosphorous concentration (mg/l) in the upper layer (0-5 cm), for five-time intervals during the research period (2020-2022).

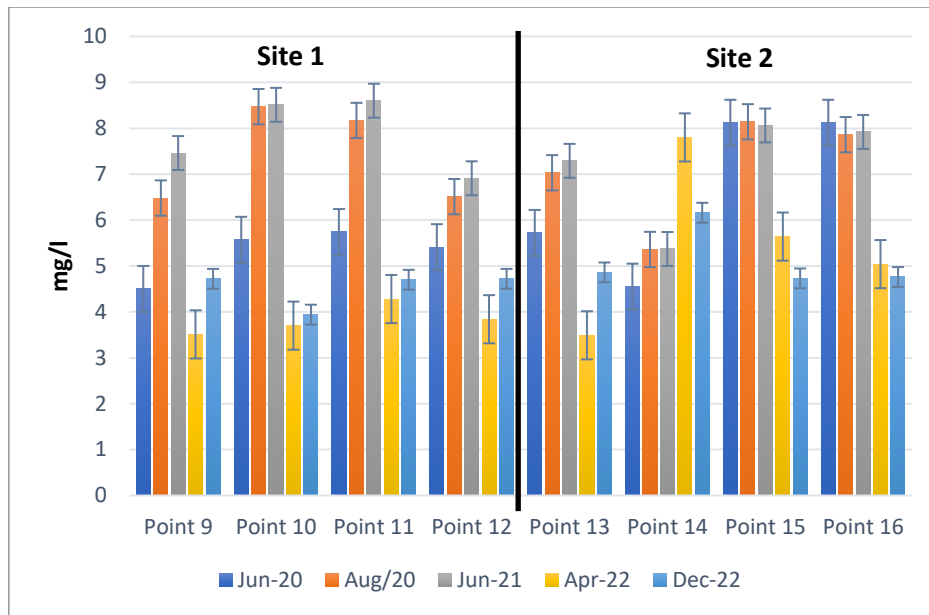


Figure 13. Sedimentary interstitial water total phosphorous concentration (mg/l) in the bottom layer (5-10 cm), for five-time intervals during the research period (2020-2022).

Descriptive analysis of phosphate ( $\text{PO}_4^{3-}$ ) variable shows that sedimentary groups mean ranged closely during the measurement intervals (Tab. 16). The t-test, proof that there is a significant means difference ( $p < 0.05$ ) between intervals, with a t-value far from the zero value (Tab. 17). Water-over-sediment during December 2022' sampling season, showed higher phosphate ( $\text{PO}_4$ ) concentration than the analyzed one in April 2022 (Fig. 14). Anyhow, December 2022' measurement, indicating lower phosphate concentration than what was before the operation of the pipelines system. Compared to the exist phosphate concentration in both layers of the sediment, water-over-sediment has less phosphate concentration ( $\text{max} \leq 0.4 \text{ mg/l}$ ).

Results of phosphate analysis of the interstitial water showed that phosphate ( $\text{PO}_4^{3-}$ ) concentration through the upper layer of sediments (0-5 cm) various for the sampling points with less concentration in year 2022 than that it was during years 2020 and 2021 (Fig. 15). There is more stored phosphate in the deeper layer of sediments than the upper one (Fig. 16). Interstitial water of the bottom layer for the last sampling season has less phosphate concentration than the observed one in April 2022, April recorded the highest obtained values. The distribution Phosphate intensity through the whole segment of sediments (water & sediments) showed that there is a higher concentration of phosphate in the interstitial water than water-over-sediment, which indicate that sediments retain this vital

element( $\text{PO}_4^{3-}$ ). There is more phosphate content at the outflow zone than the inflow zone.

Table 16. Descriptive statistics of phosphate ( $\text{PO}_4^{3-}$ ) in (mg/l) from 8 points for five-time intervals.

	N	Mean	Std. Deviation	Std. Error Mean
June 2020	24	1.69	.99	0.20
August 2020	24	1.60	.91	0.19
June 2021	24	1.85	1.21	0.25
April 2022	24	1.91	1.42	0.29
December 2022	24	1.65	1.07	0.22

Table 17. T-test statistics of phosphate ( $\text{PO}_4^{3-}$ ) in (mg/l) from 8 points for five-time intervals.

	t	df	Sig. (2-tailed)	Mean Difference	95% CI Lower	95% CI Upper
June 2020	8.388	23	.000	1.69	1.27	2.11
August 2020	8.568	23	.000	1.60	1.21	1.99
June 2021	7.481	23	.000	1.85	1.33	2.36
April 2022	6.595	23	.000	1.91	1.31	2.51
December 2022	7.564	23	.000	1.65	1.20	2.10

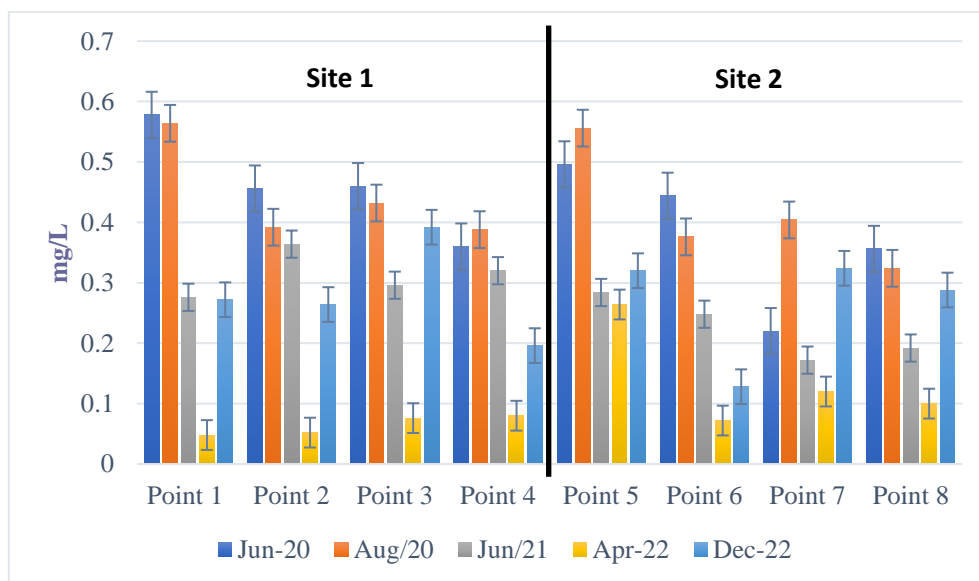


Figure 14. Phosphate concentration (mg/l) in water-over-sediment (0-10 cm), for five-time intervals during the research period (2020-2022).

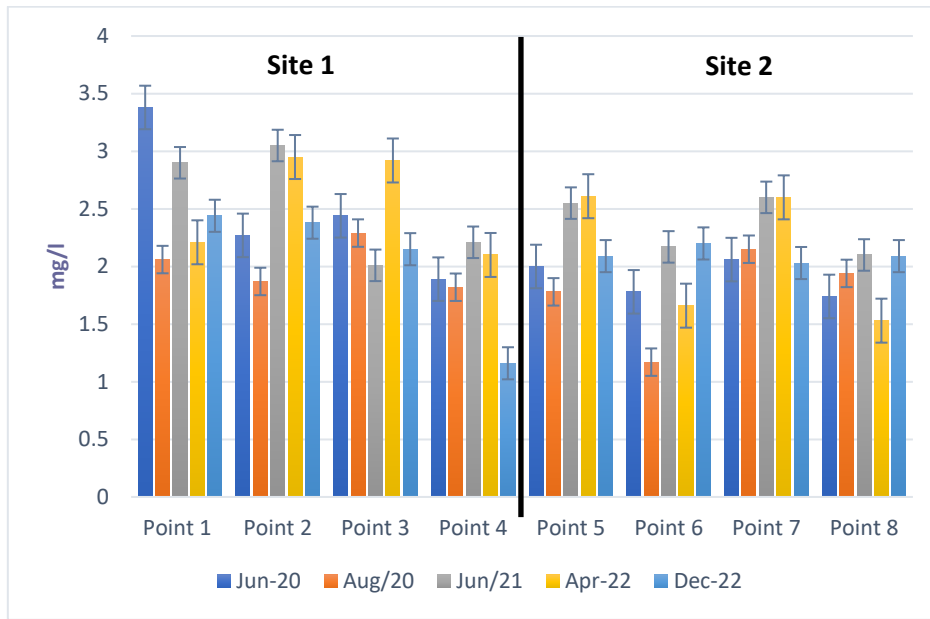


Figure 15. Sedimentary interstitial water phosphate concentration (mg/l) in the upper layer (0-5 cm), for five-time intervals during the research period (2020-2022).

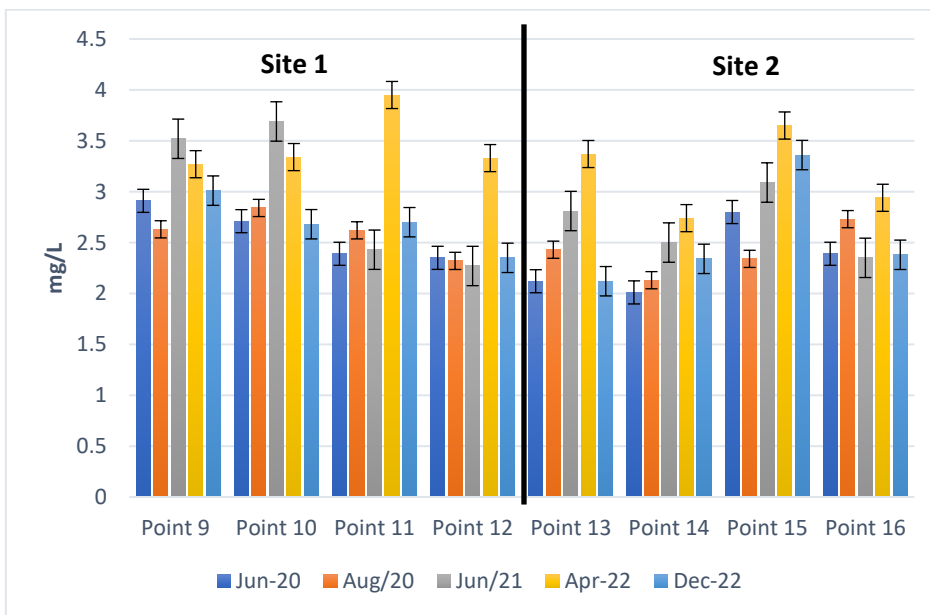


Figure 16. Sedimentary interstitial water phosphate concentration (mg/l) in the bottom layer (5-10 cm), for five-time intervals during the research period (2020-2022).

The mean variability of the organic phosphorus ( $P_{org}$ ) for the sedimentary waters varied significantly to record the lowest value in April 2022 and the highest in December 2022 (Tab. 18). The variation of organic phosphorous concentration in water over and inside of the segments, it could be deduced that all eight points over a period of three years varied significantly ( $p < 0.05$ ) (Tab. 19). During April 2022, concentration of organic phosphorus was the lowest for all sedimentary waters in all points. This value increased in December 2022, to be the highest organic phosphorus concentration in water-over-sediment at the inflow pipes outlet (Point nu. 5) (Fig. 17). The overall concentrations were reduced significantly in the year 2022, compared to analyzed  $P_{org}$  values before the restoration measurement. In general,  $P_{org}$  concentration at the outflow zone (Points nu. 1-4), is less than the one in inflow zone (Points nu. 5-8) for all sedimentary waters (Fig.s 18 & 19).

Table 18. Descriptive statistics of Organic Phosphorous (mg/l) from 8 points for five-time intervals.

	N	Mean	Std. Deviation	Std. Error Mean
June 2020	24	2.96	2.29	.46
August 2020	24	3.39	2.45	.50
June 2021	24	4.99	3.36	.68
April 2022	24	2.87	2.22	.45
December 2022	24	7.95	5.21	1.06

Table 19. T-test statistics of Organic Phosphorous (mg/l) from 8 points for five-time intervals.

	t	Df	Sig. (2-tailed)	Mean Difference	95% CI Lower	95% CI Upper
June 2020	6.347	23	.000	2.96	2.00	3.93
August 2020	6.757	23	.000	3.39	2.35	4.42
June 2021	7.263	23	.000	4.99	3.57	6.41
April 2022	6.321	23	.000	2.87	1.93	3.81
December 2022	7.468	23	.000	7.95	5.74	10.15

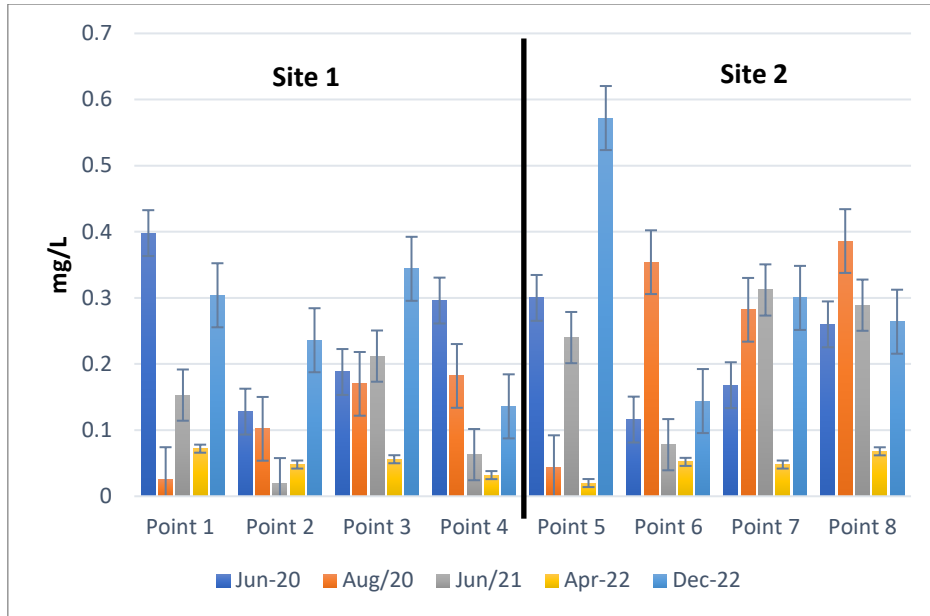


Figure 17. Organic phosphorous concentration (mg/l) in water-over-sediment (0-10 cm), for five-time intervals during the research period (2020-2022).

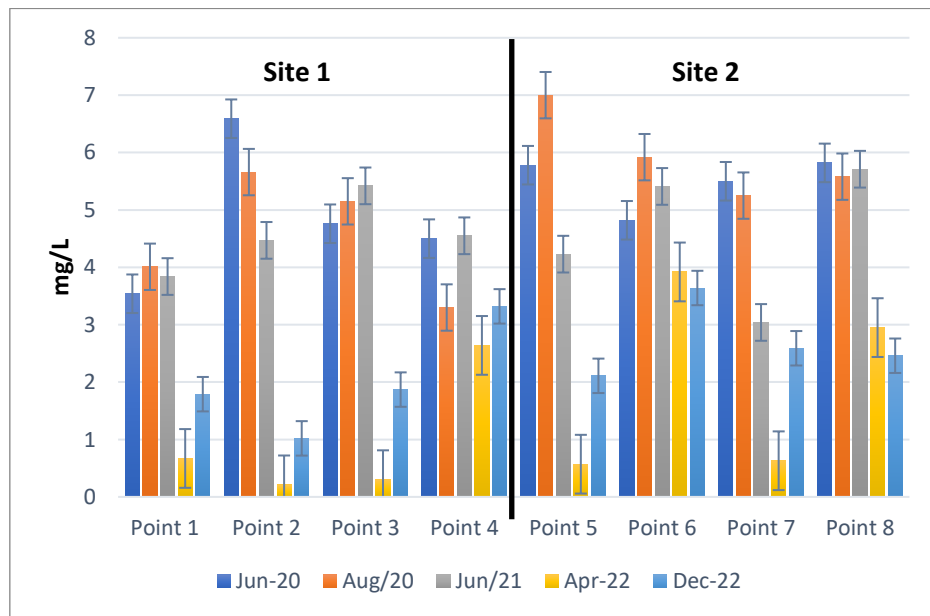


Figure 18. Sedimentary interstitial water organic phosphorous concentration (mg/l) in the upper layer (0-5 cm), for five-time intervals during the research period (2020-2022).

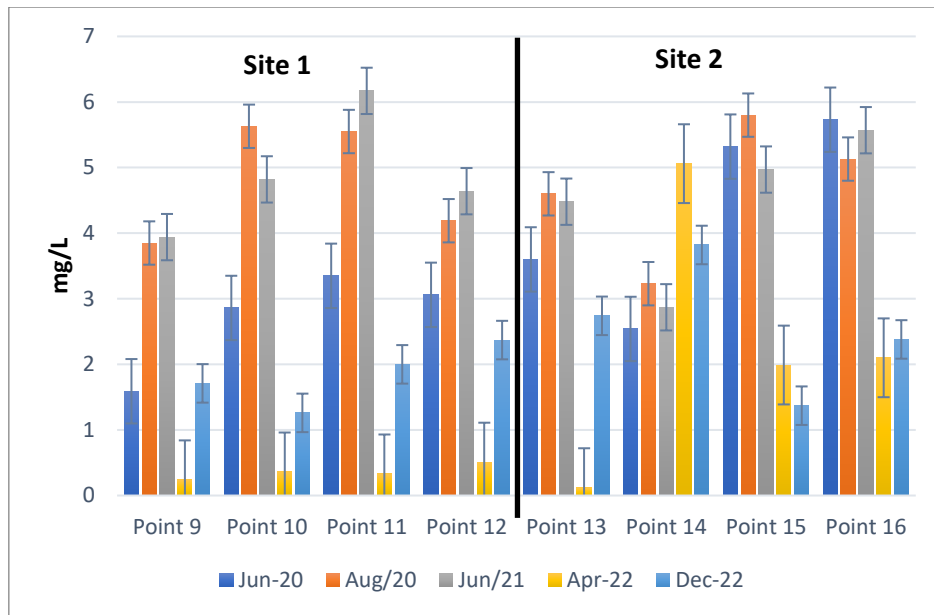


Figure 19. Sedimentary interstitial water organic phosphorous concentration (mg/l) in the bottom layer (5-10 cm), for five-time intervals during the research period (2020-2022).

The average total nitrogen (TN) concentration for the interstitial waters for all sampling points during the summer stagnation of 2020, was around 20 mg N/l and the maximum was 29.68 mg N/l. The difference between its concentration in the upper layer of sediments (0-5 cm), and the bottom one (5-10 cm), was relatively small with 2 mg N/l variance, except for two sampling points. The ammonium nitrogen (N-NH<sub>4</sub>) was the dominant form with an average of 16.9 mg N/l, while the organic form average value was 4.57 mg N/l.

The means between sample-groups of the sedimentary water analysis did not change noticeably (Tab. 20). Sedimentary waters for all eight points over a period of three years varied significantly ( $p < 0.05$ ) (Tab. 21).

Highest value of the total nitrogen (TN) in water-over-sediment has been recorded during August 2022' measurement (Fig. 20). Compared to the period before the operation of the pipelines system, the overall content of the total nitrogen (TN) declined during year 2022' sampling seasons (Fig.s 21 & 22). However, trend lines for total N within the sediment show that it did not change significantly and was almost the same for all sites of observation.

Table 20. Descriptive statistics of total nitrogen (mg/l) from 8 points for five-time intervals.

	N	Mean	Std. Deviation	Std. Error Mean
June 2020	24	14.57	7.79	1.59
August 2020	24	16.67	6.98	1.42
June 2021	24	15.76	6.85	1.39
April 2022	24	13.46	7.67	1.56
December 2022	24	13.64	44.52	9.08

Table 21. T-test statistics of total nitrogen (mg/l) from 8 points for five-time intervals.

	T	df	Sig. (2-tailed)	Mean Difference	95% CI Lower	95% CI Upper
June 2020	5.288	23	.000	3.73	2.27	5.19
August 2020	6.962	23	.000	3.87	2.72	5.03
June 2021	8.272	23	.000	5.46	4.09	6.82
April 2022	6.017	23	.000	2.88	1.89	3.87
December 2022	8.205	23	.000	13.92	10.41	17.44

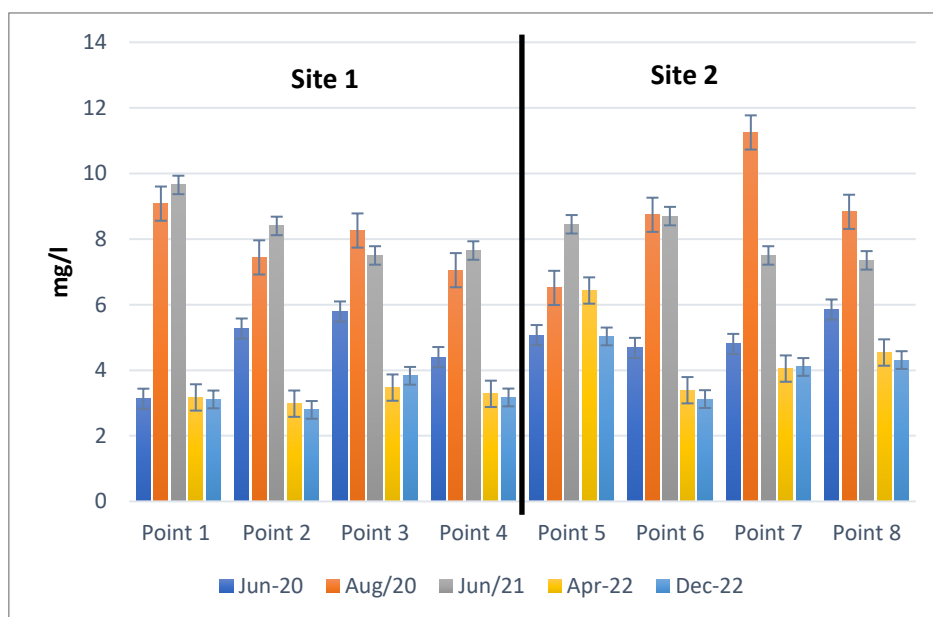


Figure 20. Total nitrogen concentration (mg/l) in water-over-sediments (0-10 cm), for five-time intervals during the research period (2020-2022).



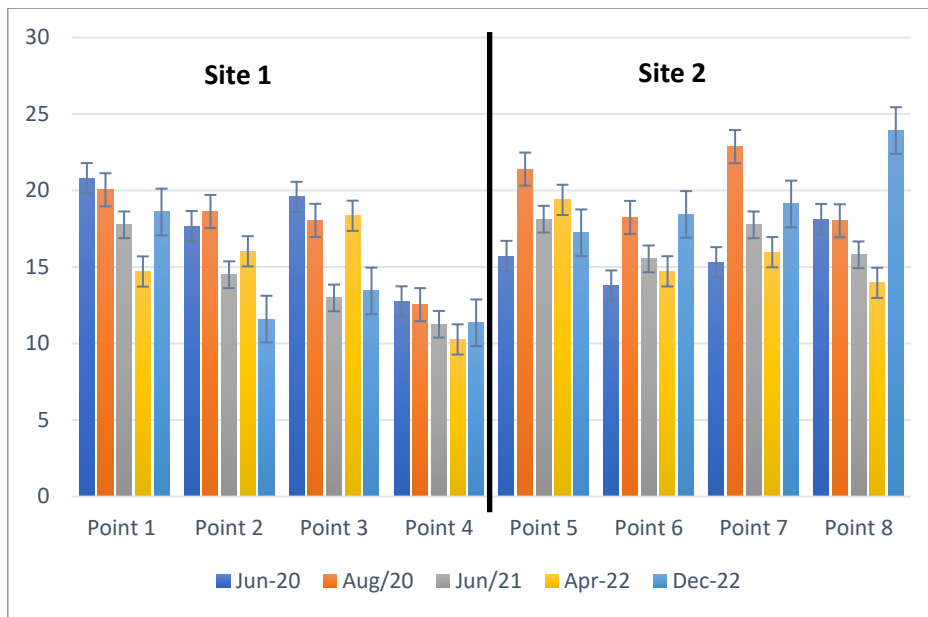


Figure 21. Sedimentary interstitial water total nitrogen concentration (mg/l) in the upper layer (0-5 cm), for five-time intervals during the research period (2020-2022).

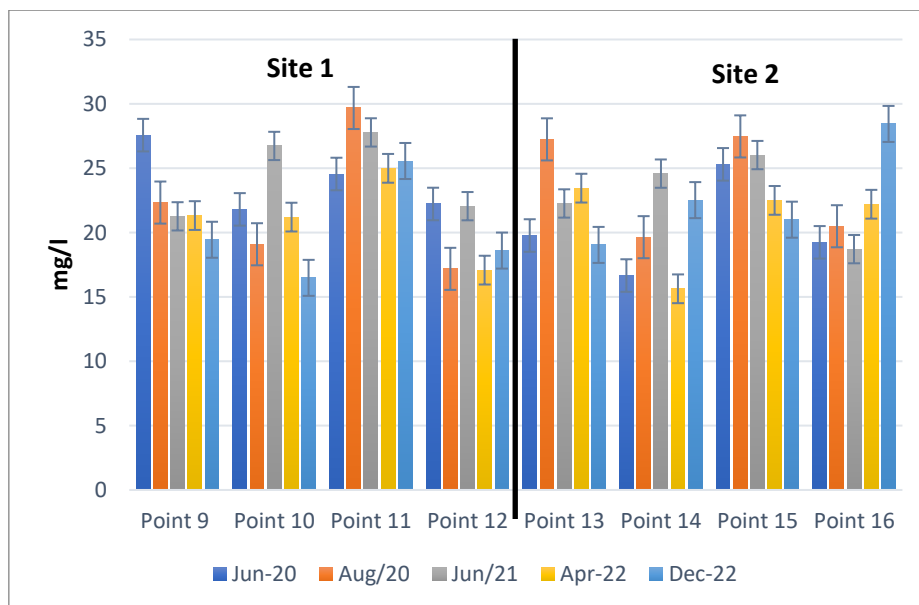


Figure 22. Sedimentary interstitial water total nitrogen concentration (mg/l) in the bottom layer (5-10 cm), for five-time intervals during the research period (2020-2022).

a) Ammonium (NH<sub>4</sub><sup>+</sup>)

Ammonium (NH<sub>4</sub><sup>+</sup>) concentration mean of sample-groups of the sedimentary water analysis decreased the half in sedimentary waters from August 2020, until December 2022 (Tab. 22). T-test indicates that the mean varied significantly ( $p < 0.05$ ) between intervals for all groups (Tab. 23).

The highest concentration of ammonium (NH<sub>4</sub><sup>+</sup>) was reported in August 2020, and the least values were recorded during December 2022. All points have almost the same concentration during the same season (June 2020 and June 2021) (Fig.s 23, 24 & 25).

Table 22. Descriptive statistics of NH<sub>4</sub><sup>+</sup> (mg/l) from 8 points for five-time intervals.

	N	Mean	Std. Deviation	Std. Error Mean
June 2020	24	10.84	6.09	1.24
August 2020	24	12.79	5.88	1.20
June 2021	24	10.30	6.98	1.42
April 2022	24	10.58	6.66	1.36
December 2022	24	5.97	4.35	.88

Table 23. T-test statistics of NH<sub>4</sub><sup>+</sup> (mg/l) from 8 points for five-time intervals.

	t	df	Sig. (2-tailed)	Mean Difference	95% CI	
					Lower	Upper
June 2020	8.711	23	.000	10.84	8.26	13.41
August 2020	10.65	23	.000	12.79	10.30	15.27
June 2021	7.227	23	.000	10.30	7.35	13.25
April 2022	7.777	23	.000	10.58	7.7658	13.3942
December 2022	6.722	23	.000	5.97	4.13	7.81

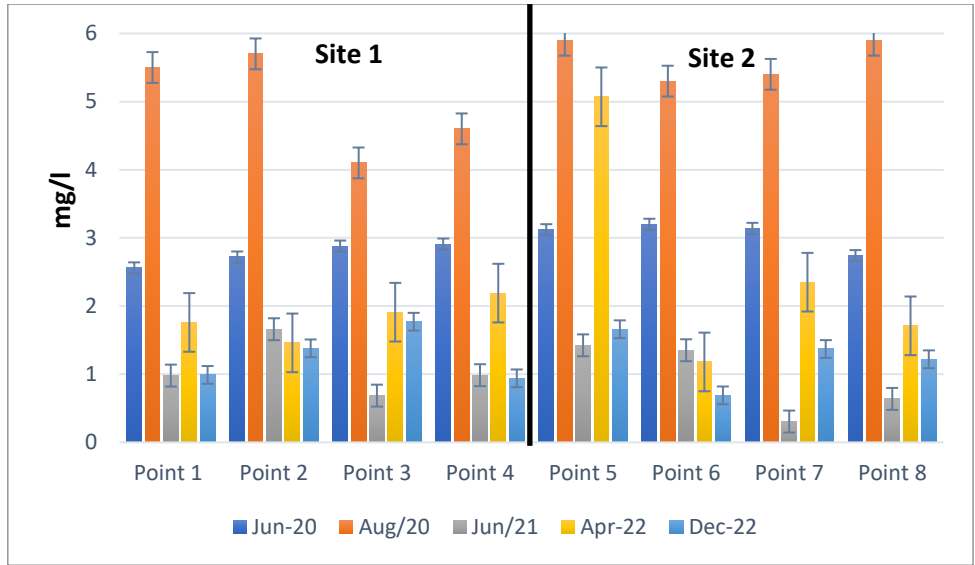


Figure 23. Ammonium concentration (mg/l) in water over sediments (0-10 cm), for five-time intervals during the research period (2020-2022).

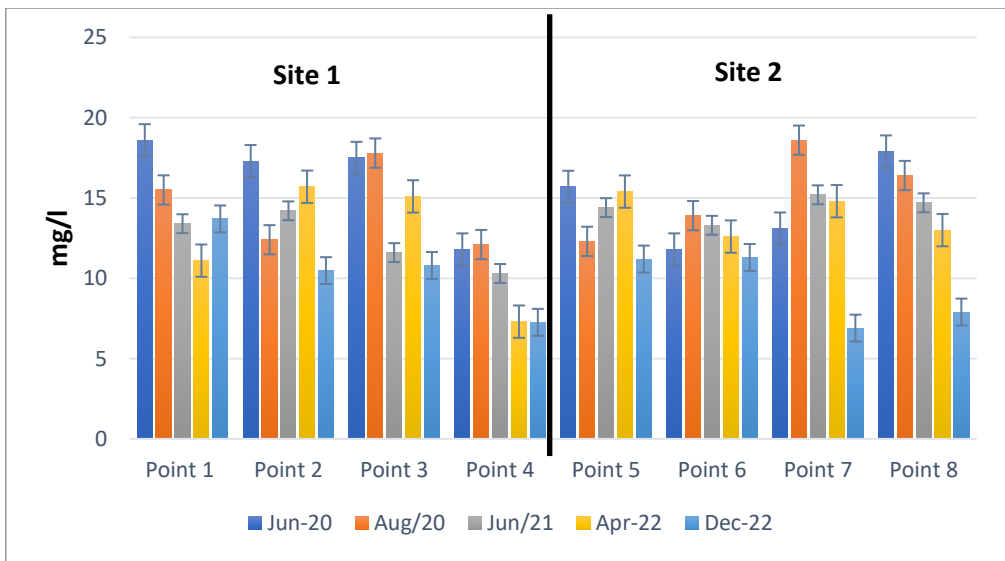


Figure 24. Sedimentary interstitial water ammonium concentration (mg/l) in the upper layer (0-5 cm), for five-time intervals during the research period (2020-2022).

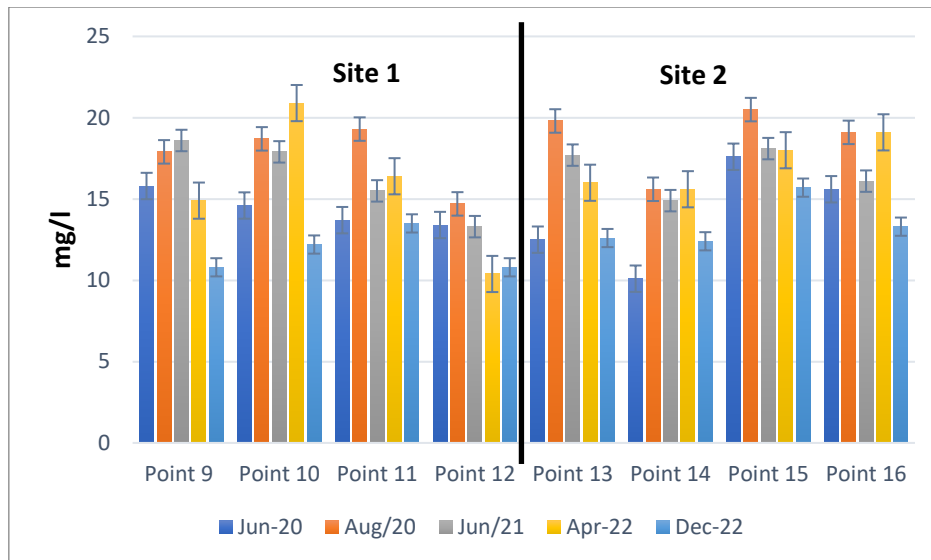


Figure 25. Sedimentary interstitial water ammonium concentration (mg/l) in the bottom layer (5-10 cm), for five-time intervals during the research period (2020-2022).

Descriptive statistics of the organic nitrogen ( $N_{org}$ ), show that the lowest mean value for sedimentary waters sample-groups obtained in April 2022 (2.88 mg/l), while the highest one observed in December 2022 (13.92 mg/l) (Tab. 24). Means of sedimentary waters varied significantly ( $p < 0.05$ ), between measurement seasons, (Tab. 25). Organic nitrogen concentration in water-over-sediment was the highest during 2021, and the lowest during 2022 (Fig. 26) In the interstitial water of both layers, the organic nitrogen concentration recorded the highest values during December 2022, besides that its content was the lowest during April measurement from the same year (Fig.s 27 & 28). Point 8 expressed the highest level of organic nitrogen concentration in both layers during December 2022. There is more organic nitrogen concentration in the interstitial waters than the water-over-sediment, these values increase in the inflow zone.

Table 24. Descriptive statistics of organic nitrogen (mg/l) from 8 points for five-time intervals.

	N	Mean	Std. Deviation	Std. Error Mean
June 2020	24	3.73	3.45	.70
August 2020	24	3.87	2.72	.55
June 2021	24	5.46	3.23	.66
April 2022	24	2.88	2.34	.48
December 2022	24	13.92	8.31	1.69

Table 25. T-test statistics of organic nitrogen (mg/l) from 8 points for five-time intervals.

	T	df	Sig. (2-tailed)	Mean Difference	95% CI Lower	95% CI Upper
June 2020	5.288	23	.000	3.73	2.27	5.19
August 2020	6.962	23	.000	3.87	2.72	5.03
June 2021	8.272	23	.000	5.46	4.09	6.82
April 2022	6.017	23	.000	2.88	1.89	3.87
December 2022	8.205	23	.000	13.92	10.41	17.44

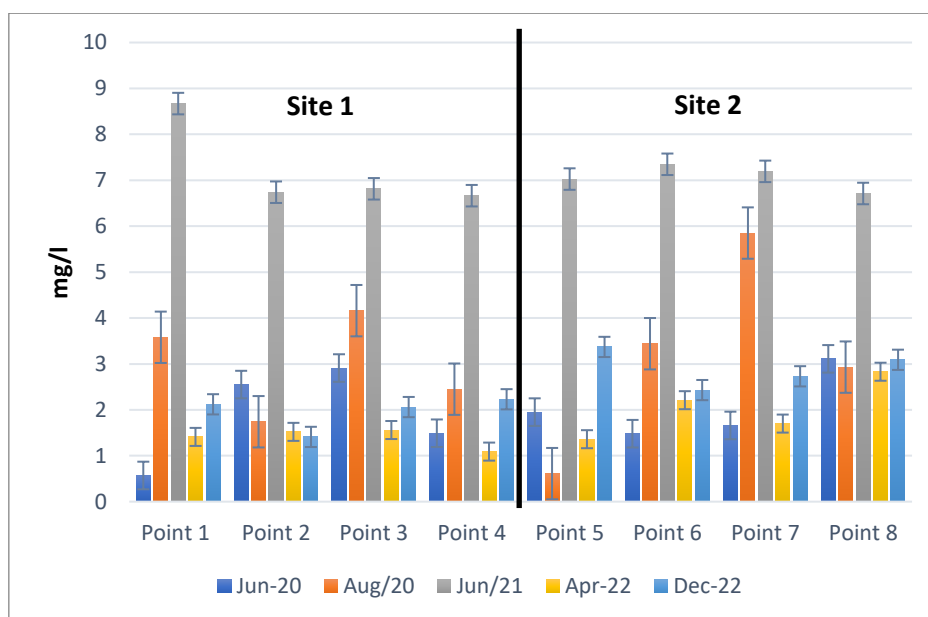


Figure 26. Organic nitrogen concentration (mg/l) in water over sediments (0-10 cm), for five-time intervals during the research period (2020-2022).

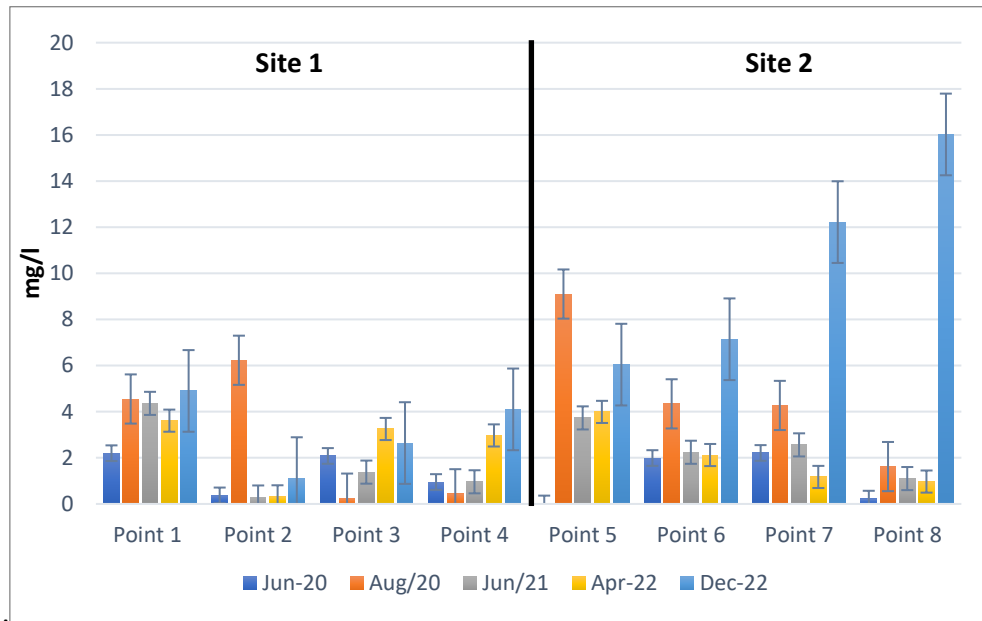


Figure 27. Sedimentary interstitial water organic nitrogen concentration (mg/l) in the upper layer (0-5 cm), for five-time intervals during the research period (2020-2022).

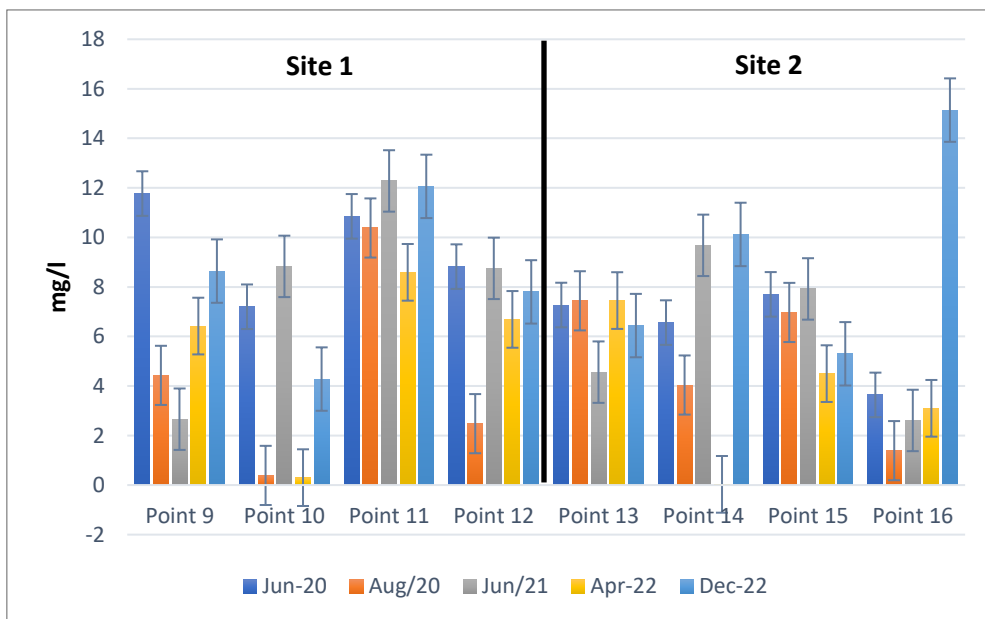


Figure 28. Sedimentary interstitial water organic nitrogen concentration (mg/l) in the bottom layer (5-10 cm), for five-time intervals during the research period (2020-2022).

By the end of the research period December 2022, the average concentration of TP, TN and TOC were 0.56 mg P/l, 3.68 mg N/l and 15.53 mg C/l, respectively. The organic form of nitrogen ( $N_{org}$ ) dominated the TN amount, while both forms of phosphorus; mineral ( $PO_4^{3-}$ ) and organic ( $P_{org}$ ) were relatively equal. The sedimentary interstitial water average concentration of phosphorus (TP) was 4.62 mg P/l with more existence of the mineral form ( $PO_4^{3-}$ ), whereas its average nitrogen concentration (TN) was 19.05 mg N/l. The ammoniacal nitrogen form ( $NH_4$ ) was more than organic form ( $N_{org}$ ), differ than the situation in water-over-sediment. Both TP and TN concentrations increase with the depth of sediment, this could be concluded by an existence of more TP and TN concentration in the bottom layer than the upper one.

The average of the total organic carbon (TOC) in the sedimentary interstitial water was 102.69 mg C/l, and in contrary to TP and TN, the upper layer showed higher content than the bottom one. The means of the total organic carbon (TOC) content in sedimentary waters declined by the time of the research period (Tab. 26).

T-test was used to compare the means of TOC concentration at all eight points, and it confirms that groups mean varied significantly ( $p < 0.05$ ) through intervals of measurements for all sampling points (Tab. 27). TOC, in water-over-sediment is much less the interstitial one for both layers, these results stayed almost similar during the research period (Fig. 29). The interstitial water content of TOC varies with a general declining trend and content of the organic matter at the upper layer (Fig. 30). The highest recorded value of TOC has been observed in deeper layer (Layer 2), in point nu. 6 during April 2022, which declined in December 2022 to half for the same point (Fig. 31).

Table 26. Descriptive statistics of TOC (mg/L) from 8 points for five-time intervals.

	N	Mean	Std. Deviation	Std. Error Mean
June 2020	24	148.05	304.78	62.21
August 2020	24	94.42	60.96	12.44
June 2021	24	81.42	50.16	10.24
April 2022	24	79.49	52.59	10.73
December 2022	24	73.64	44.52	9.08

Table 27. T-test statistics of TOC (mg/L) from 8 points for five-time intervals.

	t	Df	Sig. (2-tailed)	Mean Difference	95% CI Lower	95% CI Upper
June 2020	2.380	23	.026	148.05	19.35	276.75
August 2020	7.588	23	.000	94.42	68.68	120.16
June 2021	7.951	23	.000	81.42	60.23	102.60
April 2022	7.405	23	.000	79.49	57.28	101.70
December 2022	8.103	23	.000	73.64	54.84	92.44

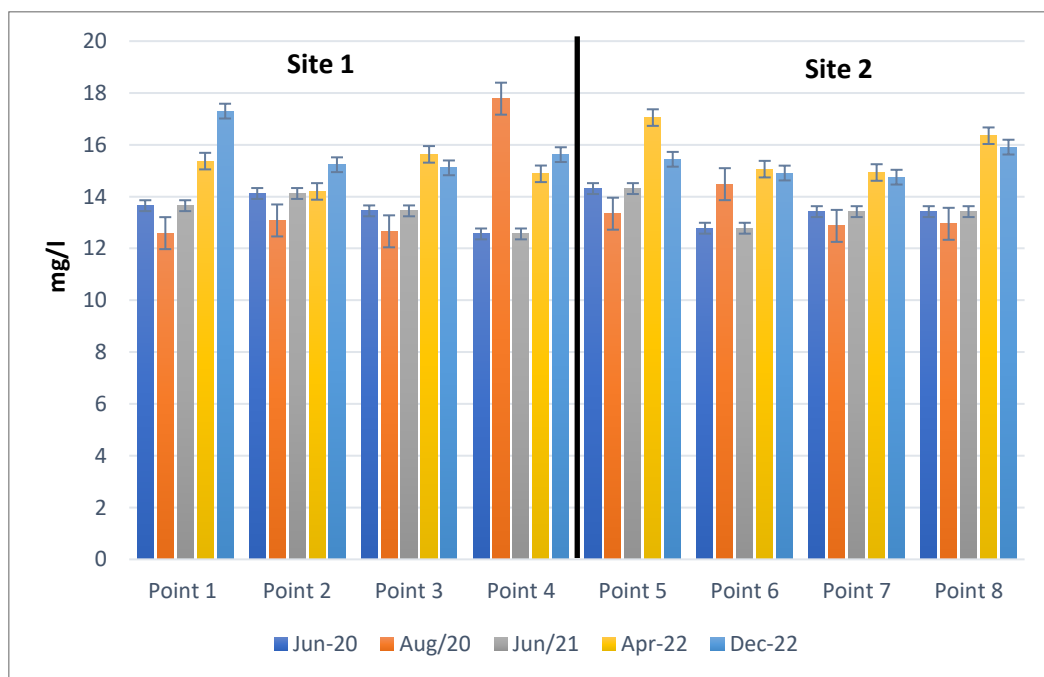


Figure 29. Total organic carbon (TOC) concentration (mg/l) in water over sediments (0-10 cm), for five-time intervals during the research period (2020-2022).



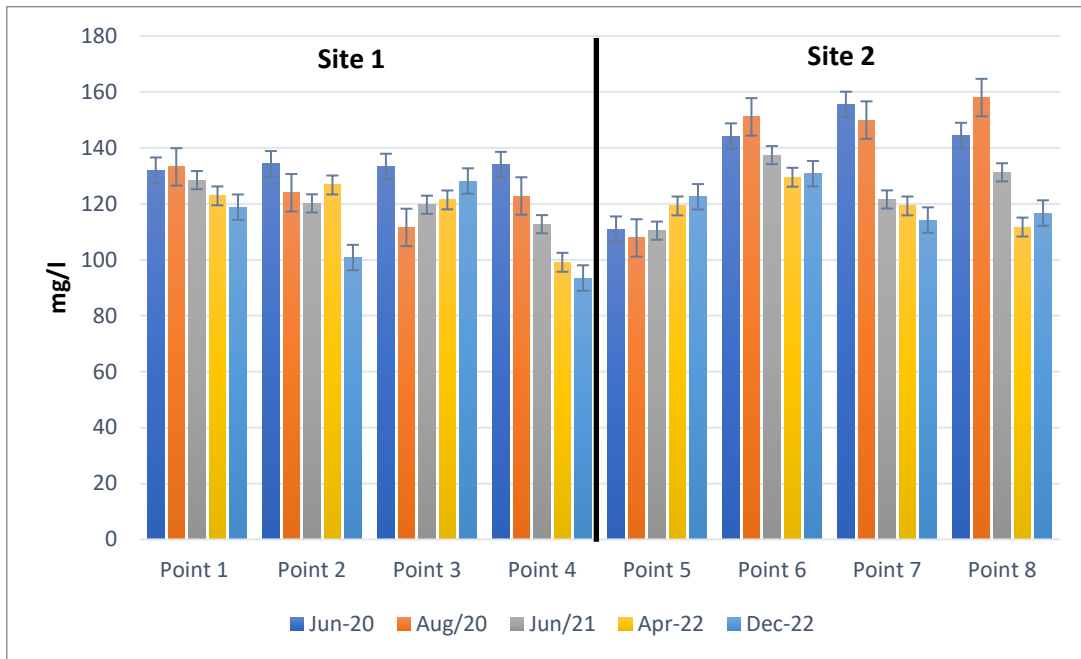


Figure 30. Sedimentary interstitial water total organic carbon (TOC) concentration (mg/l) in the upper layer (0-5 cm), for five-time intervals during the research period (2020-2022).

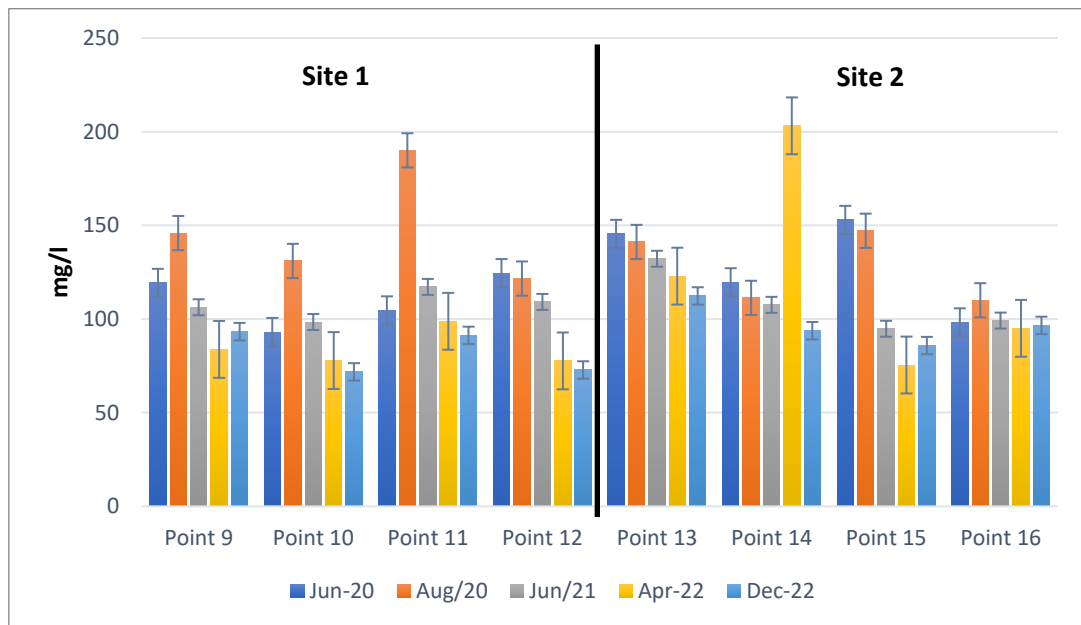


Figure 31. Sedimentary interstitial water total organic carbon (TOC) concentration (mg/l) in the bottom layer (5-10 cm), for five-time intervals during the research period (2020-2022).

#### 4.4.3 Chemical composition of the sediment

The chemical composition analysis of lake bottom sediments shows a slightly order change of the sediment-forming elements during the operation of the pipelines system, where silicon (Si), organic matter (O. M.), calcium (Ca), carbonate ( $\text{CO}_3^{-2}$ ), aluminium (Al) and magnesium (Mg) are the main constituent elements of the sediment (Tab. 30). The statistical analysis tables and figures are in the (Appendix).

Table 30. The rank order sediment chemical composition and elements average percentage for both layers of research sites in-lake during the research period (2020-2022).

Rank order		<u>1</u>	<u>2</u>	<u>3</u>	<u>4</u>	<u>5</u>	<u>6</u>	<u>7</u>	<u>8</u>	<u>9</u>	<u>10</u>
June, 2020	upper layer	SiO <sub>2</sub>	O. M.	CaO	MgO	CO <sub>3</sub> <sup>-2</sup>	Al <sub>2</sub> O <sub>3</sub>	N	P <sub>2</sub> O <sub>5</sub>	Fe <sub>2</sub> O <sub>3</sub>	MnO
		54.69%	18.33%	5.72%	5.23%	3.97%	3.31%	1.00%	0.25%	0.24%	0.05%
	Bottom layer	SiO <sub>2</sub>	O. M.	CO <sub>3</sub> <sup>-2</sup>	CaO	MgO	Al <sub>2</sub> O <sub>3</sub>	N	Fe <sub>2</sub> O <sub>3</sub>	P <sub>2</sub> O <sub>5</sub>	MnO
		56.12%	17.38%	7.02%	6.60%	4.18%	3.03%	0.89%	0.41%	0.20%	0.02%
August, 2020	upper layer	SiO <sub>2</sub>	O. M.	CO <sub>3</sub> <sup>-2</sup>	CaO	MgO	Al <sub>2</sub> O <sub>3</sub>	N	Fe <sub>2</sub> O <sub>3</sub>	P <sub>2</sub> O <sub>5</sub>	MnO
		57.20%	18.05%	6.31%	5.20%	4.16%	3.12%	0.88%	0.34%	0.17%	0.06%
	Bottom layer	SiO <sub>2</sub>	MO	CO <sub>3</sub> <sup>-2</sup>	CaO	MgO	Al <sub>2</sub> O <sub>3</sub>	N	Fe <sub>2</sub> O <sub>3</sub>	P <sub>2</sub> O <sub>5</sub>	MnO
		53.47%	16.26%	12.57%	5.14%	3.56%	3.41%	0.72%	0.29%	0.24%	0.05%
June, 2021	upper layer	SiO <sub>2</sub>	O. M.	CO <sub>3</sub> <sup>-2</sup>	Al <sub>2</sub> O <sub>3</sub>	MgO	CaO	N	Fe <sub>2</sub> O <sub>3</sub>	P <sub>2</sub> O <sub>5</sub>	MnO
		57.60%	16.88%	6.96%	5.40%	4.01%	1.66%	0.99%	0.87%	0.55%	0.15%
	Bottom layer	SiO <sub>2</sub>	O. M.	CO <sub>3</sub> <sup>-2</sup>	MgO	Al <sub>2</sub> O <sub>3</sub>	CaO	N	Fe <sub>2</sub> O <sub>3</sub>	P <sub>2</sub> O <sub>5</sub>	MnO
		58.31%	15.11%	6.80%	5.75%	5.21%	2.04%	1.86%	0.96%	0.53%	0.14%
December, 2022	upper layer	SiO <sub>2</sub>	O. M.	CO <sub>3</sub> <sup>-2</sup>	MgO	Al <sub>2</sub> O <sub>3</sub>	CaO	N	Fe <sub>2</sub> O <sub>3</sub>	P <sub>2</sub> O <sub>5</sub>	MnO
		60.47%	20.33%	5.03%	4.87%	3.09%	2.57%	0.91%	0.61%	0.56%	0.12%
	Bottom layer	SiO <sub>2</sub>	O. M.	MgO	CO <sub>3</sub> <sup>-2</sup>	Al <sub>2</sub> O <sub>3</sub>	CaO	N	Fe <sub>2</sub> O <sub>3</sub>	P <sub>2</sub> O <sub>5</sub>	MnO
		54.48%	16.06%	9.08%	6.70%	5.39%	1.18%	0.81%	0.79%	0.55%	0.16%

Silicon (Si) is the major component of sediments, and it was measured as silicon dioxide ( $\text{SiO}_2$ ) in sediment composition analysis. Its mean content share percentage of sediments for both layers ranged between 53.47% and 60.47%. The variation of silicon dioxide ( $\text{SiO}_2$ ) share percentages for all sampling points over the research period statistically varied significantly ( $p < 0.05$ ). Silicon (Si) content percentage in sediments was the lowest value during June 2020, which increased after two months to record the highest values. The fluctuations of silicon percentage content during the research period indicate that the pipelines system does not effect on lake income flow from silicon and sediment.

The second largest component of bottom sediments was organic matter, and its occurrence was inversely proportional to the silica ( $\text{SiO}_2$ ) content. Which means that its occurrence increases at the deeper parts of the lake, with higher levels in the upper layer of sediments (1-5 cm). Organic matter (O. M.) means share percentage in sediments ranged between 18.33 -20.33 % D. M. at the upper layer and between 15.11 %– 20.33 % D. M. at the bottom layer of sediments during the research period. The highest mean value has been recorded in August 2020. The performed t-test indicates that groups of samples statistically varied significantly ( $p < 0.05$ ). The organic matter content in both sediment layers during the research period were similar and slightly varied. It also shows the relative concentration at eight points of study. Initially during June 2020, the average mean O. M. concentration for all samples from both layers was around 18.86%. This increased during August 2020' measurement to 24.53 % at point nu. 1, to be the highest observed value in the upper layer of sediments.

T-test results of carbonate ( $\text{CO}_3^{2-}$ ) from t-test for the four-time intervals (sampling seasons) as Groups, which each contains 16 variables from the 8 sampling points, indicate that both sediment layers and both research sites inside the lake (site nu. 1 & 2) carbonate content varied significantly ( $p < 0.05$ ). Carbonate ( $\text{CO}_3^{2-}$ ) percentage in the upper layer varied slightly, but all the time intervals were higher than June 2020's measurement for the rest of the research period. Point nu. 4 at the outflow zone (site nu. 1), recorded the highest levels of carbonates ( $\text{CO}_3^{2-}$ ) for both layers throughout the research period.

The percentage share of nitrogen (N) content in the dry matter of sediments does not exceed 1% of the D. M., with slightly higher concentration in the upper layer of the sediments. The mean share percentage of total nitrogen (TN) in sediments recorded the highest value in June 2021' measurement time-interval over the whole research period, that found to be less than

1%. Groups of samples varied significantly ( $p < 0.05$ ) during the four-time intervals of the research period regarding their total nitrogen (TN) content. The upper layer of sediments shows a higher nitrogen (TN) content percentage than the bottom one, although the difference is little. The general trend of total nitrogen (TN) content in the upper layer of sediments is decreasing over time with more total nitrogen (TN) content in the inflow zone. The bottom layer of sediments shows a greater amount of nitrogen over the research period, especially at the inflow zone. The highest concentration was found at point nu. 7 in the upper layer, which subsequently decreased over time.

The mean of magnesium (Mg) share percentage in sediments, standard deviation and the standard error mean increased by the end of research period (Tab. 42). Magnesium (Mg) content percentage varied significantly ( $p < 0.05$ ) between the groups of samples with a wider difference range of the confidence interval.

Descriptive statistics of the analyzed phosphorus (P) content in sediments indicate that the mean of phosphorus (P) content percentage doubled twice after the operation of the pipelines system due to the mineral binding of it as a consequence of the enhanced redox potential. Phosphorus (P) content percentage for all the eight sampling points varied significantly ( $p < 0.05$ ) over the research period. Both layers of sediment showed a multiplication of their phosphorus (P) content after pipelines system operation.

Despite phosphorus (P) content percentage increase, both token measurements after the operation of the pipelines system refer to stable phosphorus (P) content with a slight increase by the last measurement.

The iron (Fe) mean percentage content in sediments during the research period was less than 1 %. Iron has been measured as iron (III) oxide / ferric oxide ( $\text{Fe}_2\text{O}_3$ ); all the sampling points varied significantly ( $p < 0.05$ ) regarding their content of iron. Both layers showed a drastically increase of their iron content percentage after the operation of the pipelines system, with more iron existence in the inflow zone. The increased amount of iron in sediment during the sampling season in June 2021, could be explained by the spring ice melt. This high iron content percentage stayed until the end of the research period (2020-2022).

Aluminum was present in a higher concentration at Pintus estuary side. The mean percentage share of aluminum (Al) content in sediments recorded the highest value during June 2021, but stayed similar by the end of the research period comparing to founds before the operation

of the pipelines system. All the sampling points statistically varied significantly ( $p < 0.05$ ) regarding its aluminum content. Aluminum content share percentage in sediments varies at both layers and for all points. The highest aluminum content was found at upper layer of point nu. 5 during December 2021' sampling measurement, while the point nu. 4 possessed the highest aluminum content at the bottom layer. In general, all inflow zone showed increased content value of aluminum with ameliorate trend during the research period. This refers to the transport of allochthonous materials as Pintus tributary fetches.

The mean share percentage of calcium (Ca) in sediments decreased dramatically after the operation of the pipeline system. Calcium oxide content in sediments varied significantly ( $p < 0.05$ ) between and within the sample's groups for the four-time intervals. At both layers of the sediment and for all sampling points the calcium (Ca) content percentage declined after the operation of pipelines system, point nu. 5 at the upper layer was the only expect.

The upper layer of sediments contains less magnesium (Mg) content than the bottom one, diagrams exhibit that the outflow zone possesses a higher content percentage of magnesium (Mg) especially the bottom layer. The highest magnesium (Mg) content found for the upper layer was at point 4 (outflow zone) before the operation of the pipelines system, which subsequently decreased over the research period. The highest recorded values were for the bottom layer at point nu. 1 and point nu. 2 (entrance of the outflow pipeline), by the end of research period.

Manganese (Mn) means share percentage in sediment increased almost three times than as it was before the operation of the pipelines system and stayed stable. The groups of samples during research period for four-time intervals varied significantly ( $p < 0.05$ ) in their manganese content. The highest content of manganese (Mn) was recorded in the upper layer for point nu. 1 (deepest point in the outflow section) of samples from August 2020, the bottom layer for the same point contained much less content of manganese. Analysis of sediments at the inflow zone for the upper layer contains more manganese than the outflow zone.

While it's the opposite regarding the bottom layer of sediment for both of the lake section, where the outflow zone contains more manganese (Mn) than the inflow zone.

#### 4.4.3.1 Phosphorus fractions in sediments

The five fractions of the sedimentary phosphorus (P-fractions) arranged according to the ease of release from sediments; readily available P ( $\text{NH}_4\text{Cl-P}$ ), redox-sensitive P (BD-P), metal oxide bound P (NaOH-P), calcium bound P (HCl-P) and the not reactive permanently bound P (res-P). The metal oxide bound P (NaOH-TP), has fractionated for; aluminum bound P (NaOH-rP) and organic matter bound P (NaOH-nrP).

Phosphorus fractions rank does not change by the end of the research period as it was before the operation of the pipelines system (NaOH-P > HCl-P > BD-P > res-P >  $\text{NH}_4\text{Cl-P}$ ). The bounded phosphorus with the organic matter (NaOH-nrP) formed majority of the metal oxide bound P (NaOH-P), despite the double-increased percentage of the bounded phosphorus with the aluminum (NaOH-rP), to form around 20 % of the metal oxide bound P fraction (NaOH-P) by end of the research period.

The main sediment components that are responsible for phosphorus binding were organic matter (NaOH-nrP) and calcium (HCl-P). This is confirmed by the high percentage of phosphorus fractions that are associated with these components in total phosphorus content in the sediment. The bound phosphorus fraction with calcium (HCl-P) percentage of phosphorus content in the sediment for August 2020 ranged between (0.08-16.05%) to drop by the followed year and record a range of (0.54-5.43%), June 2021. While it recorded a range of (9.5-23.91 %) for December 2022. This significant percentage increase of the bounded phosphorus with calcium (HCl-P) could be attributed to the high load of calcium through the Pintus inflow, where Świąte lake showed an ability to absorb calcium ( $\text{Ca}^{+2}$ ), where the carried amounts of them at the inflow were much higher than the discharged. Calcium concentrations for December 2022' measurement for the inflow and outflow were 111.2 and 41.4 mg Ca/l, respectively.

The hardly mobilized fraction of phosphorus (HCl-P) in sediments, can indicate a mineral binding of calcium phosphate in the hypolimnetic water due to the enhanced redox potential at this layer, which precipitate later. A low values of sediments phosphorus content that are easily mobilized fractions labile ( $\text{NH}_4\text{Cl-P}$ ).

The total retained content of phosphorus in sediments (TP), increased twice-fold by the end of the research period (2.57 mg P/g D. M.) compared to measured TP content before the

operation of the pipelines system (1.35 mg P/g D. M.). The lowest analyzed total phosphorus content has obtained during the June 2021' measurement (0.62 mg P/g D. M.) All fractions' groups in sediments varied significantly ( $p < 0.05$ ), regarding of their mean during the four-time intervals of the research period (Appendix).

The main components of sediments responsible for the binding of phosphorus in them were organic matter and calcium, which is confirmed by the high percentage share of phosphorus fractions associated with these components in the total phosphorus. The percentage distribution of sedimentary P-fractions during the four-time intervals of the research period indicates that the metal oxide bound phosphorus (NaOH-P) overwhelmed the rest of other fractions in sediments (Fig. 32).

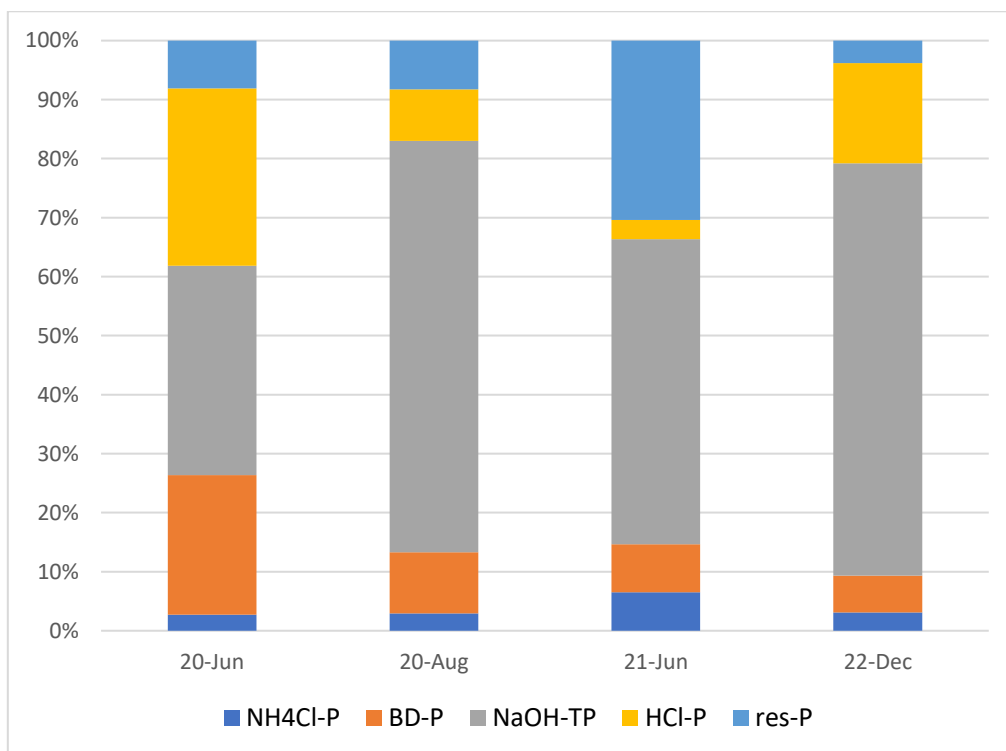


Figure 32. Percentage distribution of phosphorus fractions in sediments during four-time intervals of the research periods (2020-2022).

#### 4.4.4 correlation between sediment components

Correlation analysis of sediments components shows that phosphorous is highly correlated with manganese (Mn), iron (Fe), aluminum (Al) ( $P < 0.01$ ), and positively correlated with magnesium (Mg). Similarly, the organic matter (O.M.) is correlated positively with calcium (Ca) and Aluminum (Al) ( $P < 0.05$ ), while nitrogen (N) is correlated positively with Ca, Al, Mn, and P (Tab. 31).

Sediment components that found to be negatively correlate to each other, are; (P and O.M.), (P and Si), (P and Ca), (Fe and Ca), (Fe and O.M.), (Fe and Si), (Ca and Mg), (Ca and Mn), (Ca and Si), (Mg and O.M.), (Mg and Si), (Mg and N), (Al and O.M.), (Mn and Si), and (N and Si). Full correlation between the whole analyzed sediment components found in (Appendix).

Table 31. Correlations analysis of sediments components.

	Fe <sub>2</sub> O <sub>3</sub> (%)	CaO (%)	MgO (%)	Al <sub>2</sub> O <sub>3</sub> (%)	MnO (%)	O. M. (%)	SiO <sub>2</sub> (%)	P <sub>2</sub> O <sub>5</sub> (%)	N (%)
Fe <sub>2</sub> O <sub>3</sub> (%)	1								
CaO (%)	-.271*	1							
MgO (%)	.243	-.205	1						
Al <sub>2</sub> O <sub>3</sub> (%)	.545**	.145	.002	1					
MnO (%)	.648**	-.489**	.306*	.353**	1				
OM (%)	-.095	.267*	-.113	.261*	-.062	1			
SiO <sub>2</sub> (%)	-.117	-.212	-.271*	-.022	-.070	.128	1		
P <sub>2</sub> O <sub>5</sub> (%)	.576**	-.514**	.209	.403**	.656**	-.153	-.050	1	
N (%)	.195	.079	-.165	.090	.131	-.022	-.102	.140	1

\*. Correlation is significant at the 0.05 level (2-tailed).

\*\* . Correlation is significant at the 0.01 level (2-tailed).



#### 4.4.5 Sediments nutrients ratios

Descriptive statistics of TN:TP mean ratio during the research period for both research sites of Świąte lake was below 16:1, which indicating a mineral binding of P with sediments rather than the organic binding. The maximum TN:TP mean ratio observed at point nu. 6 during June 2020' measurement found to be 20.55 (Tab. 32). These ratios did not vary significantly ( $P>0.05$ ) during the research period, neither between nor within the groups of sediment samples (Tab. 33).

Table 32. Descriptives of TN:TP and O.M.:TN ratios in sediments.

						95% Confidence			
				Std. Deviation		Interval for Mean			
		N	Mean	n	Std. Error	Lower Bound	Upper Bound	Minimum	Maximum
TN:TP	Site 1	32	3.19	3.26	0.58	2.02	4.37	0.62	15.12
	Site 2	32	4.75	4.99	0.88	2.95	6.55	1.47	20.55
	Total	64	3.97	4.25	0.53	2.91	5.04	0.62	20.55
O.M.: TN	Site 1	32	34.64	46.15	8.16	18.00	51.28	1.86	259.95
	Site 2	32	20.65	4.40	0.78	19.07	22.24	13.59	38.58
	Total	64	27.65	33.28	4.16	19.33	35.96	1.86	259.95

Table 33. ANOVA of N:P and O.M.:TN in sediments.

		Sum of Squares	df	Mean Square	F	Sig.
TN:TP	Between Groups	38.860	1	38.860	2.187	.144
	Within Groups	1101.607	62	17.768		
	Total	1140.468	63			
O.M.: TN	Between Groups	3131.297	1	3131.297	2.914	.093
	Within Groups	66628.627	62	1074.655		
	Total	69759.924	63			

The mean value of TN:TP ratio in the inflow zone sediments was found to be higher than the outflow zone, the ratio means of TN:TP varied slightly between sites for the same layer.

In contrast, O.M.:TN mean ratio for the upper layer of sediments at both sites is similar but varied in the bottom layer with higher ratio value at outflow zone (Fig. 33).

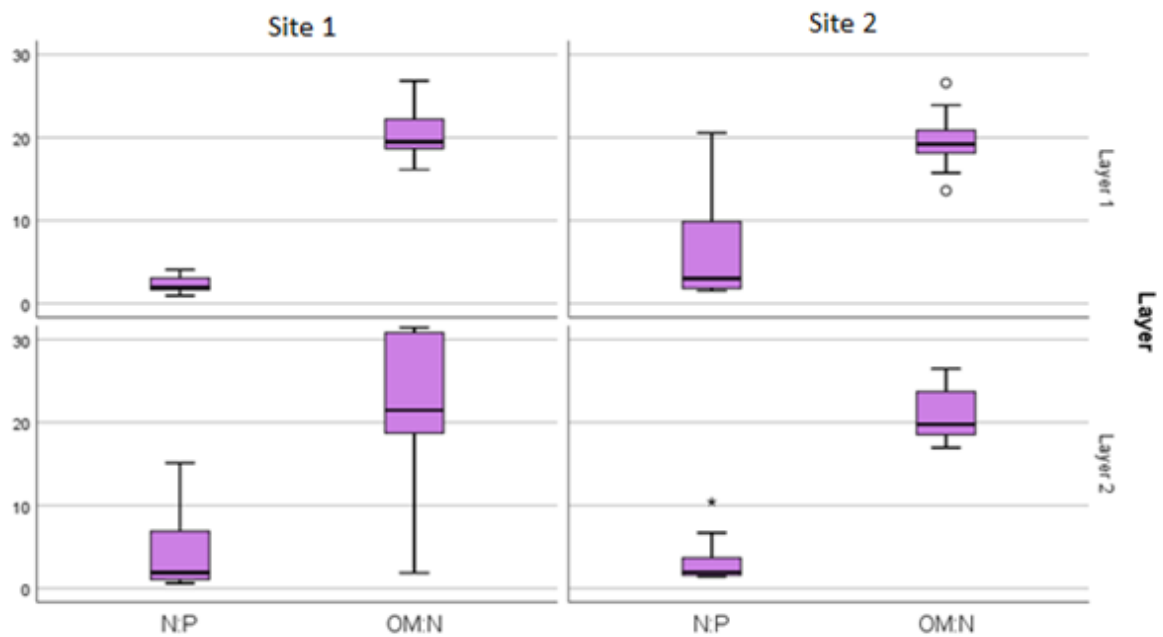


Figure 33. Status of TN:TP and O.M.:TN mean ratios in sediments for the whole research period (2020-2022).

## 4.5 Lake ecosystem

### 4.5.1 Phytoplankton

During the early spring period of year 2018, a small number of phytoplankton of low species diversity was recorded in the lake waters. The dominant group were diatoms of the genus *Cyclotella*, chlorophyta (green algae) and organisms belonging to cyanoprokaryota were present in smaller amounts. While in the following months was a noticeable increase in the species diversity of algae. Until September, when the prevalence of the potentially toxic species of cyanobacteria from the order Oscillatoriales and *Planktothrix* species.

In July of the 2018 year, the presence of *Ceratium hirundinella* (Genus of dinoflagellates) was recorded. This in turn can be related to the large number of mineral substances in the lake's waters, where this species is rarely found in waters rich in organic compounds. Organisms belonging to the Cryptophyceae and Euglenophyta were also determined in the analyzed samples.

A total of 94 taxa of algae (orders, families, genera, species) were determined in 2020 at both research sites before the operation of the pipelines system. Algae taxa distribution as follows; 22 taxa belonging to cyanoprokaryota were, 3 taxa of Chrysophyceae, 13 taxa of Bacillariophyceae, 1 taxon of Cryptophyceae, 3 taxa of Dinophyceae, 50 taxa of Chlorophyceae and 2 taxa of Euglenophyta. All the observed algae belong to common organisms, occurring mostly in the plankton of moderately and more eutrophic waters.

The most enriched species of the analyzed phytoplankton samples from August 2022, were characterized by chlorophyta and cyanobacteria, which is typical for the summer phytoplankton community of many lakes. Increased share of cryptophytes in the quantitative structure of phytoplankton in the August 2022 sample could be related to the temporary instability of the conditions in the reservoir. These algae are typical representatives of phytoplankton that develop in unstable conditions. Their presence may also result from the inflow of an increased amount of organic matter.

The observed algae after the operation of the pipelines system for are a common organism, which occurring mostly in the plankton of moderately and more eutrophic waters. A total of 61 taxa of algae were observed in October 2022, as follows: 19 taxa of cyanobacteria and representing 30% of the studied population, 16 taxa of chlorophyta with a share of 25.8%

from the quantitative structure, 9 taxa of Bacillariophyceae (diatoms) with a 14.5% of the total population. while the remaining algae taxa formed less than 10%), 4 taxa of cryptophyceae, 4 taxa of dinophyceae, 4 taxa of euglenophyceae, 2 taxa of klebsormidiophyceae, 2 taxa of chrysophyceae, and 1 taxon of zygnematophyceae.

In May 2022, the average number of phytoplankton was 1,002,335 indiv. /l, cyanobacteria were dominant, especially the colonial form of it -trichomes/ filamentous-. In August, the average number of phytoplankton amounted to 1,170,000 indiv. /l, of which 46.7% were cyanobacteria of the genus: aphanocapsa and aphanothece in colonial forms, and 31.8% were chlorophyta. In October 2022, a large decrease in the number of phytoplankton was observed, but cyanobacteria still prevailed as a filamentous colony, planktothrix. however, their number, compared to august, was much lower and amounted to an average of 193,680 indiv. /l.

#### **4.5.2 Zooplankton**

Before conducting the restoration activities of Świąte lake, the main zooplankton taxa in the lake were rotifera, cladocera (rowers) and copepoda species. in addition, individuals belonging to the order bdelloidea and larval stages of copepods (nauplius and copepodites) were observed. The zooplankton biomass was overwhelmingly dominated by crustaceans. The zooplankton research results indicate a moderate trophic state of the lake. Even though the number of zooplankton is relatively high, species characteristic of high-water trophy was not dominant. Moreover, the relatively low biomass of ecologically desirable rowers (<1 mg/l) indicates a high food pressure of small cyprinids.

In each month and at both measuring site nu. 1 & 2, rotifera were the definite quantitative dominants, constituting over 90% of the total number of zooplankton. keratella was the quantitative dominant species among rotifera species keratella cochlearis constituting at least 44% of the number of rotifers every month. The highest number of species was recorded in July 2018 with a density, the lowest in October 2018. Among the rowing species, Bosmina dominated in numbers of longirostris (23% share in the number of rowers), and among species belonging to copepods were copepodites and nauplius, especially the mesocyclops leuckarti genus.

During the consecutive years after the undertaken reclamation process of the lake, a various number of zooplankton was observed during the research period. In each month, a high number of zooplankton was observed, dominated by rotifers constituting over 80% of the total number of zooplankton in each month and at each measuring site. This is a typical arrangement of zooplankton structures in this type of lake. Their density was higher in May and August though lower than in previous years. In August 2020, over 2,000 individuals per liter of zooplankton was observed. For the rest of the research-year months the number was smaller comparing to previous years, due to the lower abundance of rotifers.

Despite this, it must be recognized that the density of zooplankton was still relatively high. The high number of zooplankton in summer indicates a high availability of food and good conditions for the development of zooplankton typical of eutrophic lakes.

In total, 40 taxa of zooplankton were found throughout the study period in 2022, species. 27 taxa belonged to rotifera, 9 to cladocera and 4 to copepoda. crustacean larva forms of copepods were copepodites and nauplius.

Rotifers were quantitatively dominant, by small species, which is characteristic of lakes with a high trophic status. The main species of Rotifers taxonomic group was *Keratella cochlearis*. *Bosmina longirostris* was the dominant among the cladocera. Both taxa are typical species for all water reservoirs, but their population increases with the trophic status of the water body. copepodites and nauplius were clearly dominant among the copepods group. This is a characteristic symptom of the high trophic status of lakes.

#### **4.5.3 Macrobenthos**

The conducted study before applying the restoration procedure confirmed a presence of 24 taxa of macrobenthos belonging to: annelida, isopoda, amphipoda, insecta, bivalvia, gastropoda -snails- and hydracarina (water mites). Moreover, the presence of an invasive species, as *Dreissena polymorpha* -zebra mussel-, albeit with a slight concentration. The qualitative and quantitative composition of the macroinvertebrates of the studied reservoir indicates that the reservoir is covered with dense growth in the littoral zone by macrophytes. The lack of species sensitive to pollution may indicate a large impact of anthropopressure on the lake.

By the end of the research period (2018-2022), 19 taxa of macro zoobenthos were found with no significant difference in the number of taxa and the number of individuals between spring (May 2022) and autumn (October 2022). In both of the previous mentioned research seasons, the most numerous groups of benthos were zebra mussels (*Dreissena polymorpha*) and bloodworms (*Chironomus*). In addition, the larvae of dragonflies of the species *Coenagrion puella* and *Coenagrionidae*, were quite numerous in autumn.

The small number of ubiquitous taxa and a lack of clear dominance of these taxa and a large share of insect larvae, indicate the progressing stabilization of the ecosystem of the lake towards the improvement of trophic conditions.

#### 4.5.4 Macrophytes

The average aquatic vegetation cover of Świąte lake ecosystem during 2017-2018 represents 11% of the bottoms surface, the largest covered zone exist on the Halophyte belt which is the largest zone of aquatic vegetation in the lake (Pho. 16). Macrophytes of Świąte lake are mainly shaped by; Common reed *Phragmites australis* represent 29% of, narrow-leaved cattail form 27%, and *Myriophyllum spicatum* cover a 20% of the area covered by macrophytes. The cover percentage of the rest of minor groups were as follows; *Acorus calamus* growing on 1%, *Glyceria maxima* (2%), white-lily *Nymphaea alba* (1%), *Nymphaea lutea* (7%), elodeids (7%), represented by a *Ceratophyllum demersum*, and *Potamogeton crispus* (4%). In addition, a few communities of moss from the *Fontinalis antipyretica* were found in the lake, with a coverage area of 3% in the total area that occupied by macrophytes.

The average aquatic vegetation covers almost 31% of the bottom surface of Świąte lake after launch the restoration process (Pho. 17). The helophyte belt, shaped by 30% of *Phragmites australis* (the common reed), 24% by cattail (*Typha*). Among the amphiphytes, *Acorus calamus* covers 1% of the surface of aquatic plants, and *Glyceria maxima* formed 2%. while the share of the nymphoids were 10% of *Nymphaea lutea* (yellow-water lily), and 2% of *Nymphaea alba* (white-water lily). The elodeids (submerged macrophytes) covered 29% of the total occupied area by macrophytes. This percentage was shared as follows; 6% covered by *Ceratophyllum demersum*, 20% by *Myriophyllum spicatum* and 3% by *Potamogeton crispus*. in addition, the lake was found to have a rare occurrence of *Fontinalis antipyretica* (Willow Moss), whose coverage area in the total area was determined at 2%.

In 2022, aquatic vegetation covered the bottom to a depth of about 2.8 m, which is 0.6 m more than in the previous year.



Photo 16. Map of macrophyte distribution in the Świąte lake, 2018.



Photo 17. Map of macrophyte distribution in the Świąte lake, 2022.

#### 4.5.5 Ichthyofauna

Before conducting the biomanipulation process biological analysis of 775 fish with a total biomass of 4535g, shows that caught fish belong mainly to 11 species, as follow; 8 of them belongs to cyprinidae/carp, 2 to perch (ruffe and perch) and one to pike.

Despite the small length and unit body weight of the common roach (cyprinidae), it turned out to be not only a quantitative dominant, but also a weight dominant in the lake accounted for 78% of the biomass of all caught fish. Followed by silver bream species, also despite the low values of length and unit body weight. The total share of these two quantitative dominants in fish biomass was as much as 85%. Adding to this value the percentage of



biomass of other cyprinidae species i.e., carp, we get almost 93%, which proves the high biomass of non-predatory fish. Fish species share percentage (Fig.34).

According to the analysis of the ichthyofauna of the Święta lake, the lake waters are lacking predatory fish in such size and weight. That would inhibit the development and growth of the dominant small cyprinid fish, that feed on zooplankton which filter the water from plant cells and detritus.

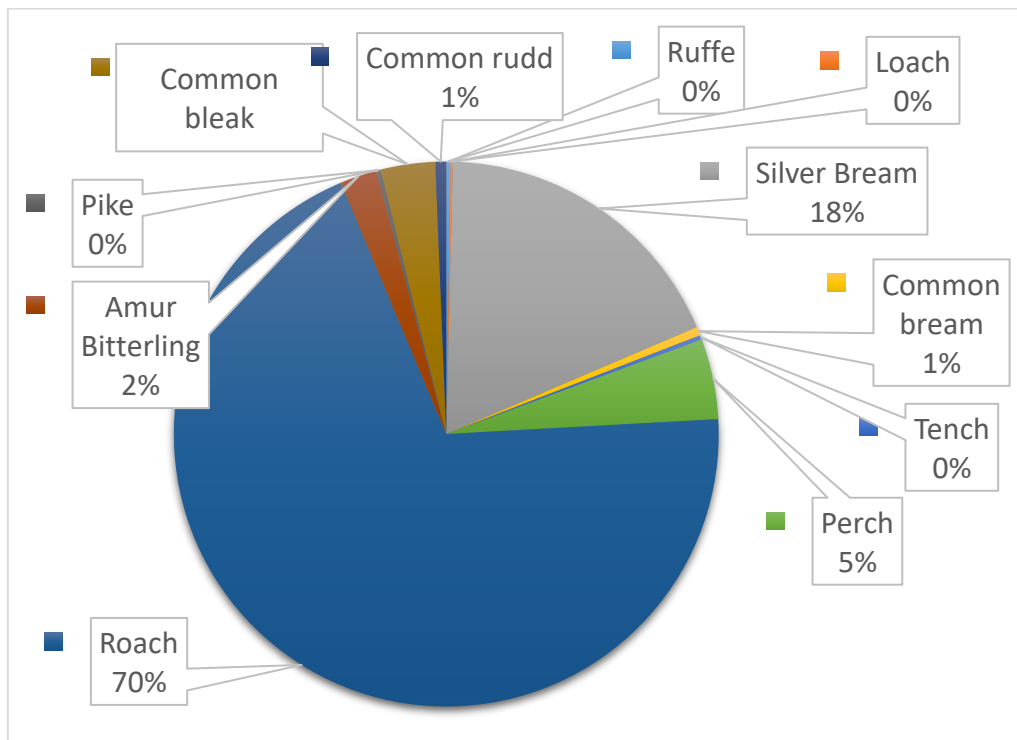


Figure 34. Fish species share percentage in Święta lake for year of 2018.

The caught fish during the biological sampling seasons for year 2022, mainly distributed to 3 families that contain 13 species, as follow; 9 species belong to cyprinidae family, whose are *misgurnus fossilis*, silver bream, common bream, tench, roach, amur bitterling, common bleak, common rudd and asp, a 3 species belong to percidae family; zander, ruff and perch, and 1 specie form esocidae family; pike.

In total, 957 fish with a total biomass of 10,180 g were caught from ten points. However, the obtained information from anglers confirms the existence of common crucian carp, catfish and 3 invasive species, grass carp, silver carp, and prussian carp. Asp and zander presence is due to the conducted stocking.

Roach was the quantitative dominant among the caught fish species, constituting 67% with an average body length of 8 cm, year 2022. The silver bream species formed 16%, and characterized by a body length of 7 cm. While Perch found to be 7%. Other cyprinids species had a small share in the number of the total, approx. 3%. Typically, predatory species, like perch, pike, zander, and asp accounted for about 9-10% of all fish caught, which were found to be half amounted as it was in previous years. Ruff can also be considered as a predatory species, whose food also occasionally contains other fish, but in the entire sample of fish it accounted for only 1%. In general, all fish species were characterized by their small body length. Share percentage distribution of fish species in Święte lake (Fig. 35).

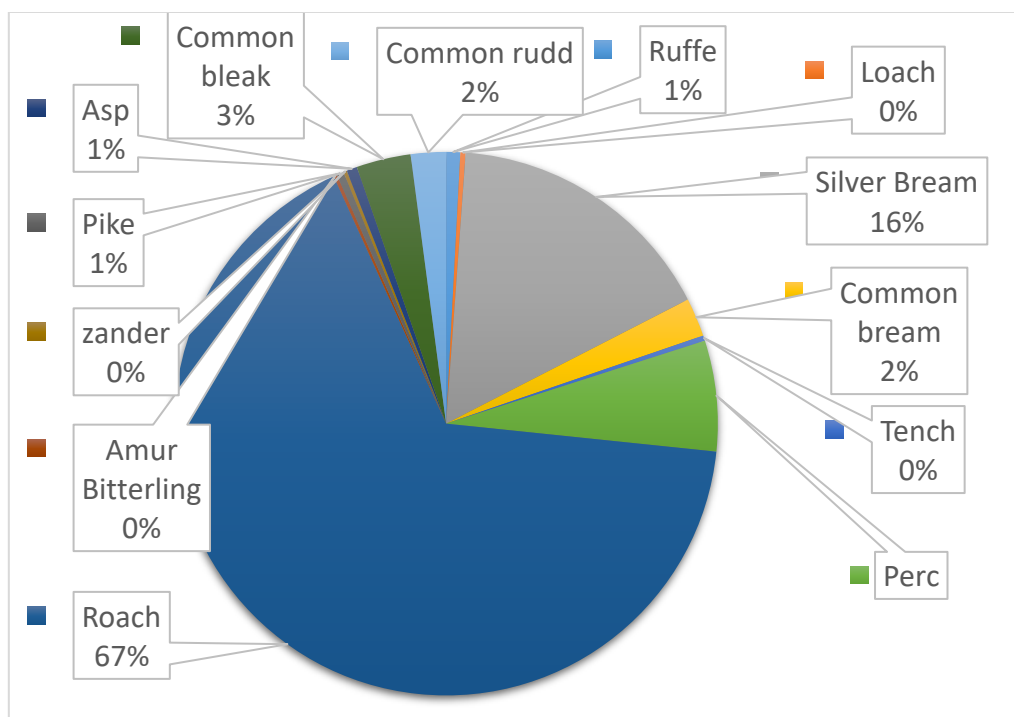


Figure 35. Fish species share percentage in Święte lake for year of 2022.

Among the analyzed predatory fish Święte lake ecosystem during the one-year monitoring cycle (2017-2018), and in terms of weight of biomass, perch was the dominant one, constituting 4% of the total weight of caught fish. It can be concluded that this value is not so small in relation to the shape of the trophic pyramid and the weight ratios. However, the lake may contain pike perch/ zander (*sander lucioperca*), stickleback (*gasterosteus aculeatus*), eel (*anguilla anguilla*), spined loach (*cobitis taenia*), catfish (*silurus glanis*) and carp (*cyprinus carpio*). The obtained information indicates a significant number of cyprinids.

Tench was characterized by the highest mean value of unit body weight in the lake before the biomanipulation treatment and significantly different from other fish species. Another species with the highest unit weight was pike, which, considering the largest sizes of this species compared to others. The average fish condition index in Świąta lake (Fig. 36). The average unit weight of roach and silver bream were 7 g and 2 g, respectively. Perch was also characterized by low values of the unit body weight, only on average 5 g. This result may also indicate the dwarfing of the carp fish population in the lake.

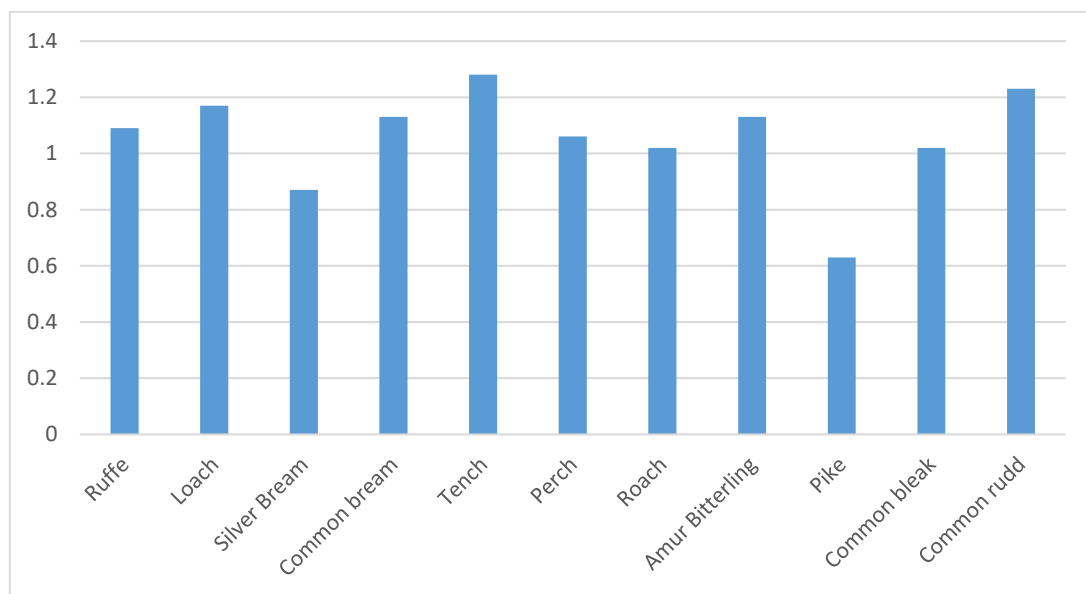


Figure 36. Average fish condition index in Świąta lake for year of 2018.

During the year 2022, the highest average value of unit body weight in the lake was found in pike species and significantly differing from other fish species. The next species with the highest unit weight was Zander. The unit weight of the remaining fish was much lower. Roach and Silver bream, which were the most important in terms of quantitative dominance, had an average unit weight of 8 g and 5 g, respectively (Fig. 37).

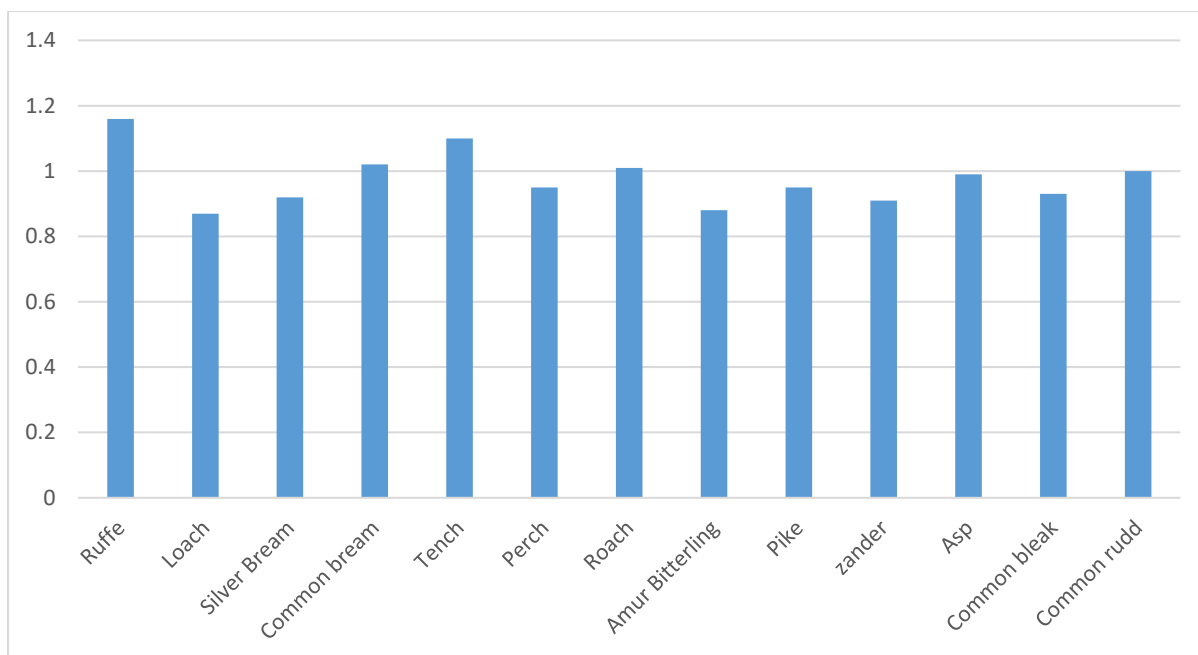


Figure 37. Average fish condition index in Święte lake for year of 2022.

## 5. Discussion

Lake's ecological condition is affected by the caused impact of catchment area as a source of its external load of nutrients. Lakes are remarkably diverse ecosystems, where susceptibility to degradation of each ecosystem is determined by its individual characteristics. Morphometric indicators as spatial dimensions of the lake basin, hydrological and catchment features specify its rate of deterioration (Dearing et. al., 1981).

Shallow and small water bodies are weaker to resist the eutrophication process. Low water resources make it difficult to dilute pollutants and maintain a better water quality (Qin et. al., 2013). On the other hand, flow-through lakes always degrade faster because they have larger catchments (Lau and Lane, 2002).

Hypolimnion layer considers as an oxygen reservoir for the biochemical transformations that occur in this fragment of waters, where it is some kind isolated from the rest of the water body during the summer stagnation. In this zone, suspensions of sediments take place and any oxygen deficient in it affect negatively on the whole waterbody and exacerbated by the muddy nature of the bottom (Mao et. al., 2018). Lakes with large hypolimnion volume do not suffer oxygen deficiency, due to the small organic load from the surface area during the growing season towards the bottom of the lake. On the contrary, the small hypolimnion volume rapidly overload by the precipitated organic matter. (Gantzer et. al., 2009).

Absence of the dissolved oxygen in water decreases its redox potential. This in turn affects phosphorus sorption by sediments (Kirf et. al., 2015). The sediments start to release the adsorbed phosphorus to the water over it and become a very efficient source of nutrients that contribute to increase the phytoplankton abundancy and growth of algae blooms, causing a self-degradation of the lake, (Rossi and Premazzi, 1991). There is a positive correlation between oxygen deficiency and the released phosphorus load from the sediments (Hupfer and Lewandowski, 2008). Moreover, under anaerobic conditions, poisonous hydrogen sulphide may appear in the profundal zone, this is considered as a symptom of advanced lake degradation. A consequence of algae abundance, the dead remains of it fall down the bottom of the lake increasing the organic matter load. Decomposing of this new organic load will cause greater oxygen deficit (Mortimer, 1971).

The carried sulphate ( $\text{SO}_4^{2-}$ ) amounts to lake from both surface and ground waters, reduced to sulphide ( $\text{HS}^-$ ) in the sediment. The interaction between sulphide ( $\text{HS}^-$ ) and phosphorus sorption complex elements generate an alkaline medium that affects their chemical bonding and stimulates the waters mineralization due to minerals release from sediment. Besides that, sulphide ( $\text{HS}^-$ ) is toxic to planktonic macrophyte, lake enrichment of sulphate ( $\text{SO}_4^{2-}$ ) increase the eutrophication severity due to its cycle inside lake (Giordani et. al., 1996). The increased iron (Fe) concentrations inside the sediments interstitial water can reduce the adverse effects of sulphate ( $\text{SO}_4^{2-}$ ) pollution (Holmer and Storkholm, 2008).

The lake internal load usually prevents the reservoir from returning to good water status, where the reservoir maintains excessive fertility from its own sources, and even after cutting off the external load of nutrients from the catchment area. Under such circumstances, conducting restoration plans to assist the lake to recover its aquatic ecosystem status become necessary (Alhamarna and Tandyrak, 2021; Zamparas and Zachrias, 2014; National research council, 1992).

Bottom sediments play a considerable key role in aquatic ecosystems, where it works as a trap that holds the excess nutrients, especially phosphorus, the most important nutrient, and the main culprit of lake eutrophication (Giguët-Covex et. al., 2010). The amount of nutrients in the bottom sediments of the lake is extremely large, which makes them the main, inexhaustible source of nutrients in polluted lakes. 90% of the total phosphorus content is found only in the upper layer of the bottom sediments -10 cm. This clearly indicates the need to limit the participation of this source in the internal load process (Łopata et. al., 2013).

The keystone to understanding the played role by sediments in the lake regime is by its sequential physicochemical analysis. That includes the determination of the chemical composition of the sediment with the division into mineral and organic parts, analysis the water chemistry of the sediment pore water -interstitial water- and the overlaying water-over-sediments (Mudroch et. al., 1996).

The basic condition for starting a restoration process of the water ecosystem is to eliminate, or at least reduce the external load of nutrients. A complete elimination of nutrients from seeping toward the lake is impossible, due to the constant natural supply of the delivered

water along with surface runoff and underground seepage from the direct and indirect catchment area, as well as the impact of precipitation (rJeppesen et. al., 2007).

Święte lake catchments are strongly transformed and exposed to anthropopressure with a weak existence of natural plant cover, which is a kind of filter of impurities. The nature of Święte lake's catchment area management is unfavorable, where most of its surrounding area is arable land, partially grassland and development areas of surrounding villages. Greater-Poland region -Wielkopolska-, is characterized by a large agricultural production potential with a significant population fragment still living outside agglomerations with unregulated water and sewage management.

The observed concentration mass of sulphur-bacteria by late 2017's summer (Pho. 18), consider a confirming symptom of the cumulative nature of pollutants in lake from the catchment area (Steenbergen, 1982). By the autumn turn-over cycle, the sulphur released to the euphotic zone. The occurrence of this phenomenon is one of the advanced symptoms of eutrophication (Karhunen et. al., 2013).



Photo 18. Bacterial biofilms, Święte lake, Sep. 2017 (author: Dr. K. Parszuto/Personal).

Quality decline of Święte lake came because of both the internal load of nutrients from bottom sediments and external supply from the catchment area, by the surface inflow (Pintus). The findings of Święte lake monitoring cycle (2017-2018), indicated that the critical loads of phosphorus and nitrogen have been exceeded (Tab. 34). Święte lake was exposed to the excessive influence of the catchment area, which, according to the standards adopted in limnology and hydrobiology, will result in a further degradation of its ecosystem.

Table 34. List of P and N loads from individual sources for the Święte lake (on the base of Czerniawski et al., 2018).

source	phosphorus		nitrogen	
	kg / year	participation	kg / year	participation
<b>Intermediate catchment</b>	282.65	77.70%	4907.92	74.80%
<b>Direct catchment</b>	62.48	17.20%	1365.85	20.80%
<b>Fishing ground bait</b>	8.37	2.30%	24.30	0.40%
<b>Bather</b>	0.1875	0.10%	4.50	0.10%
<b>Atmospheric sources</b>	10.20	2.80%	257.60	3.90%
<b>Total</b>	363.88	100	6560.13	100

Fortunately, the dominated nutrients load that supply Święte lake from the intermediate catchment area through Pintus ditch as a previously connection between the lake and Berzyńskie lake, been diverted to Dojca river ending to Obra canal as an implementation of the first stage of the restoration plan.

The restoration plan of Święte lake consist mainly of a hydraulic pipelines system, and secondary of a biomanipulation treatment processes of its ecosystem. The expected environmental impacts of the applied pipelines system installation are:

- Providing oxygen to the lake deep layer of the lake waters, approximately 1600 kg O<sub>2</sub>, and could be twice more in case of preparing the trench-section of the Pintus for more effective self-oxygenation e.g., cleaning the trench, forcing turbulent flow, cascades.
- Redirection of the surface inflow to hypolimnion instead the epilimnion will contribute to decrease the accessible nutrients for algae, thus mitigation the peak of the growing season (Dunalska, 2020).



- Shortening the period of summer stagnation to extend the circulation period, due to the reduction of the stability of thermal layers of water in summer and accelerating the autumn turn-over cycle (Casamitjana et. al., 2003).
- Possibility of future use of the filling pipeline to dose additional oxygen or water purification preparations directly into the hypolimnion of the lake, without costly installation (Łopata et al, 2013).
- Discharging the most polluted waters from the deep-water layer of the lake.

The favorable period of pipelines system operation is during the summer stagnation when the lake is thermally stratified e.g., the installed hypolimnion withdraw system Kortowskie lake (Mientki and Teodorowicz, 1996). The planned operation periods for the filling pipeline is from June to September, and for the discharging pipeline from July to October.

The amount of received water by Święte lake from Krutla drainage pumping station that flow through Pintus tributary, should be adjusted to limit the excess water inflow to the lake. Usually, in June, the inflow waters could build up water in the lake by 0.2 m (46,600 m<sup>3</sup>), as a natural retention capacity of the lake, this state would be maintained during the summer months. The sufficient inflow will help to flush the hypolimnetic water and prevent sedimentation of organic matter and nutrients. As a result of the lake's partition by the underwater curtain, two separate hypolimnion sections. Currently, the hypolimnion of Święte lake is on average less than 10 m deep and contains 278,500 m<sup>3</sup> of water, half of this volume should be considered for each pipeline as the minimum yearly flow volume.

As the operation of both pipelines (filling/ draining) linked together to maintain water balance of the lake, the failure to apply the planned pumping schedule for Krutla drainage pumping station, in case of scarcity of the collected water from the melioration drainage network leave the functionality of the pipelines system vulnerable to the meteorological conditions, as the spring ice melt in 2021 and the drought in 2022.

In year 2021, the delivered nutrients by Pintus inflow within a few days has exhausted the annual self-cleaning capacity of this reservoir. Phosphorus and nitrogen (P & N) concentration exceeded 1.1 mg P /l of phosphorus, and almost 12 mg N /l of nitrogen, as well as a significant load of organic matter measured as total organic carbon (TOC) about 24 mg C /l with an estimated load of phosphorus amount to at least 30 kg and 300 kg of nitrogen. This came because of the spring ice melt issue, where the inflow quantity volume was approximately 25,000 m<sup>3</sup>. For comparison of the annual permissible load for Święte lake according to the

Vollenweider criteria (Vollenweider, 1975) are 29.6 kg of phosphorus and 474 kg of nitrogen (Czerniawski et. al., 2018).

During the 2022 drought there was low to no inflow, therefore the outflow was reduced to maintain the water level in the lake and prevent its shrunken. As a consequence of the summer drought of year 2022, it was necessary to drain water from the areas flooded around the pumping site. The quality of water in the fields quickly deteriorated due to the leaching of nutrients from the flooded soil and rotting of the plant cover at the buffer reservoir of the pumping site. Moreover, water pumping impetus washed loose fractions of soil and sediments from the ditch, which further aggravated its disastrous quality.

The increased concentration of the nutrients (P & N) in the waterbody by the end of the research period is a consequence of the meteorological conditions and not a glitch of pipelines system functionality, as it indicated by the concentration declining trend of nutrients (P & N) until April 2022 (Fig. 38) where It has not been reported about any kind of malfunctions of the installed pipelines system.

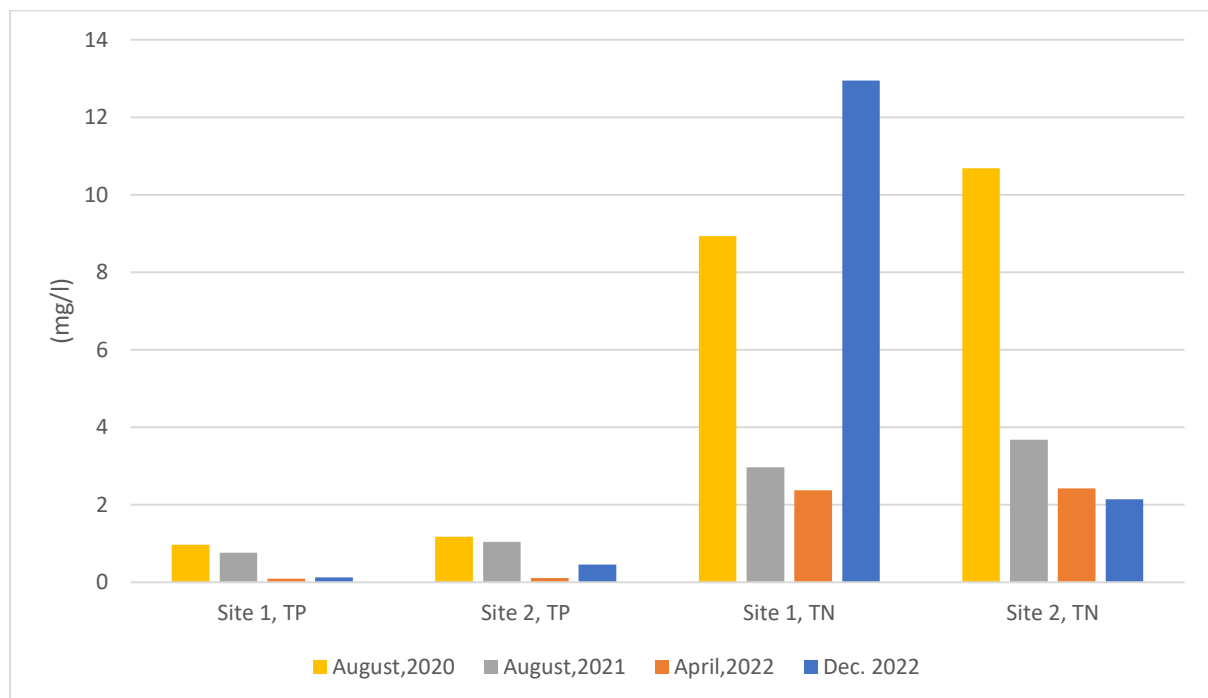


Figure 38. The change of nutrients (P & N) concentration at the deep waters.

The pipeline system showed an efficiency to remove a sufficient amount of the hypolimnetic phosphorus content, approximately three times from the outflow section than the delivered phosphorus (TP) before the summer stagnation when lake is a relatively weakly stratified. In

April 2022, the discharged phosphorus (TP) with the outflow was 0.434 mg P/l, in time, when the phosphorus (TP) concentration in the inflow water was 0.146 mg P/l. And for the same measurement, nitrogen (TN) concentration for the inflow and outflow were 2.4 and 2.44 mg N/l, respectively. Almost the same delivered amount of nitrogen to Świąte lake by Pintus inflow is discharged through Pintus outflow, indicating a slow process of nitrogen (N) removal.

Hydrogen sulphide (H<sub>2</sub>S), showed a significant decrease in its concentrations and depth of its occurrence along with operation time of the pipelines system is a success symptom of the applied restoration activities. In 2020, prior the operation of the restoration installation, this toxic gas was noticeably existing below 9 m depth, in significant amounts. During the summer stagnation of year 2021, the depth of hydrogen sulphide (H<sub>2</sub>S) occurrence gets deeper by 3-4 m with much smaller amounts that slightly exceed 1 mg S<sup>-</sup>/l. In compared with the remarkable concentrations of hydrogen sulphide from the previous stagnation, which reached more than 17 mg S<sup>-</sup>/l. Seems highly, that the source of hydrogen sulphide for deep waters is the bacterial reduction of sulphates (SO<sub>4</sub><sup>-2</sup>), which takes place under the anaerobic conditions (Tandyrak and Lizuraj, 2008). Occasionally, Pintus inflow brought significant amounts of sulphates and Świąte lake form a deposit pool for sulphates. The inflow/ outflow analysis for April 2022, showed that the carried amount of sulphates (SO<sub>4</sub><sup>-2</sup>) was 185 mg S<sup>-</sup>/l and the discharged concentration was much more less 35 mg S<sup>-</sup>/l. The amount of the transported sulphates to the lake is not stable during the year months e.g., for December 2022' measurements the sulphate concentration was 34.4 mg S<sup>-</sup>/l and 33 mg S<sup>-</sup>/l for the inflow and outflow, respectively. The delivered dissolved oxygen with the inflow partially prevented sulphates reduction to hydrogen sulphide. Another source of hydrogen sulphide for lake waters may be the decomposition of sulphur-containing organic matter (Holmer and Storkholm, 2008). This justifies the higher concentrations of the toxic hydrogen sulphide (H<sub>2</sub>S) gas. The odor pollution of hydrogen sulphide (H<sub>2</sub>S) at the outflow was noticeable in the first period after the pipelines system start-up and it was determined to be strong, currently after removal of significant amounts of hydrogen sulphide from deep water layers, it is weakly and very poorly palpable organoleptically.

The pipelines system succussed to decrease the BOD<sub>5</sub> content in the discharged outflow to the half comparing to the incoming inflow value of BOD<sub>5</sub> (1:2, inflow/outflow), December 2022. Total organic compounds (TOC) for the inflow to outflow could be generally represented

as data from April 2022 (12.94 to 16.43 mg C/l, respectively), which represent an expulsion process of the organic matter from the hypolimnion layer. The discharged seston from the outflow section is much higher than the delivered one to inflow section through Pintus to record 3.2 to 28.5 mg/l, April 2022. The amount of the delivered seston to discharged one from both pipelines sections are not always with high differences i.e., the recorded seston values for December 2022 were 4.4 mg/l for Pintus inflow and 2.8 mg/l for Pintus outflow. Total Hardness (TH) showed the same and it was almost 3 times higher than its value in the discharged outflow, this explain magnesium ( $Mg^{+2}$ ) order change in sediments. (2.46 mval/l), April 2022.

The decrease in phosphorus-TSI ( $TSI_{TP}$ ) during the summer stagnation of year 2021 could be attributed to its absorption by phytoplankton and macrophytes, but also can be considered as a succeed symptom of the installed pipelines system of targeting the phosphorus content in water and lowering its TSI rank rather than sustaining it. What support the second assumption is that chlorophyll a-TSI ( $TSI_{Chl a}$ ) productivity as an indicator of lake productivity during the summer does not change (Tab.s 35 & 36).

Beside the decline of phosphorus-TSI ( $TSI_{TP}$ ) the stability of rest of the trophic state indexes [ $TSI_{Chl a}$ ,  $TSI_{SD}$  and  $TSI_{TN}$ ] during the stagnation indicates that the summer operation of the pipelines system does not disturb the thermal regime of Świąte lake, where the water measurements done for the epilimnion layer (Carlson, 1977). Indexes of the trophic state (TSI) improved by end of the research period as expressed in (Results).

Table 35. Trophic State Index (TSI) of Świąte lake for 21<sup>st</sup> June 2021.

<b>TSI Index</b>	<b>Site nu. 1</b>	<b>Site nu. 2</b>
<b><math>TSI_{TP}</math></b>	76	78
<b><math>TSI_{Chl a}</math></b>	60	58
<b><math>TSI_{SD}</math></b>	55	55
<b><math>TSI_{TN}</math></b>	61	62

Table 36. Trophic State Index (TSI) of Świąte lake for 31<sup>st</sup> August 2021.

<b>TSI Index</b>	<b>Site nu. 1</b>	<b>Site nu. 2</b>
<b><math>TSI_{TP}</math></b>	65	69
<b><math>TSI_{Chl a}</math></b>	59	58
<b><math>TSI_{SD}</math></b>	55	55
<b><math>TSI_{TN}</math></b>	61	62

Biodegradability Index (ratio of BOD<sub>5</sub> to COD) for organic matter content of the lake waters were 0.49 (ave.) at site nu.1 (outflow zone) and 0.42 at site nu.2 (inflow zone) during the research period (2020-2022), which refer to an average biodegradability of water (Klepacz-Smolka, 2013). The higher BOD<sub>5</sub>:COD ratio at the inflow zone indicates the influence of the catchment area in matter supply, especially at the surface layer (Weerasinghe and Handapangoda, 2019).

The gradients of nitrogen concentrations through the water column depth show that the conditions of the deep water layer of Świąte lake were favorable for nitrogen transfer from the sedimentary interstitial water to the water-over-sediments, and later on and during the turn-over cycle it circulates with the whole water body. Nitrogen was found to be correlated with the sediments organic matter percentage (Peters et. al., 1978).

The analysis of the bottom sediments of Świąte lake showed that the sedimentary interstitial water characterized by higher concentrations of both nutrients than water-over-sediments (Löfgren and Boström, 1989).

During year 2020, a significant increase in the sediment's phosphorus content (up to 2.074 mg P/g D. M.) was recorded in the upper layer of the sediments core at site nu. 2. These amounts were higher than at site nu. 1. This is related to the high organic matter content in it and its associated phosphorus, which is an easily mobilized fraction of phosphorus. However, the phosphorus amount in sediments is not that high comparing to founds of eutrophic lakes e.g. Dianchi Lake/ China has reached 6.66 g/kg (Gao et. al., 2005). In the year 2022, a decrease in these values was observed, but they are still higher than in the year 2020.

The N:P ratio for both of the sediment layers (site nu. 1), it found at the outflow zone to be higher than its relative one at the inflow zone (site nu. 2). Ratio of N:P in the upper layer of sediments at the inflow zone found to be higher than the same layer at the outflow zone, regarding to the incoming flow.

The summed percentage of the analyzed sediment sorption complex elements [calcium, magnesium, iron, manganese, aluminum] varied annually between 14.68 % and 16.47 % during the research period. It found that calcium (Ca<sup>+2</sup>) is the dominant sorbent in Świąte lake case, with a larger share percentage of aluminum and iron at the inflow zone (site.nu. 2).

Order of the chemical compositions of sediment before the operation of the pipelines system found to be [Si > O.M. > Ca > CO<sub>3</sub><sup>-2</sup> > Mg > Al > N > Fe > P > Mn]. The rank altered during year 2021 to be [Si > O.M > CO<sub>3</sub><sup>-2</sup> > Mg > Al > Ca > N > Fe > P > Mn], with an increase of carbonate and a decline of calcium contents. Calcium average percentage changed from 6.54% before the operation of the pipelines system to 1.89% by end of the research period. Ranking of the chemical compositions of the sediments by the end of the research period altered to be [Si > O.M > Mg > CO<sub>3</sub><sup>-2</sup> > Al > Ca > N > Fe > P > Mn]. By comparing the two periods before and after the operation of the pipelines system, by the end of the research period (2018-2022) magnesium (Mg) showed a significant increase in its content, while calcium (Ca) content decreased significantly than it was before (Appendix) . Magnesium and calcium are natural components of surface water, and their concentrations can be shaped by a range of factors, mostly the geological structure of a catchment area, soil class and type, plant cover, weather conditions, land relief type and intensity of water supply (Potasznik and Szymczyk, 2015). In Kinneret lake, it was found that the main source of Ca<sup>2+</sup> and Mg<sup>2+</sup> components was calcite, which was dominant in the catchment. Calcite crystalized in the epilimnion, then the cation Ca<sup>2+</sup> and Mg<sup>2+</sup>, precipitated together with Ca<sup>2+</sup>, moved in the water column because of the mixing process. In consequence, cations were partly dissolved in the hypolimnion. Apart from the geological structure and acidity, the literature emphasizes the impact of climate change on the formation of cation concentrations in surface waters (Bhat et al. 2014). Furthermore, an increase in the mineral content of water leads to a greater abundance of magnesium ions than calcium ions and a low Ca:Mg ratio. Mineral levels can be significantly affected by the carbonate balance. Depending on the physicochemical parameters of the local environment, calcium can be precipitated or transferred from bottom sediments to water (Gałczyńska et. al., 2014). A positive magnesium balance was observed in Symsar lake where the lake retained magnesium in bottom deposits and prevented its spread outside, mostly at the inflow zone (Potasznik and Szymczyk, 2015).

Nitrogen-phosphorus ratio in sediments was below 16:1, which indicates a mineral binding of P with sediments rather than the organic binding. Organic matter-nitrogen ratio in sediment (O.M.:TN) found to be higher than 10:1, which refers to growth of terrestrial plants within the sediments and it confirmed by the field observation (Kaushal and Binford, 1990). No land

plants grow in the place where the sediments are collected. The plant cover (macrophytes) increased from 11% by the beginning of the reporting period to 31% by end of it.

Biomanipulation is a method of shaping the structure of ichthyofauna to reduce the excessive number of zooplanktivorous and benthosivorous fish. Fish stocking into the lake with predatory species -pike and zander-, form a food pressure on planktivorous, thus limiting their pressure on zooplanktons. The abundant planktonic crustaceans are the natural controller of the number of planktonic algae. Therefore, such a reconstruction of the species structure of fish contributes to the improvement of the water quality in the lake (Zhang et. al., 2020).

For Święte lake, fishing biomanipulation was adopted as complementary but necessary stage of the restoration process. The lake ichthyofunistic monitoring study, indicating a clear disturbance of the trophic pyramid structure at the level of fish (Czerniawski et al, 2018). There is a justified necessity to reduce the number of small cyprinids, especially roaches and silver bream to increase the population of predators.

Phytoplankton composition did not change significantly, where the taxa biodiversity in Święte lake are common plankton species. During 2022, monocultures with mass appearances of a single phytoplankton species e.g., blooms does not take place, with no mass appearances of sulfur bacteria, as recorded before the year 2020.

The variability of the phytoplankton communities in the can be considered typically for moderate to eutrophic lakes. The occurrence of genus *Oocystis*, chlorophyta, may indicate a minor water pollution. its presence observed in period that preceded eutrophication and after the implemented restoration measurement (Czerniawski et al., 2022). Cryptophytes algae tolerate the changing of the environmental conditions, where the recorded cryptomonas genus of algae belongs to eurytopic species. Both genus *Aphanocaps*, cyanobacteria and genus *Coenochloris*, chlorophyta are stress-tolerant algae. They could appear in eutrophic reservoir, but their presence also indicates possible periods of lake stability (Mikami et. at., 2021; Holzinger and Pichrtová, 2016). Since phytoplankton has not changed significantly, there has not been a strong enough change in the feeding pressure of zooplankton on phytoplankton. It stills an early stage of the biomanipulation process to confirm.

Due to its central location in the trophic pyramid of lakes, zooplankton is sensitive to abiotic and biotic changes in the environment, caused by natural and anthropogenic factors. It plays a vital role in aquatic ecosystems, where it controls the development of phytoplankton and forms a food base for fish (Lampert et. al., 1986). Phytoplankton does not mark any change in its structure by the end of the research period (2020-2022). This means that it still benefits from the stored nutrients in bottom sediments from previous years during the internal loading of the lake.

In Świąte lake, various zooplankton abundances were observed during the study period and before the biggining of the lake restoration. High zooplankton abundancy was observed dominated by rotifers. In May and August 2020, an exceedingly high number of zooplankton was recorded, over 2000 individuals per liter. This abundance indicates a high availability of food and particularly good conditions for the development of zooplankton, typical of highly eutrophic lakes. The high proportion of copepods among crustaceans proves the high degree of trophies of the studied reservoir. The lack of a dominant share in the biomass of large rowers may also indicate the high pressure of fish.

Świąte lake zooplankton observation during the period of May to October 2021, showed that the zooplankton structure in this lake are typical for eutrophic water body. The most common dominants in the zooplankton abundance were small species of rotifers, Cladocera and nauplius. In comparison with the period before the operation of the pipeline, the zooplankton state of the lake's water has not changed in 2021. It even seems to have deteriorated slightly without a significant change, but with an improvement in the average number of large crustaceans e.g., daphnia during the research period compared to the obtained results from the one-year monitoring cycle. This could be interpreted as the beginning of a decrease in the pressure of cyprinids on zooplankton. But generally, for the biomanipulation effect to occur the ecosystem needs time to change in populations (Łopata et. al., 2020).

Macrobenthos are organisms that are associated with the bottom of water reservoirs at least at one stage of their lives. These organisms are an essential element of the trophic pyramid in aquatic ecosystems. Benthic macroinvertebrates in the littoral part are subject to local influences related to the management of the direct vicinity of the lake's catchment area. The qualitative and quantitative structures of macrobenthos have not deteriorated in year 2022 compared to the previous years and remain at a quite stable level. This indicates a moderate



ecological status with a tendency to improve the physicochemical conditions in the bottom zone, habitat of these organisms.

Macrophytes distribution pattern does not refer to an eutrophicated lake, where macrophytes succession in this type of lakes is usually very intensive. In 2022, Elodeids occupied a slightly larger area of the bottom, which enrich the natural self-cleaning of the lake. Charophytes were observed for the first time in the lake since the beginning of the observing period (2017-2022). These favorable symptoms state that the light's penetration through the water column reaching deeper areas of the lake's bottom. Thus, abundance of submerged macrophytes as Elodeids can increase.

All the observed algae during 2018-2020, belong to common organisms, occurring mostly in the plankton of moderately and more eutrophic waters.

Based on the ichthyofauna research results for the one-year monitoring cycle (2017-2018), it can be concluded that the species and quantitative structure of ichthyofauna in Święte lake is typical for highly eutrophic lakes, where the size of the stocked carp fish is much higher than that of predatory fish. It can be assumed that without a biomanipulation treatment for the lake ecosystem, its trophic conditions will only get worse. Based on the obtained results of ichthyofauna studies (2017-2018), it can be concluded that the ichthyofauna structures of the Święte lake are characterized by unfavorable ichthyofauna indexes.

The selection of fish species for the biomanipulation treatment was a result from the natural potential of the Święte lake habitats. Littoral zone determines pike habitats, the sublittoral zones with good habitat conditions consider the habitat of zander species, and the open water zone is a proper habitat for asp species. In this species system, predators will explore all ecological zones of the lake without competing for food excessively. Pike will remain the dominant, as its habitats are the most abundant. Asp is a fish that occurs naturally mainly in rivers but attempts to introduce it into reservoirs of lentic waters with good water quality are successful. In addition, asp species are difficult to catch for anglers, so it will not be subject to such strong anthropogenic pressure as pike or zander. Stocking with any carp species was not recommended, except for Asp, which is considered a predator.

Pike introduced directly into the zone of coastal vegetation with a depth of 0.8 - 1.2 m. Zander introduced in deeper water (depth 1.2 - 1.6 m). Asp introduced in small groups of several

pieces outside the coastal vegetation zone. After being brought in by the (boat's method), fish freely disperse in the water and take positions that are natural for their behavior (Czerniawski et al, 2018).

Implementation of stocking individual stages depend on the selection of the assortment of stocking material: foraging brood, spring, summer, or autumn fry. Stocking material should come from fish breeding and breeding centers located in the vicinity of the lake. The short distance means that fish are not tired with transport, shortly after harvesting and in good condition. Stocking material must have a valid veterinary health certificate.

## 6. Conclusion

The research purpose of investigating the initial occurred changes of the restored reservoir is achieved by analyzing its biophysicochemical parameters during the study period. The installed pipelines system (filling/drainage) works without reported malfunctions. The functionality of the installed pipelines system does not disturb the lake thermal regime, and succeeded to discharge significant amounts of phosphorus, hydrogen sulphate, total organic carbon and dry matter seston from the hypolimnetic water. The discharged organic compound from the lake indicated by its biological oxygen demand ( $BOD_5$ ) was twice higher than the entered one with the inflow. The 3-years plan of biomanipulation has improved the biological state of Święte lake from the bottom of the trophic pyramid by limiting external load, and from the top of the trophic pyramid stocking predators. The correction of the trophic pyramid happens slowly, as the formation of the ichthyofauna structure takes about 4-5 years and needs to maintain a long-term strategy of limiting the excessive number of cyprinids.

The implemented restoration activities of Święte lake succeeded significantly to decrease hydrogen sulphide ( $H_2S$ ) gas in its concentrations and depth of its occurrence along the water column, slightly exceed 1 mg S/l. Transparency of water increased, with decline of the Chlorophyll a concentration by the end of the research period (2020-2022). The main nutrients (P & N) concentration in the hypolimnetic water showed a decline trend during the operation time of the pipelines system. In April 2022, the concentration of TP through the outflow was almost three times higher than the inflow. Święte lake bottom sediments manifest an ability to retain phosphorus quite effectively due to the delivered oxygen which enhanced the redox potential conditions of the hypolimnetic water.

Phytoplankton composition did not change significantly, where the taxa biodiversity in Święte lake are common plankton species dominated by characterized by chlorophyta and cyanobacteria, typically for moderate to eutrophic lakes with no mass appearances of sulfur bacteria as the recorded before the biomanipulation treatment. The zooplankton research results indicate a moderate trophic state of the lake and dominated by rotifers. Qualitative and quantitative structures of macrobenthos have not deteriorated in year 2022 compared to the previous years and remain at a quite stable level. Macrophytes distribution pattern

does not refer to an eutrophicated lake. Roach was the quantitative dominant among the caught fish species, constituting 67% with an average body length of 8 cm, year 2022.

## Summary

Święte lake restoration plan has been set based on the obtained biophysiochemical parameters during a one-year monitoring program (2017-2018) for the lake and its surrounding catchment. The unsatisfactory limnological parameters of Święte lake left the lake unable to defend itself against its own productivity, as pollution has reached a critical level and this situation sustains an excessive primary production, including algae blooms.

The obtained results of the abovementioned monitoring program, Święte lake considered as a trophic reservoir and its ecological condition was rated below good. It resulted from both internal supply of nutrients from bottom sediments and their supply from the catchment basin mainly via the surface inflow. Hydrogen sulphide was present in the hypolimnion of the lake in exceptionally high concentrations of 8.5 - 10 mg HS<sup>-</sup> /l. A probable significant source of this gas is the bacterial reduction of sulphates, where sulfur bacteria were present in concentrations up to 136 mg /l.

Święte lake restoration approach have been implemented by Department of water protection engineering and environmental microbiology at University of Warmia and Mazury in Olsztyn and Department of Hydrobiology of University of Szczecin, that consists of following stages:

A. regulating the directions of water flow through the lake hydrological network, and cut its connection with Berzyńskie lake.

B. construct an innovative pipelines system: a) filling pipeline, which directs the water flowing directly from the surface of the Pintus directly to the bottom of the northern deep, b) discharging hypolimnion water from the southern deep to the surface of the Pintus, and c) partially divide the hypolimnetic water by underwater curtain. The pipelines system were launched in October 2020.

C. biomanipulation process that consists of: a) systematic lake stocking with species of predatory fish, and b) regulatory catches which selectively focused to elimination of small cyprinids.

- The restoration activities planned to be completed by phosphorus inactivation using PIX 111 iron coagulant and PAX 18 aluminum coagulant. But in view of the tangible effects of the conducted restoration activities and the increase the iron mean content percentage in

sediments from 0.24% before the operation of the pipelines system to 0.79% by the end of the research period (2020-20) meaning a more sediment absorption capacity for phosphorus (P).

Water transparency before the application of the restoration activities ranged between 1.90 m and 1.82 m for the inflow and outflow zones, respectively. The visibility range registered up to 5 m by end of the research period, December 2022.

The most pronounced effect of the applied restoration process is the improvement of the oxygen conditions in the lake. Phosphorus (P) and nitrogen (N) as main nutrients showed a change of their concentrations. The deep-water layer of Święte lake, showed a significant reduce of their levels for both sites. The obtained results for the deep waters concentration of P and N, indicate the effectiveness of the applied restoration measurements. Both pipelines, filling pipeline and the discharge one, are functionally sufficient to reduce the amount of the stored nutrients at the hypolimnion layer. This took place by discharging the nutrient rich hypolimnetic water from outflow zone, and by enhancing the redox potential at inflow zone. Hydrogen sulfide concentrations did not exceed 1.19 mg HS<sup>-</sup>/l.

Reducing the abundance of small cyprinids will assist to relieve the formed graze pressure by it on zooplankton communities. The introduced predators fish species as, zander and asp through the biomanipulation process will enhance the lake' trophic pyramid and limit its disturbance for the coming years.

## Streszczenie

Plan rekultywacji Jeziora Świętego został opracowany na podstawie parametrów biofizykochemicznych uzyskanych w trakcie rocznego programu monitoringu jeziora i jego otaczającej zlewni (2017-2018). Niezadowalające parametry limnologiczne Jeziora Świętego sprawiły, że jezioro nie było w stanie obronić się przed własną produktywnością, ponieważ zanieczyszczenie osiągnęło poziom krytyczny, a sytuacja ta powoduje nadmierną produkcję pierwotną, w tym zakwity glonów.

Uzyskane wyniki ww. programu monitoringu Jeziora Świętego spowodowały, że uznano je za zbiornik troficzny, a jego stan ekologiczny oceniono poniżej dobrego. Wynikało to zarówno z wewnętrznego zaopatrzenia w składniki pokarmowe z osadów dennych, jak i zaopatrzenia ze zlewni, głównie poprzez doływ powierzchniowy. Siarkowodór występował w hipolimnionie jeziora w wyjątkowo wysokich stężeniach 8,5 – 10 mg HS<sup>-</sup>/l. Prawdopodobnym znaczącym źródłem tego gazu jest bakteryjna redukcja siarczanów, gdzie bakterie siarkowe występowały w stężeniach do 136 mg/l.

Podejście renaturyzacyjne Jeziora Świętego zostało zrealizowane przez Katedrę Inżynierii Ochrony Wód i Mikrobiologii Środowiskowej Uniwersytetu Warmińsko-Mazurskiego w Olsztynie oraz Katedrę Hydrobiologii Uniwersytetu Szczecińskiego i składało się z następujących etapów:

A. uregulowanie kierunków przepływu wód przez sieć hydrologiczną jeziora i przecięcie jego połączenia z Jeziorem Berzyńskim.

B. wybudowanie innowacyjnego systemu rurociągów: a) rurociąg wypełniający, który kieruje wodę wyptywającą bezpośrednio z powierzchni Pintus na dno głębi północnej, b) rurociąg odprowadzający wody hipolimnionowe z głębi południowej na powierzchnię Pintus, oraz c) częściowe przedzielenie wody hipolimnetycznej kurtyną podwodną. System rurociągów został uruchomiony w październiku 2020 roku.

C. procesu biomanipulacji polegającego na: a) systematycznym zarybianiu jezior gatunkami ryb drapieżnych, oraz b) połowach regulacyjnych, które selektywnie skupiały się na eliminacji małych karpiowatych.

Planowane zakończenie prac renowacyjnych polega na inaktywacji fosforu koagulantem żelazowym PIX 111 i koagulantem aluminiowym PAX 18. Jednak biorąc pod uwagę wymierne efekty przeprowadzonych działań rekultywacyjnych i zwiększenie średniej zawartości żelaza w osadach z 0,24% przed eksploatacją systemu rurociągów do 0,79% do końca okresu badawczego, wpłynęło bardziej na pochłaniania osadu przez fosfor (P).

Przejrzystość wody przed zastosowaniem działań renaturyzacyjnych wahała się od 1,90 m do 1,82 m odpowiednio dla strefy dopływu i odpływu. Zasięg widoczności zarejestrowany do 5 m do końca okresu badawczego, grudzień 2022 r.

Najbardziej wyraźnym efektem zastosowanego procesu rekultywacji jest poprawa warunków tlenowych w jeziorze. Fosfor (P) i azot (N) jako główne składniki pokarmowe wykazały zmianę swoich stężeń. Warstwa głębinowa Jeziora Świętego wykazała w obu stanowiskach znaczne obniżenie ich poziomu. Uzyskane wyniki stężeń P i N w wodach głębokich wskazują na skuteczność zastosowanych pomiarów renaturyzacyjnych. Obydwa rurociągi, napełniający i odprowadzający, są funkcjonalnie wystarczające do zmniejszenia ilości magazynowanych składników biogenych w warstwie hipolimnionu. Odbyło się to poprzez usunięcie bogatej w składniki odżywcze wody hipolimnetycznej ze strefy odpływu i zwiększenie potencjału redoks w strefie dopływu. Stężenia siarkowodoru nie przekraczały 1,19 mg HS<sup>-</sup>/l.

Zmniejszenie liczebności małych karpiowatych pomoże złagodzić powstającą przez nie presję wypasu na zbiorowiska zooplanktonu. Wprowadzone w procesie biomanipulacji gatunki ryb drapieżnych, jak sandacz i boleń, wzmocnią piramidę troficzną jeziora i ograniczą jej zaburzenia w nadchodzących latach.



## Acknowledgements

This work wouldn't be done without support of Dr hab. inż. Renata Tandyrak 😊.

Mohammed Alhamarna is a recipient of a scholarship from the Programme Interdisciplinary Doctoral Studies in Bioeconomy (POWR.03.02.00-00-I034/16-00), which is funded by the European Social Funds.

Thanks to Pani inż. Marzena Karpienia<sup>1</sup>, Chemical laboratory specialist at University of Warmia and Mazury in Olsztyn, for the kindly help through the chemical analysis.

Thanks to Dr hab. inż. Michał Łopata<sup>2</sup>, Assistant Professor at University of Warmia and Mazury in Olsztyn, to assist with field measurement.

Thanks to Dr Sajed Ali<sup>3</sup>, Assistant Professor at University of Management and Technology-Sialkot Campus, for the assistance through the statistical analysis.

Thanks to Designer. Mohammed Abojayab<sup>4</sup>, to edit photos.

<sup>1</sup> marzena.karpienia@uwm.edu.pl

<sup>2</sup> michal.lopata@uwm.edu.pl

<sup>3</sup> sajed.ali@skt.umt.edu.pk

<sup>4</sup> Mj.jayyab@gmail.com

## References

- Alhamarna, M. and Tandyrak, R. (2021). Lake's restoration approaches. *Limnological Review*, 21:105-118.
- Andersen, T. (1997). Pelagic nutrient cycles: Herbivores as sources and sinks. *Ecological Studies*, V. 129. Springer, Berlin.
- Ashley, K. (2011). Hypolimnetic Aeration of A Naturally Eutrophic Lake: Physical and Chemical Effects. *Canadian Journal of Fisheries and Aquatic Sciences*, 40: 1343-1359.
- Augustyniak, R. (2018). Wpływ Czynn timer Fizyczno-Chemicznych i Mikrobiologicznych na Zasilanie Wewnetrzne Fosforem w6d Wybranych Jezior Miejskich. Polish Academy of Sciences, Environmental Engineering Committee Publishing House: Lublin, Poland.
- Augustyniak, R., Grochowska, J., 6opata, M., Parszuto, K., Tandyrak, R., Tunowski, J. (2019). Sorption Properties of the Bottom Sediment of a Lake Restored by Phosphorus Inactivation Method 15 Years after the Termination of Lake Restoration Procedures. *Water*, 11(10):2175.
- Augustyniak, R., Neugebauer, M., Kowalska, J., Szymański, D., Wiśniewski, G., Filipkowska, Z., ... & Tandyrak, R. (2017). Bottom deposits of stratified, seepage, urban lake (on the example of Tyrsko Lake, Poland) as a factor potentially shaping lake water quality. *Journal of Ecological Engineering*, 18(5), 55-62.
- Bajkiewicz-Grabowska, E., Magnuszewski, A. (2009). Guide to exercises in general hydrology . Ed. OWN.
- Balasubramanian, A. (2015). Classification of lakes. University of Mysore, November, 8.
- Bhagowati, B. and Ahamad, K. (2020). A review on lake eutrophication dynamics and recent developments in lake modeling. *Ecohydrology and Hydrobiology*, 19(1):155-166.
- Bhat, S.A., Meraj, G., Yaseen, S., Pandit A.K.(2014). Statistical assessment of water quality parametes for pollution source identification in sukhnag stream: an inflow stream of Lake Wular (Ramsar Site), Kashmir Himalaya. *J. Ecosyst.*, 2014: 1-18.
- Bhateria, R. and Jain, D. (2016). Water quality assessment of lake water: a review. *Sustain. Water Resour. Manag.*, 2:161–173.

- Birge, E.A. (1916). The work of the wind in warming a lake. *Trans. Wis. Acad. Sci. Arts Lett.*, 18(2):341–391.
- Boehrer, B., Schultze, M. 2008. Stratification of lakes. *Reviews of Geophysics*, 46(2).
- Bormans, M., Maršálek, B. and Jančula, D. (2016). Controlling internal phosphorus loading in lakes by physical methods to reduce cyanobacterial blooms: a review. *Aquat. Ecol.*, 50: 407–422.
- Brooks, J. L. and Dodson, S. I. (1965). Predation, body size, and composition of plankton. *Science* 150: 28–35.
- Brouwer, E., Bobbink, R., and Roelofs, J. (2002). Restoration of aquatic macrophyte vegetation in acidified and eutrophied softwater lakes: An overview. *Aquatic Botany*. 73: 405-431.
- Butcher, J. B., Nover, D., Johnson, T. E., and Clark, C. M. (2015). Sensitivity of lake thermal and mixing dynamics to climate change. *Climate Change*, 129:295–305.
- Carlson, R.E. (1977). A trophic state index for lakes. *Limnol. Oceanogr*, 22(2): 361-369.
- Casamitjana, X., Serra, T., Colomer, J., Baserba, C., Pérez-Losada, J. (2003). Effects of the water withdrawal in the stratification patterns of a reservoir. *Hydrobiologia*, 504: 21–28.
- Casenave, C. and Vinçon-Leite, B. (2018). Modelling eutrophication in lake ecosystems: A review. *Science of The Total Environment*, 651.
- Cole, J. J., Carpenter, S. R., Kitchell, J. F., and Pace, M. L. (2002). Pathways of organic carbon utilization in small lakes: Results from a whole-lake C-13 addition and coupled model. *Limnology and Oceanography*, 47(6): 1664–1675.
- Cooke, D.G., Welch, E.B., Peterson, S.A. and Nichols, S.A. (2005). Restoration and management of lakes and reservoirs. 3rd ed. Boca Raton (FL): CRC Press, Taylor and Francis Group.
- Cooke, G.D. and Carlson, R.E. (1989). Reservoir Management for Water Quality and THM Precursor Control, AWWA Research Foundation, Denver, CO.
- Czerniawski, R., Tandyrak, R., Łopata, M., Karpienia, M.(2018). Eutrophication of Święte lake in view of the ecological condition, threats, possibilities of protection and reclamation. University of Warmia and Mazury in Olsztyn.

- Czerniawski, R., Tandyrak, R., Łopata, M., Karpienia, M.(2022). Monitoring studies of Święte lake waters - stage I (2020-2022). University of Warmia and Mazury in Olsztyn.
- Daoliang, L. and Shuangyin, L. (2019). Water Quality Detection for Lakes. Water Quality Monitoring and Management. Pp. 221-231.
- Darryl, J. (2023). Statistical Tests. Researchgate. 10.13140/RG.2.2.36635.34088.
- Dearing, J., Elner, J., & Happey-Wood, C. (1981). Recent Sediment Flux and Erosional Processes in a Welsh Upland Lake-Catchment Based on Magnetic Susceptibility Measurements. *Quaternary Research*, 16(3): 356-372.
- Dufera, A., Liu, T., and Xu, J. (2023). Regression models of Pearson correlation coefficient. *Statistical Theory and Related Fields*, 7: 1-10.
- Dunalska, J. (2003). Impact of limited water flow in a pipeline on the thermal and oxygen conditions in a lake restored by hypolimnetic withdrawal method. *Polish Journal of Environmental Studies*, 12(4), 409-416.
- Dunalska, J. (2020). How the integrated engineering solutions can support the lakes restoration?. *Ecohydrology & Hydrobiology*. 21(1): 36-45.
- Dunalska, J.A., Wiśniewski, G. and Mientki, C. (2007). Assessment of multi-year (1956–2003) hypolimnetic withdrawal from Lake Kortowskie, Poland. *Lake Reserv Manage.*, 23(4):377– 387.
- Emiliani, C. (1991). Planktic/planktonic, nektic/nektonic, benthic/benthonic. *Journal of Paleontology*, 65(2): 329-329.
- Faizi, N. and Alvi, N. (2023). *Biostatistics Manual for Health Research: Statistical tests of significance*. Academic Press, Pp.: 45 62.
- Faraś -Ostrowska, B., Lange, W. (1998). Water transparency as a measure of the intensity of lake eutrophication. *Degradation threats and protection of lakes*. Department of Limnology, UG. *Bad. Limnol .*, 1: 181-191.
- Findlay, D.D.L., Vanni, M.M.J., Paterson, M.J., Mills, K.H., Kasian, S.E.M., Findlay, W.J. and Salki, A.G. (2005). Dynamics of a boreal lake ecosystem during a long-term manipulation of top predators. *Ecosystems*, 8: 603– 618.
- Gałczyńska, M., Gamrat, R., Burczyk, P., Horak, a., Kot, M. (2013). The influence of human impact and water surface stability on the concentration of selected mineral

macroelements in mid-field ponds. *Water-Environment-Rural Areas*, 3(3/43): 41-54 (in Polish).

- Gantzer, P. A., Bryant, L. D., John C. Little, J. C. (2009). Effect of hypolimnetic oxygenation on oxygen depletion rates in two water-supply reservoirs, *Water Research*, 43 (6): 1700-1710.
- Gao, L., Zhou, J.M., Yang, H., Chen. J. (2005). Phosphorus fractions in sediment profiles and their potential contributions to eutrophication in Dianchi Lake. *Environ. Geol.* 48: 835–844.
- Giguët-Covex, C., Arnaud, F., Poulenard, J., Enters, D., Reyss, J., Millet, L., Lazzaroto, J., Vidal, O. (2010). Sedimentological and geochemical records of past trophic state and hypolimnetic anoxia in large, hard-water Lake Bourget, French Alps. *Journal of Paleolimnology* 43 (1): 171–190.
- Giordani, G., Bartoli, M., Cattadori, M., Viaroli, P. (1996). Sulphide release from anoxic sediments in relation to iron availability and organic matter recalcitrance and its effects on inorganic phosphorus recycling. In: Caumette, P., Castel, J., Herbert, R. (eds) *Coastal Lagoon Eutrophication and ANaerobic Processes (C.L.E.AN.)*. Developments in Hydrobiology, vol 117. Springer, Dordrecht. Vollenweider, R.A. (1975). Input-output models. *Schweiz. Z. Hydrologie*, 37, 53–84.
- Golachowska, J. (1977). Determination of the total content of mineral and organic phosphorus in lake bottom sediments. *Year Science. Rol. H.*, 98: 39-49.
- Górniak D., Tandyrak R., Parszuto K., Misiun J. 2014. Relationships between physico-chemical and microbiological parameters in monimolimnion of in-forest meromictic lake, *Journal of Limnology*, 73(3):511–522.
- Grimm, M.P. and Backx, J.J.G.M. (1990). The restoration of shallow eutrophic lakes, and the role of northern pike, aquatic vegetation and nutrient concentration. *Hydrobiologia* 200: 557-566.
- Grønkjær, P., Skov, C. and Berg, S. (2004). Otolith-based analysis of survival and size-selective mortality of stocked 0+year pike related to time of stocking. *J. Fish. Biol.* 64: 1625-1637.

- Gulati, R.D., Pires, L.M.D., Van Donk, E., 2008. Lake restoration studies: failures, bottlenecks and prospects of new ecotechnological measures. *Limnologica*, 38: 233–248.
- Haddout, S., Priya, K.L., and Boko, M. (2018). Thermal response of Moroccan lakes to climatic warming: first results. *Annales de Limnologie - International Journal of Limnology*, 54(2).
- Hakala, A., 2004. Meromixis as a part of lake evolution; observations and a revised classification of true meromictic lakes in Finland. *Boreal environment research*, 9(1): 37.
- Hansson, L., Annadotter, H., Bergman, E., Hamrin, S., Jeppesen, E., Kairesalo, T., Luokkanen, E., Nilsson, P., Søndergaard, M., Strand, J. (1998). Minireview: Biomanipulation as an Application of Food-Chain Theory: Constraints, Synthesis, and Recommendations for Temperate Lakes. *Ecosystems*. 1: 558-574.
- Hansson, L.-A., Annadotter, H., Bergman, E., Hamrin, S.F., Jeppesen, E., Kairesalo, T., Luokkanen, E., Nilsson, P.-A. , Søndergaard, M., Strand, J. (1998). Biomanipulation as an application of food-chain theory: constraints, synthesis, and recommendations for temperate lakes. *Ecosystems*, 1: 558–574.
- Hermanowicz, W., Dojlido, J., Dożańska, W., Kozirowski, B., Zerbe, J. (1999). *Physico-chemical testing of water and sewage* . Arkady, Warsaw.
- Holmer, M., & Storkholm, P. (2001). Sulphate reduction and sulphur cycling in lake sediments: a review. *Freshwater Biology*, 46(4), 431-451.
- Holzinger, A., Pichrtová, M. (2016). Abiotic Stress Tolerance of Charophyte Green Algae: New Challenges for Omics Techniques. *Front Plant Sci.*, 20(7):678.
- Hullebusch, E. Van Auvray, F., Deluchat, V., Chazal, Ph. M., Baudu, M. (2003). Phosphorus fractionation and short-term mobility in the surface sediment of a polymictic shallow lake treated with a low dose of alum (Courtille Lake, France). *Water, Air and Soil Pollution*, 146: 75-91.
- Hupfer, M. and Lewandowski, J. (2008), Oxygen Controls the Phosphorus Release from Lake Sediments – a Long-Lasting Paradigm in Limnology. *International Review of Hydrobiology*, 93: 415-432.

- Ikeda, S., Adachi, N. (1976). Dynamics of the nitrogen cycle in a lake and its stability. *Ecological Modelling*, 2(3): 213-234.
- Imboden, M. (1974). Phosphorus model of lake eutrophication. *Limnology and Oceanography*, 19: 297-304.
- Januskiewicz, T. (1978). A study on the methodology of chemical analysis of the composition of contemporary lake bottom sediments . *Zesz. Science. ART. In Olsztyn*, 8.
- Januskiewicz, T. (1980). Chemistry of recent sediments of Grabowskie Lake in Kashubian Lake district in Northern Poland. *Pol. Arch. Hydrobiol.*, 27(3): 319-336.
- Jarosz, A., Wołoszyn, J. (1966). *Hydraulika*. Państwowe Wydawnictwo Rolnicze i Leśnicze, Warsaw. (In Polish).
- Jasser, I., Kostrzevska-Szlakowska, I., Ejsmont-Karabin, J., Kalinowska, K., WĘGLEŃSKA, T. (2009). Autotrophic versus heterotrophic production and components of trophic chain in humic lakes: The role of microbial communities. *Polish Journal of Ecology*, 57:423-439.
- Jeppesen, E. and Sammalkorpi, I. (2002). Chapter 14 "Lakes". In: M. Perrow & T. Davy (eds.): *Handbook of Restoration Ecology*, Cambridge University Press, Volume 2: 297-324.
- Jeppesen, E., Jensen, J.P., Søndergaard, M., Lauridsen, T. and Landkildehus, F. (2000). Trophic structure, species richness and biodiversity in Danish lakes: changes along a phosphorus gradient. *Freshw. Biol.*, 45: 201–213.
- Jeppesen, E., Søndergaard, M., Lauridsen, T., Davidson, T., Liu, Z., Mazzeo, N., Trochine, C., Özkan, K., Jensen, H., Trolle, D., Starling, F., Lazzaro, X., Johansson, L., Bjerring, R., Liboriussen, L., Larsen, S., Landkildehus, F., Egemose, S., Meerhoff, M. (2012). Biomanipulation as a Restoration Tool to Combat Eutrophication Recent Advances and Future Challenges. *Advances in Ecological Research.*, 47. 411-487.
- Jeppesen, E., Søndergaard, M., Meerhoff, M., Lauridsen, T., and Jensen, J. (2007). Shallow lake restoration by nutrient loading reduction—some recent findings and challenges ahead. *Hydrobiologia*. 584: 239-252.
- Jeppesen, E., Søndergaard, M., Meerhoff, M., Lauridsen, T.L., Jensen, J.P. (2007). Shallow lake restoration by nutrient loading reduction—some recent findings and

challenges ahead. In: Gulati, R.D., Lammens, E., De Pauw, N., Van Donk, E. (eds) *Shallow Lakes in a Changing World. Developments in Hydrobiology*, vol 196.

- Jöhnk, K. D., Huisman, J., Sharples, J., Sommeijer, B., Visser, P. M. and Stroom, J. M. (2008). Summer heatwaves promote blooms of harmful cyanobacteria. *Glob. Change Biol.*, 14: 495–512.
- Johnson, T. C. (1984). Sedimentation in Large Lakes. *Annual Reviews of Earth and Planetary Sciences*, 12: 179–204.
- Karhunen, J., Arvola, L., Peura, S., Tirola, M. (2013). Green sulphur bacteria as a component of the photosynthetic plankton community in small dimictic humic lakes with an anoxic hypolimnion. *Aquat Microb Ecol*, 68:267-272.
- Kasprzak, P., Koschel, R., Krienitz, L., Gonsiorczyk, T., Anwand, K., Laude, U., Wysujack, K., Brach, H. and Mehner, T. (2003). Reduction of nutrient loading, planktivore removal and piscivore stocking as tools in water quality management: The feldberger haussee biomanipulation project. *Limnologica*, 33:190–204.
- Katsev, S., Tsandev, I., L'Heureux, I. and Rancourt, D.G. (2006). Factors controlling long-term phosphorus efflux from lake sediments: Exploratory reactive-transport modeling. *Chemical Geology*, 234: 127–147.
- Katz, A., Nishri, A. (2013). Calcium, magnesium and strontium cycling in stratified, hardwatres lakes: Lake Kinneret (Sea of Galilee, Israel). *Geochim. Cosmochimi. Acta*, 105: 372-394.
- Kaushal, S., Binford, M.W. (1999). Relationship between C:N ratios of lake sediments, organic matter sources, and historical deforestation in Lake Pleasant, Massachusetts, USA. *Journal of Paleolimnology* 22, 439–442.
- Kirf, M.K., Røy, H., Holtappels, M., Fischer, J. P., Schubert, C. J., Wehrli, B. (2015). Redox gradients at the low oxygen boundary of lakes. *Aquatic Sciences*, 77: 81-93.
- Kirillin, G. and Shatwell, T. (2016). Generalized scaling of seasonal thermal stratification in lakes. *Earth-Science Reviews.*, 161: 179–190.
- Klapper, H. (2003). Technologies for Lake Restoration. *Journal of Limnology*, 62(1): 73-90.
- Klepacz-Smolka, Anna. (2013). Re: How to correlate COD/BOD ratio and biodegradability?. Retrieved



from:[https://www.researchgate.net/post/How\\_to\\_correlate\\_COD\\_BOD\\_ratio\\_and\\_biodegradability/51c2c2bcd039b13919311893/citation/download](https://www.researchgate.net/post/How_to_correlate_COD_BOD_ratio_and_biodegradability/51c2c2bcd039b13919311893/citation/download).

- Kondracki, J. (2002) *Geografia Fizyczna Polski (Physical Geography of Poland)*, PWN, Warszawa, Pp. 450 (in Polish).
- Kucklantz, V. and Hamm, A. (1988). *Möglichkeiten und Erfolgsaussichten der Seenrestaurierung*. Bayrische Landesanstalt für Wasserforschung, München, Germany. Pp. 212.
- Lampert, Winfried, Fleckner, Walter, Rai, Hakumat, Taylor, Barbara E., (1986), *Phytoplankton control by grazing zooplankton: A study on the spring clear-water phase*, *Limnology and Oceanography*, 3.
- Lau, S.S.S., Lane, S.N. (2002). Biological and chemical factors influencing shallow lake eutrophication: a long-term study, *Science of The Total Environment*, 288 (3):167-181.
- Lauridsen, T.L., Jeppesen, E., Søndergaard, M. and Lodge, D.M. (1997). Horizontal migration of zooplankton. Predator-mediated use of macrophyte habitat. In: Jeppesen, E., Søndergaard, M., Søndergaard, M. & Christoffersen, K. (eds.): *The Structuring Role of Submerged Macrophytes in Lakes*. Springer. *Ecological Studies*, 131: 233-239
- Lean, D.R.S., and Nalewajko, C. (1976). Phosphate exchange and organic phosphorus excretion by algae. *J. Fish. Res. Board. Can.*, 33: 1312–1323.
- Lerman, A., Imboden, D. and Gat, J. [Eds.]. (1995). *Physics and chemistry of lakes*. Springer-Verlag, Berlin.
- Lewtas, K., Paterson, M., Venema, H.D., Roy, D., (2015). *Manitoba Prairie Lakes: Eutrophication and In-Lake Remediation Treatments*, International Institute for Sustainable Development (IISD), Manitoba, Canada. Source: [www.jstor.org/stable/resrep14759](http://www.jstor.org/stable/resrep14759).
- Löfgren, S., Boström, B. (1989). Interstitial water concentrations of phosphorus, iron and manganese in a shallow, eutrophic swedish lake—Implications for phosphorus cycling. *Water Research*, 23(9): 1115-1125.
- Łopata, M., Augustyniak-Brzozowska, R., Grochowska, J., Parszuto, K., Tandyrak, R. (2020). *Selected Aspects of Lake Restorations in Poland*, [in:] Ewa Korzeniewska E.,

Harnisz M. (eds). Polish River Basins and Lakes – Part II, Springer-Nature, Switzerland: 327-352.

- Łopata, M., Gawrońska, H., Wiśniewski, G., Jaworska, B. (2013). *Restoration of two shallow, urban lakes using the phosphorus inactivation method - preliminary results*. Water Science and Technology, 68(10): 2127-2135
- Łopata, M., Grochowska, J. K., Augustyniak-Tunowska, R., & Tandyrak, R. (2023). Possibilities of Improving Water Quality of Degraded Lake Affected by Nutrient Overloading Form Agricultural Sources by the Multi-Point Aeration Technique. Applied Sciences, 13(5), 2861.
- Łopata, M., Tandyrak, R., Augustyniak-Tunowska, R., Parszuto, K., Płachta, A., Cybulska, Z. (2019). Interstitial Water of Deep, Stratified Lake as Potential Source of Internal Phosphorus Loading - Implications for Preventing Eutrophication, Environmental Problems, 4: 32-38.
- Łopata, M., Wiśniewski, G. (2013). The use of surface water flow to improve oxygen condition in hypertrophic lake. Global Journal of Advances in Pure and Applied Sciences, 1: 710-715.
- Lynch, A. J., Taylor, W. W., Beard Jr., T. D., and Lofgren, B. M. (2015). Climate change projections for lake whitefish (*Coregonus clupeaformis*) recruitment in the 1836 Treaty Waters of the Upper Great Lakes, J. Gt. Lakes Res., 41: 415–422.
- Macdonald, R.H., Lawrence, G.A. and Murphy, T.P. (2004). Operation and evaluation of hypolimnetic withdrawal in a shallow eutrophic lake. Lake and Reserv. Manage, 20:39-53.
- MacKay, M. D., Neale, P. J., Arp, C. D., De Senerpont Domis, L. N., Fang, X., Gal, G., Jöhnk, K. D., Kirillin, G., Lenters, J.D., Litchman, E., MacIntyre, S., Marsh, P., Melack, J., Mooij, W. M., Peeters, F., Quesada, A., Schladow, S. G., Schmid, M., Spence, C., and Stokes, S. L. (2009). Modeling lakes and reservoirs in the climate system. Limnol. Oceanogr., 54: 2315–2329.
- Mackie, C., Lackey, R., Levison, J., Rodrigues, L. (2022). Groundwater as a source and pathway for road salt contamination of surface water in the Lake Ontario Basin: A review. Journal of Great Lakes Research, 48(1): 24-36.

- Magee, M.R., Wu, C.H. (2017). Response of water temperatures and stratification to changing climate in three lakes with different morphometry. *Hydrol. Earth Syst. Sci.*, 21:6253–6274.
- Mahowald, N., Bryant, R., Corral, J., and Steinberger, L. (2003). Ephemeral lakes and desert dust sources. *Geophysical Research Letters*, 30(2): 1074-1078.
- Mao, Y., He, Q., Li, H., Su, X., Ai, H. (2018). Thermal Structure-Induced Biochemical Parameters Stratification in a Subtropical Dam Reservoir. *Water* 90 (12): 2036-2048.
- Marszelewski W., *Zmiany warunków abiotycznych w jeziorach Polski północno – wschodniej*. Publishing house UMK Toruń.
- McQueen, D.J., Story, V.A. (1986). Impact of hypolimnetic aeration on zooplankton and phytoplankton populations. *Environmental Technology Letters*, 7: 31–44.
- Mehner, T., Benndorf, J., Kasprzak, P., Koschel, R. (2002). Biomanipulation of lake ecosystems: Successful applications and expanding complexity in the underlying science. *Freshwater Biology*, 47(12): 2453–2465.
- Mercier, P., Perret, J. (1949) Aeration station of Lake Bret, *Monatsbull, Schweiz. Ver. Gas, u Wasserfach. Monatsbull.*, 29: 25–30.
- Messenger, M. L., Lehner, B., Grill, G., Nedeva, I., and Schmitt, O. (2016). Estimating the volume and age of water stored in global lakes using a geo-statistical approach. *Nature Communications*, 7: 1–11.
- Michael A. Anderson, Andy Komor, Keisuke Ikehata. (2014) Flow routing with bottom withdrawal to improve water quality in Walnut Canyon Reservoir, California. *Lake and Reservoir Management* 30:2, pages 131-142.
- Mientki, C. and Dunalska, J. (2002). Phosphorus balance at various water flows in a lake restored by hypolimnetic withdrawal. *Ecohydrology and Hydrobiology*, 1: 417-422.
- Mientki, C., Teodorowicz, M. (1996). Assessment of the Effects of Hypolimnion Water Removal from the Kortowskie Lake. In: Pawłowski, L., Lacy, W.J., Uchrin, C.G., Dudzińska, M.R. (eds) *Chemistry for the Protection of the Environment 2*. Environmental Science Research, vol 51. Springer, Boston, MA.
- Mikami, K., Takio, S., Hiwatashi, Y., Kumar, M. (2021). Environmental Stress-Promoting Responses in Algae. *Frontiers in Marine Science*, 8.

- Minnesota, P.C.A. (1991). Citizen Lake Monitoring Program - 1990 report on the transparency of Minnesota lakes. Minnesota Pollution Control Agency. Division of Water Quality. St. Paul, MN.
- Mudroch, A., Azcue, J. M., and Mudroch, P. (1996). Manual of physico-chemical analysis of aquatic sediments. CRC Press.
- Munson, B. R. (2016). Munson, Young, and Okiishi's Fundamentals of fluid mechanics. Philip M. Gerhart, Andrew L. Gerhart, John I. Hochstein, Donald F. Young, T. H. Okiishi (8th ed.). Hoboken, NJ. ISBN 978-1-119-08070-1. OCLC 916723577.
- National Research Council. (1992). Restoration of aquatic ecosystems: science, technology, and public policy. National Academies Press.
- Nürnberg, G. K. (2007). Lake responses to long-term hypolimnetic withdrawal treatments, *Lake and Reservoir Management*, 23(4):388- 409.
- Nürnberg, G.K. (2020). Hypolimnetic withdrawal as a lake restoration technique: determination of feasibility and continued benefits. *Hydrobiologia*, 847:4487–4501.
- Nutz, A., Schuster, M., Ghienne, J. F., Roquin, C., Bouchette, F. (2016). Wind-driven waterbodies: a new category of lake within an alternative sedimentologically-based lake classification. *Journal of Paleolimnology*, 59: 189-199.
- Ofir E., Heymans J.J., Shapiro J., Goren M., Spanier E., Gal, G. (2017). Predicting the impact of Lake Biomanipulation based on food-web modelingmodelling - Lake Kinneret as a case study, *Ecol. Modell.*, 348:14–24.
- Olszewski P., Paschalski J. (1959). Initial limnological characteristics of some lakes in the Masurian Lake District . *Zesz. Science. ART. Olsztyn.*, 4: 1–100.
- Paerl, H. W., Gardner, W. S., Havens, K. E., Joyner, A. R., McCarthy, M. J., Newell, S. E., Qin, B. and Scott, J. T. (2016). Mitigating cyanobacterial harmful algal blooms in aquatic ecosystems impacted by climate change and anthropogenic nutrients. *Harmful Algae*, 54:213-222.
- Paul, L. and Klapper, H. (2001). Vorrichtung zur destratifikation von standgewaessern. WPC02/F259,1985. Pp. 6.
- Paytan, A., Roberts, K., Watson, S., Peek, S.,Chuang, P.C., Defforey, D., Kendall, C. (2017). Internal loading of phosphate in Lake Erie Central Basin. *Science of The Total Environment*, 579: 1356-1365.

- Perks, C. (2006). Dealing with stratification within a water supply reservoir. In 69th Annual Water Industry Engineers and Operators' Conference, Pp. 30-36.
- Persson, L. and Greenberg, L.A. (1990). Interspecific and intraspecific size class competition affecting resource use and growth of perch, *Perca-Fluviatilis*. *Oikos* 59: 97-106.
- Peters, K. E. Sweeney, R. E. Kaplan, I. R., (1978), Correlation of carbon and nitrogen stable isotope ratios in sedimentary organic matter, *Limnology and Oceanography*, 23.
- Pettersson, K. (1998). Mechanisms for internal loading of phosphorus in lakes. *Hydrobiologia* 373, 21–25.
- Pond, G.R., Caetano, S.J. (2022). Essential Statistical Tests. In: Piantadosi, S., Meinert, C.L. (eds), *Principles and Practice of Clinical Trials*. Springer, Cham., Pp.: 1703-1716.
- Potasznik, A., and Szymczyk, S. (2015). Magnesium and calcium concentrations in the surface water and bottom deposits of a river-lake system. *Journal of Elementology*, 20: 677-692.
- Priet-Mahéo, M. C., Ramón, C. L., Rueda, F. J. and Andradóttir, H. Ó. (2018). Mixing and internal dynamics of a medium-size and deep lake near the Arctic Circle. *Limnology and Oceanography*, 64(1): 61-80.
- Psenner, R., Boström, B., Dinka, M., Pettersson, K., Pucsko, R. and Sager., M. (1988). Fractionation of phosphorus in suspended matter and sediment. *Archiv für Hydrobiologie Beihefte, Ergebnisse der Limnologie*, 30: 98-110.
- Qin, B., Gao, G., Zhu, G., Zhang, Y., Song, Y., Tang, X., Xu, H., Deng, J. (2013). Lake eutrophication and its ecosystem response. *Chinese Science Bulletin*, 58(9):961-970.
- Rice, E., Dam, H. G., and Stewart, G. (2015). Impact of Climate Change on Estuarine Zooplankton: Surface Water Warming in Long Island Sound Is Associated with Changes in Copepod Size and Community Structure. *Estuaries Coasts*, 38: 13–23.
- Rossi, G., Premazzi, G. (1991). Delay in lake recovery caused by internal loading. *Water Research*, 25 (5): 567-575.
- Ryanzhin, S. V., Subetto, D. A., Kochkov, N. V., Akhmetova, N. S., and Veinmeister, N. V. (2010). Polar lakes of the World: Current data and status of investigations. *Water Resources*, 37(4): 427–436.

- Sampl, H. (1993). Kärntner Seenbericht 1993. Kärntner Institute für Seenforschung, Klagenfurt. Pp. 144.
- Schindler, D. (2012). The dilemma of controlling cultural eutrophication of lake. *Proceedings. Biological sciences / The Royal Society*, 279: 4322-33.
- Schönach, P., Tapio, P., Holmroos, H., Horppila, J., Niemistö, J., Nygrén, N.A., Tammeorg, O., Massa I. (2017). Persistency of artificial aeration at hypertrophic Lake Tuusulanjärvi: A sociohistorical analysis. *Ambio* 46 (8): 865-877.
- Sieńska, J., Dunalska, J. and Szymański, D. (2015). Hourly and daily variability in nitrogen and phosphorus in a lake restored by the hypolimnetic withdrawal method. *Oceanological and Hydrobiological Studies*, 44(3): 381-392.
- Silvonen S., Niemistö, J., Csibrán, A., Jilbert, T., Torma, P., Krámer, T., Nurminen, L., Horppila, J., (2021). A biogeochemical approach to evaluate the optimization and effectiveness of hypolimnetic withdrawal. *Science of The Total Environment*, 755(2):1-14.
- Singleton, V. L., Little, J.C. (2006). Designing hypolimnetic aeration and oxygenation systems – A review. *Environmental Science and Technology*, 40: 7512–7520.
- Siwek, H., Włodarczyk, M., Czerniawski, R. (2018). Trophic state and oxygen conditions of waters aerated with pulverising aerator: the results from seven lakes in Poland. *Water*, 10(2): 219.
- Skov, C. and Berg, S. (2003). Udsætning af geddeyngel i Københavns indre søer 2002: Overlevelse, habitatvalg, vækst, fødevalg og afledte effekter. København: Københavns kommune. pp15 .
- Skowron, R., 2022. The summer thermal stratification of water in the lakes in the polish Lowlands. Publishing house UMK Toruń, ss 336.
- Smith, V.H., Schindler, D.W. (2009). Eutrophication science: where do we go from here?. *Trends in Ecology & Evolution*, 24(4): 201-207.
- Spieker, J. (2002). Application of ecotechnologies for lake restoration—present state, trends, prospects (German). *Wasser & Boden*, 54:5-13.
- Steenbergen, C.L.M. (1982). Contribution of photosynthetic sulphur bacteria to primary production in Lake Vechten. In: Gulati, R.D., Parma, D.S. (eds) *Studies on*

Lake Vechten and Tjeukemeer, The Netherlands. *Developments in Hydrobiology*, vol 11. Springer, Dordrecht.

- Stephen, D., Moss, B. and Phillips, G. (1997). Do rooted macrophytes increase sediment phosphorus release?. *Hydrobiologia* 342: 27–34.
- Susann, W., Rita, A. (2007). Impact of summer warming on the thermal characteristics of a polymictic lake and consequences for oxygen, nutrients and phytoplankton. *Freshwater Biology*, 53(2): 226–37.
- Tandyrak, R., & Lizuraj, M. (2008). Multiannual observations of iron and sulphur content in the waters of recultivated Lake Starodworskie waters, with comparison to selected physical and chemical parameters. *Limnological Review*, 8(4): 129-136.
- Tandyrak, R., Gołaś, I., Parszuto, K., Bowszys, M., Szymański, D., Harnisz, M., Brudniak, A., Wysocka, I. (2016). The effect of lake restoration by the hypolimnetic withdrawal method on the intensity of ambient odour, *Journal of Limnology*, 75(36).
- Ter Heerdt, G., Hootsmans, M. (2007). Why biomanipulation can be effective in peaty lakes. *Hydrobiologia* 584(1): 305–316.
- Thomas, C. D., Cameron, A., Green, R. E., Bakkenes, M., Beaumont, L. J., Collingham, Y. C., Erasmus, B. F. N., de Siqueira, M. F., Grainger, A., Hannah, L., Hughes, L., Huntley, B., van Jaarsveld, A. S., Midgley, G. F., Miles, L., Ortega-Huerta, M. A., Townsend Peterson, A., Phillips, O. L., and Williams, S. E. (2004). Extinction risk from climate change. *Nature*, 427: 145–148.
- Triest, L., Stiers I., Van Onsem, S. (2016). Biomanipulation as a nature-based solution to reduce cyanobacterial blooms, *Aquat Ecol'*, 50: 461–483.
- USBR Water Measurement Manual – Chapter 2 – Basic Concepts Related to Flowing Water and Measurement, Section 11. Hydraulic Mean Depth and Hydraulic Radius". [www.usbr.gov](http://www.usbr.gov). Retrieved 2022-03-14.
- Von Eye, A. and Wiedermann, W. (2023). *The General Linear Model: A Primer: Analysis of Variance (ANOVA)*. Cambridge: Cambridge University Press, Pp.:124-161.
- Wang, J., Chen, J., Guo, J., Sun, Q. and Yang, H. (2018). Combined Fe/P and Fe/S ratios as a practicable index for estimating the release potential of internal-P in freshwater sediment. *Environmental Science and Pollution Research* 25: 10740–10751.

- Ward, B.A., Follows, M.J. (2016). Marine mixotrophy increases trophic transfer efficiency, mean organism size, and vertical carbon flux. *Proc. Natl. Acad. Sci. USA.*, 113(11): 2958–2963.
- Weerasinghe, V.P.A., Handapangoda, K. (2019). Surface water quality analysis of an urban lake; East Beira, Colombo, Sri Lanka. *Environmental Nanotechnology, Monitoring & Management* 12: 100249.
- Wetzel, R.G. (2001). *Limnology, Lake and River Ecosystems*, Academic Press, San Diego and London. Pp. 1006.
- Zamparas, M., & Zacharias, I. (2014). Restoration of eutrophic freshwater by managing internal nutrient loads. A review. *Science of the Total Environment*, 496: 551-562.
- Zhang, Y., Luo, P., Zhao, P., Kang, S., Wang, P., Zhou, M., Lyu, J. (2020). Control and remediation methods for eutrophic lakes in the past 30 years. *Water Sci. Technol.*, 81 (6): 1099–1113.



## Appendix

### A. Sediments chemical composition

#### 1 . The organic matter (O. M.)

Table 1. Descriptive statistics of organic matter (%) in sediment.

	N	Mean	Std. Deviation	Std. Error Mean
Jun-20	16	18.86	4.249	1.062
Aug-20	16	24.53	20.044	5.011
Jun-21	16	18.00	1.370	.342
Dec-22	16	19.26	2.242	.560

Table 2. T-test statistics of organic matter (%) in sediments for four-time intervals.

	t	df	Sig. (2-tailed)	Mean Difference	95% Confidence Interval of the Difference	
					Lower	Upper
Jun-20	17.755	15	.000	18.863	16.60	21.13
Aug-20	4.894	15	.000	24.526	13.84	35.21
Jun-21	52.552	15	.000	17.997	17.27	18.73
Dec-22	34.372	15	.000	19.262	18.07	20.46

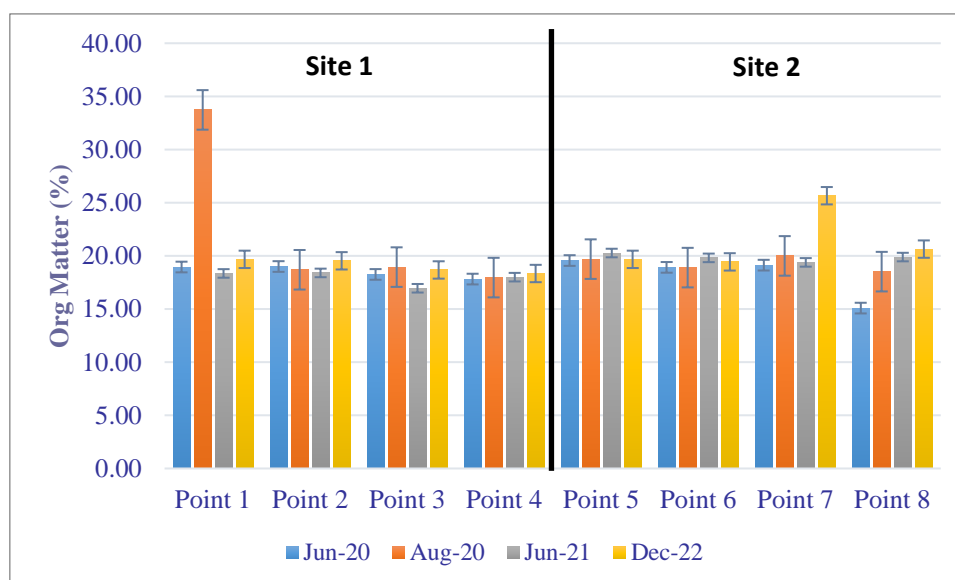


Figure 1. Organic matter share percentage in the upper layer of sediments (0-5 cm), during the research period (2020-2022).

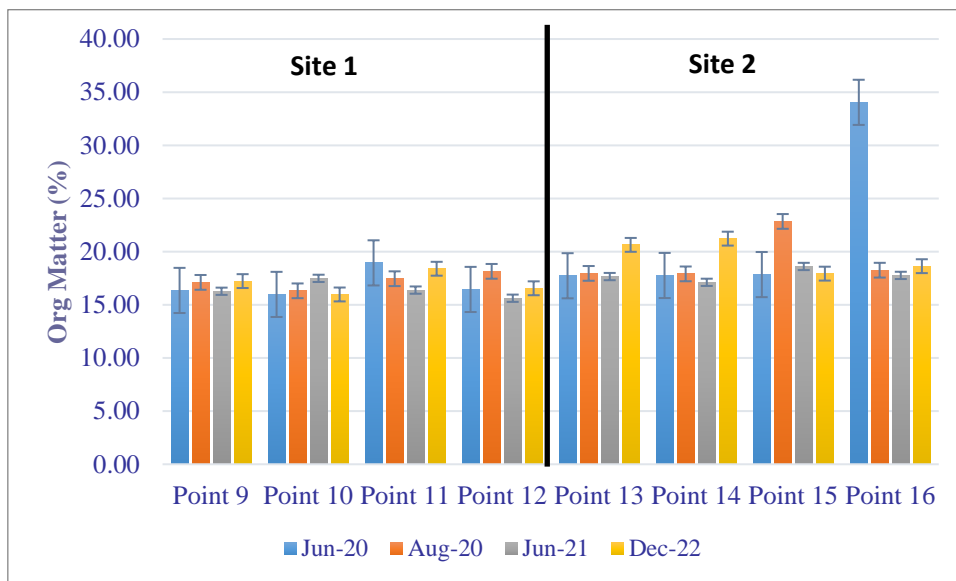


Figure 2. Organic matter share percentage in the bottom layer of sediments (5-10 cm), during the research period (2020-2022).

## 2. Carbonate (CO<sub>3</sub><sup>2-</sup>)

Table 3. Descriptive statistics of carbon dioxide (CO<sub>2</sub>) (%) in sediment.

	N	Mean	Std. Deviation	Std. Error Mean
Jun-20	16	22.73	3.498	.875
Aug-20	16	25.20	2.604	.651
Jun-21	16	23.28	5.939	1.485
Dec-22	16	30.27	21.855	5.464

Table 4. T-test statistics analysis of carbon dioxide (%) in sediments for four-time intervals.

	t	df	Sig. (2-tailed)	Mean Difference	95% Confidence Interval of the Difference	
					Lower	Upper
Jun-20	25.994	15	.000	22.734	20.87	24.60
Aug-20	38.715	15	.000	25.201	23.81	26.59
Jun-21	15.682	15	.000	23.284	20.12	26.45
Dec-22	5.541	15	.000	30.274	18.63	41.92

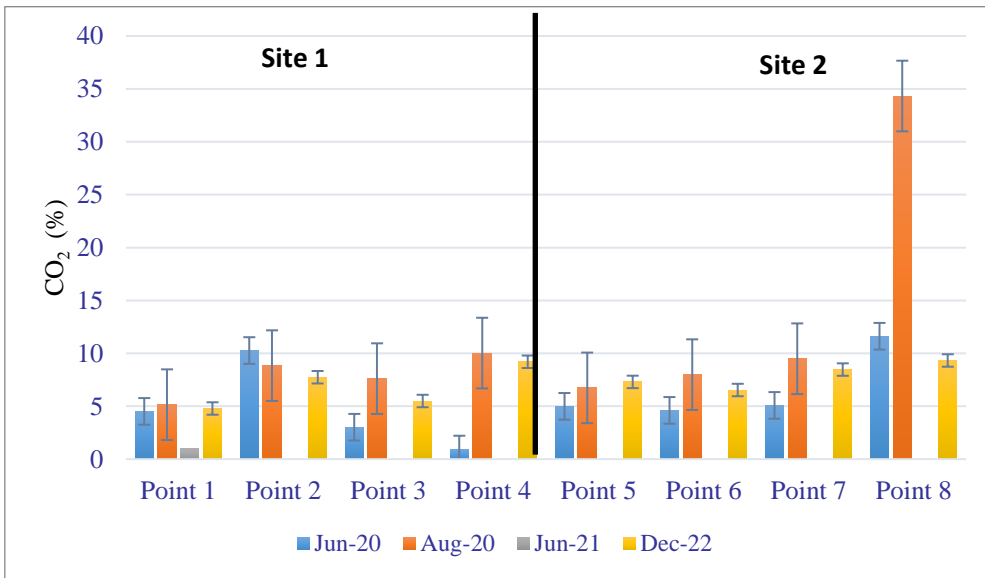


Figure 3. Carbon dioxide (CO<sub>2</sub>) share percentage in the upper layer of sediments (0-5 cm), during the research period (2020-2022).

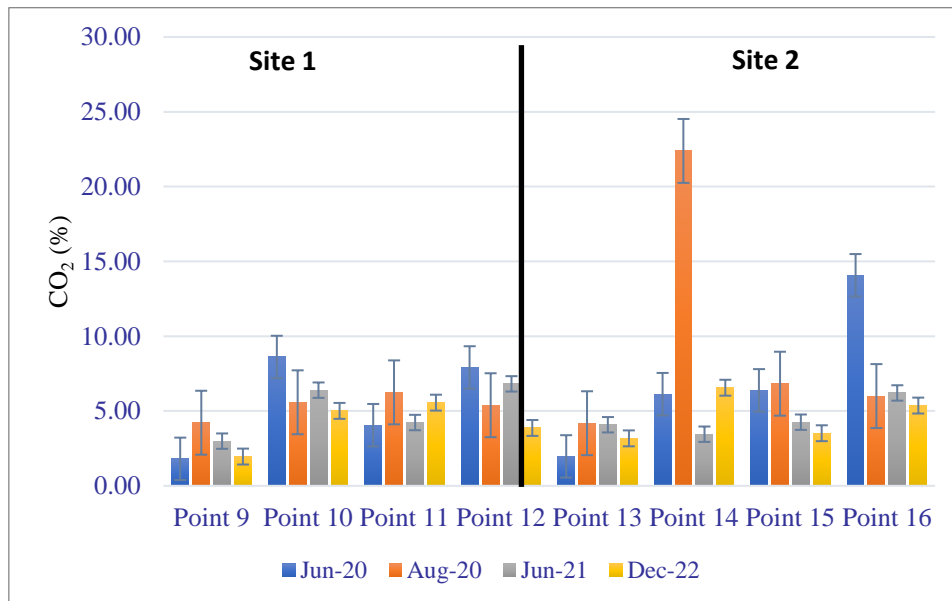


Figure 4. Carbon dioxide (CO<sub>2</sub>) share percentage in the bottom layer of sediments (5-10 cm), during the research period (2020-2022).

### 3. Silicon (Si)

Table 5. Descriptive statistics of Silicon dioxide (SiO<sub>2</sub>) (%) in sediment.

	N	Mean	Std. Deviation	Std. Error Mean
Jun-20	16	59.91	14.993	3.748
Aug-20	16	65.58	9.415	2.354
Jun-21	16	62.46	8.075	2.019
Dec-22	16	60.47	9.001	2.250

Table 6. T-test statistics of silicon dioxide (%) in sediments for four-time intervals.

	t	df	Sig. (2-tailed)	Mean Difference	95% Confidence Interval of the Difference	
					Lower	Upper
Jun-20	15.983	15	.000	59.908	51.92	67.90
Aug-20	27.863	15	.000	65.584	60.57	70.60
Jun-21	30.936	15	.000	62.456	58.15	66.76
Dec-22	26.875	15	.000	60.475	55.68	65.27

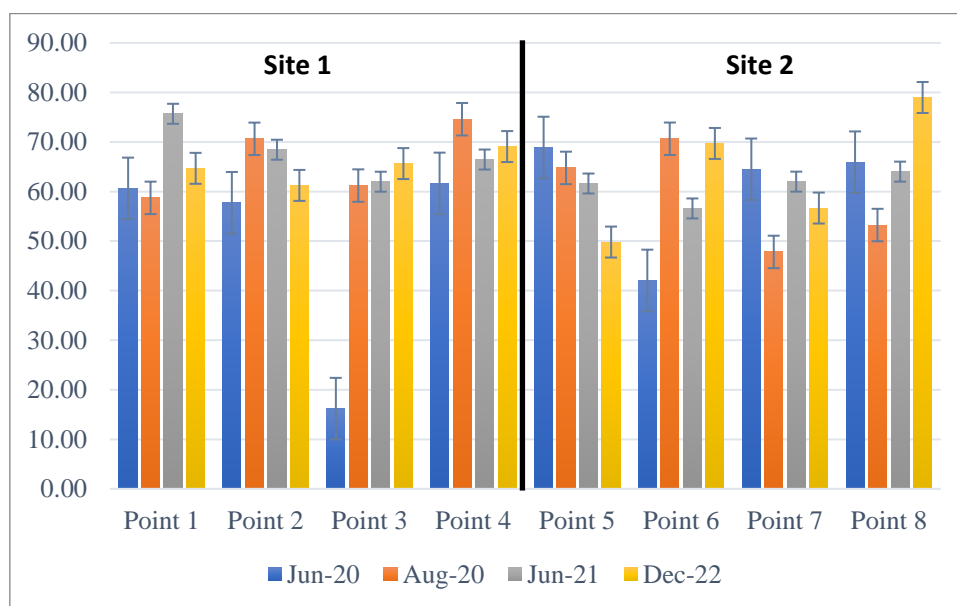


Figure 5. Silicon dioxide (SiO<sub>2</sub>) share percentage in the upper layer of sediments (0-5 cm), during the research period (2020-2022).

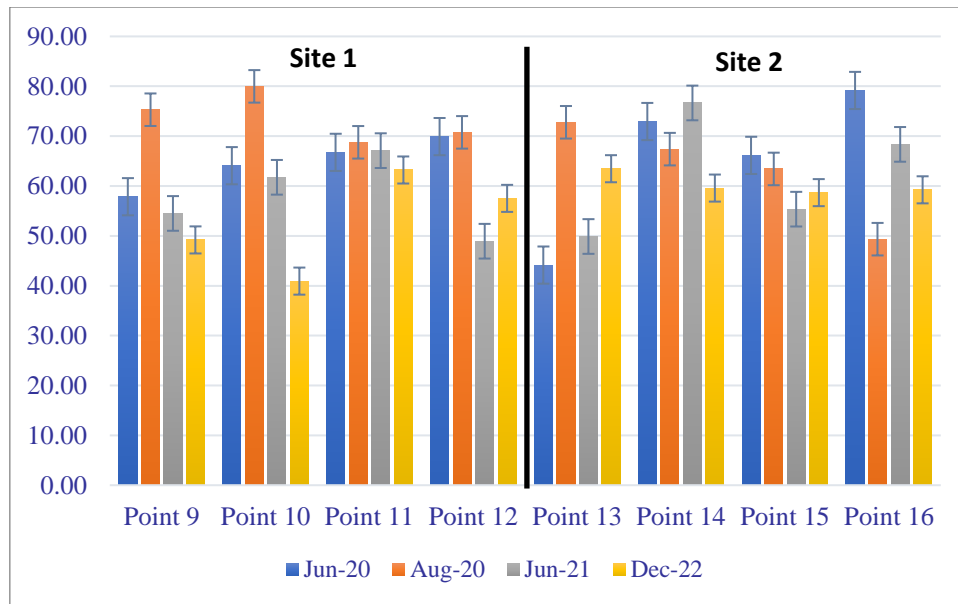


Figure 6. Silicon dioxide (SiO<sub>2</sub>) share percentage in the bottom layer of sediments (5-10 cm), during the research period (2020-2022).

#### 4. Iron (Fe)

Table 7. Descriptive statistics of ferric oxide (Fe<sub>2</sub>O<sub>3</sub>) percentage in sediment.

	N	Mean	Std. Deviation	Std. Error Mean
Jun-20	16	.33	.316	.079
Aug-20	16	.31	.362	.091
Jun-21	16	.91	.208	.052
Dec-22	16	.70	.357	.089

Table 8. T-test statistics of ferric oxide (Fe<sub>2</sub>O<sub>3</sub>) percentage in sediments for four-time intervals.

	t	df	Sig. (2-tailed)	Mean Difference	95% Confidence Interval of the Difference	
					Lower	Upper
Jun-20	4.198	15	.001	.331	.16	.50
Aug-20	3.466	15	.003	.314	.12	.51
Jun-21	17.558	15	.000	.915	.80	1.03
Dec-22	7.876	15	.000	.703	.51	.89

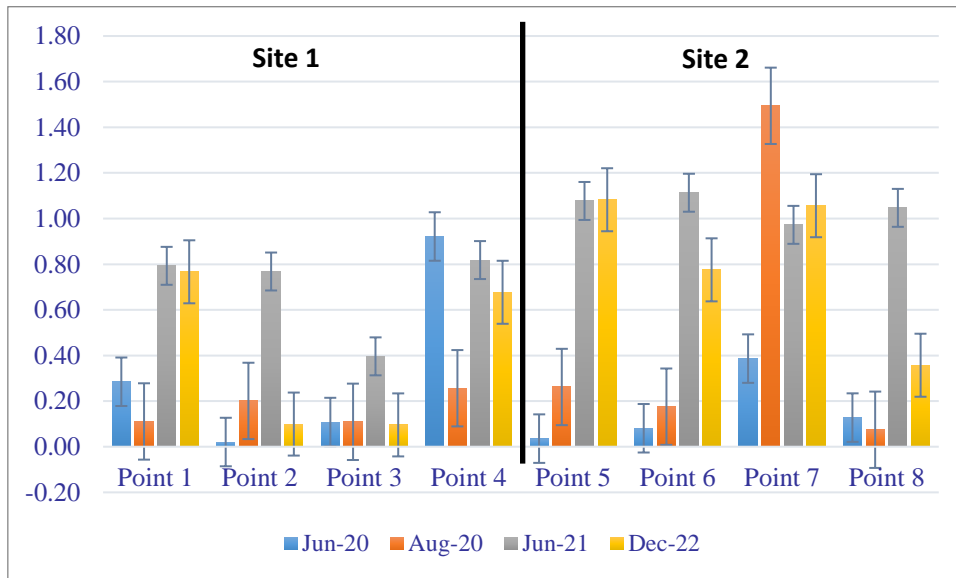


Figure 7. Ferric oxide (Fe<sub>2</sub>O<sub>3</sub>) share percentage in the upper layer of sediments (0-5 cm), during the research period (2020-2022).

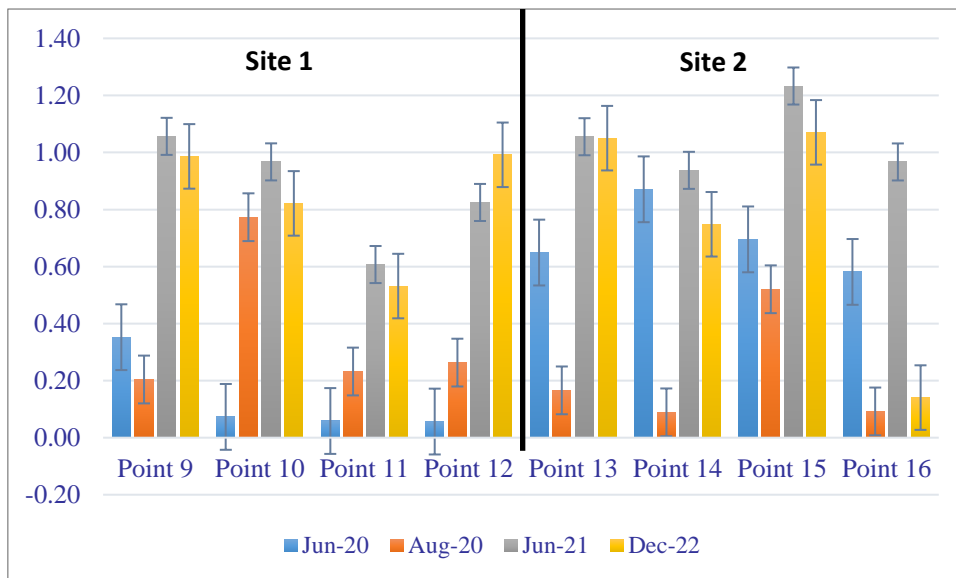


Figure 8. Ferric oxide (Fe<sub>2</sub>O<sub>3</sub>) share percentage in the bottom layer of sediments (5-10 cm), during the research period (2020-2022).

5. Aluminum (Al)

Table 9. Descriptive statistics of aluminum oxide (Al<sub>2</sub>O<sub>3</sub>) percentage in sediment.

	N	Mean	Std. Deviation	Std. Error Mean
Jun-20	16	3.53	3.012	.753
Aug-20	16	4.28	2.723	.681
Jun-21	16	5.66	1.301	.325
Dec-22	16	4.74	2.546	.636

Table 10. T-test statistics of aluminum oxide (Al<sub>2</sub>O<sub>3</sub>) percentage in sediments for four-time intervals.

	t	df	Sig. (2-tailed)	Mean Difference	95% Confidence Interval of the Difference	
					Lower	Upper
Jun-20	4.681	15	.000	3.525	1.92	5.13
Aug-20	6.282	15	.000	4.276	2.82	5.73
Jun-21	17.393	15	.000	5.657	4.96	6.35
Dec-22	7.450	15	.000	4.741	3.38	6.10

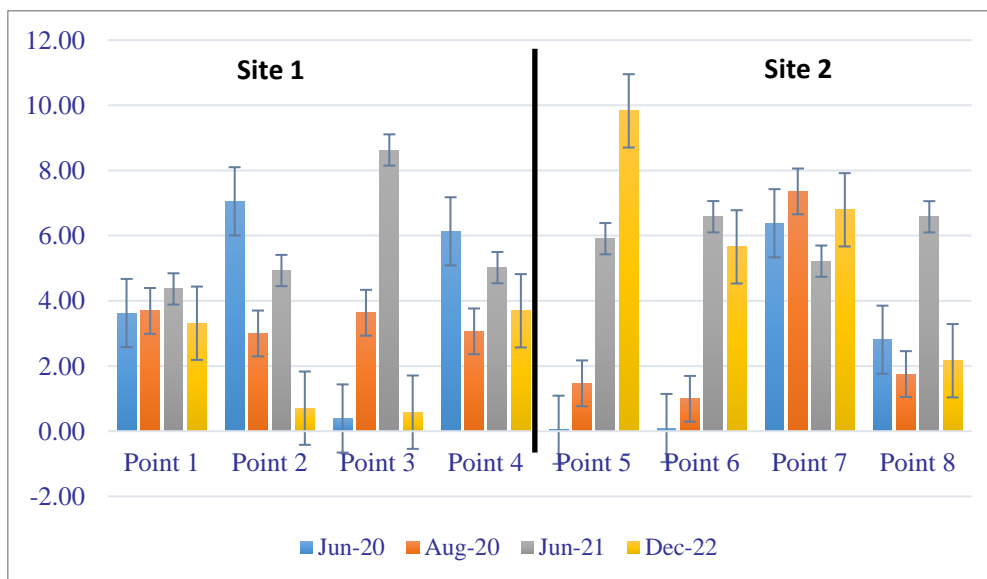


Figure 9. Aluminum oxide (Al<sub>2</sub>O<sub>3</sub>) share percentage in the upper layer of sediments (0-5 cm), during the research period (2020-2022).

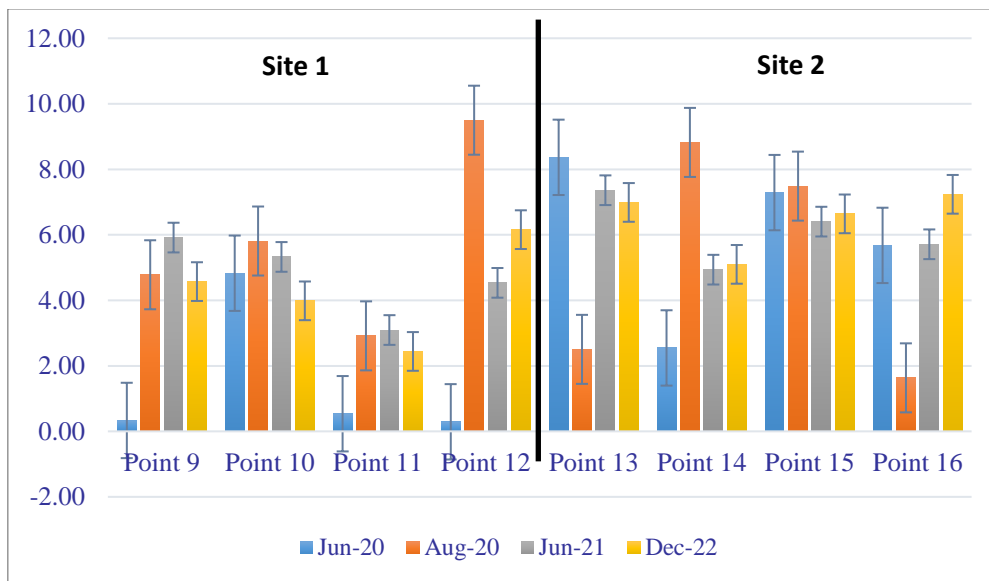


Figure 10. Aluminum oxide (Al<sub>2</sub>O<sub>3</sub>) share percentage in the bottom layer of sediments (5-10 cm), during the research period (2020-2022).

#### 6. Manganese (Mn)

Table 11. Descriptive statistics of Manganese (II) oxide (MnO) percentage in sediment.

	N	Mean	Std. Deviation	Std. Error Mean
Jun-20	16	.04	.044	.011
Aug-20	16	.05	.080	.020
Jun-21	16	.14	.032	.008
Dec-22	16	.14	.042	.011

Table 12. T-test statistics of manganese(II) oxide (MnO) percentage in sediments for four-time intervals.

	t	df	Sig. (2-tailed)	Mean Difference	95% Confidence Interval of the Difference	
					Lower	Upper
Jun-20	3.454	15	.004	.038	.01	.06
Aug-20	2.738	15	.015	.055	.01	.10
Jun-21	18.161	15	.000	.145	.13	.16
Dec-22	12.961	15	.000	.137	.11	.16



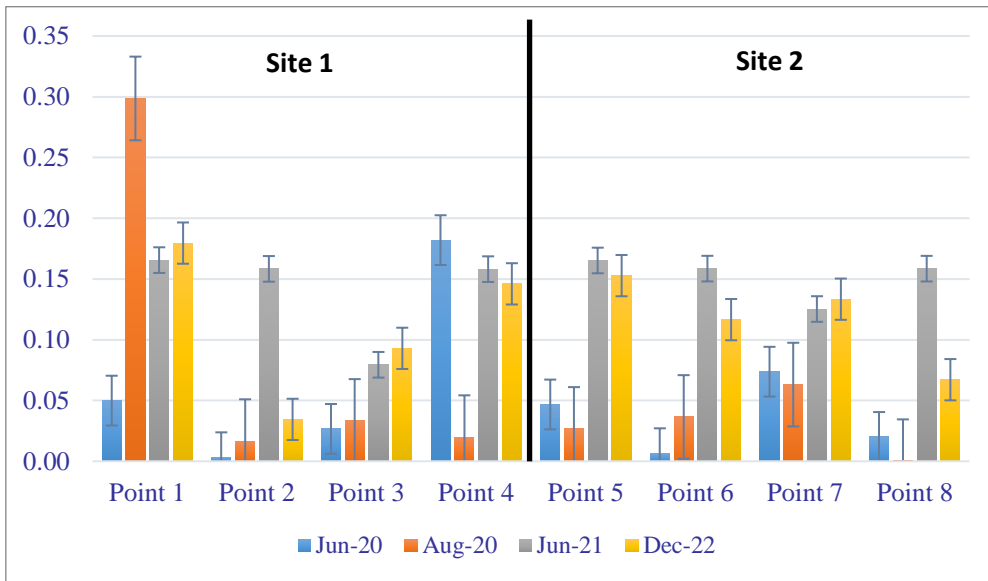


Figure 11. Manganese (II) oxide (MnO) share percentage in the upper layer of sediments (0-5 cm), during the research period (2020-2022).

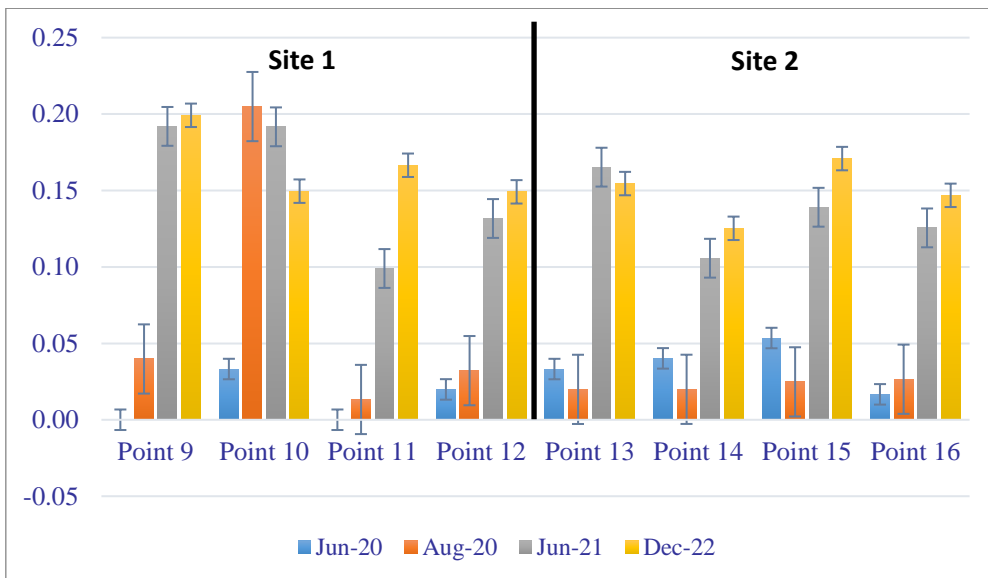


Figure 12. Manganese (II) oxide (MnO) share percentage in the bottom layer of sediments (5-10 cm), during the research period (2020-2022).

## 7. Calcium (Ca)

Table 13. Descriptive statistics of calcium oxide (CaO) percentage in sediment.

	N	Mean	Std. Deviation	Std. Error Mean
Jun-20	16	6.67	5.096	1.274
Aug-20	16	6.17	2.722	.680
Jun-21	16	1.85	1.636	.409
Dec-22	16	1.87	2.160	.540

Table 14. T-test statistics of calcium oxide (CaO) percentage in sediments for four-time intervals.

t	df	Sig. (2-tailed)	Mean Difference	95% Confidence Interval of the Difference		
				Lower	Upper	
Jun-20	5.233	15	.000	6.667	3.95	9.38
Aug-20	9.065	15	.000	6.168	4.72	7.62
Jun-21	4.514	15	.000	1.846	.97	2.72
Dec-22	3.472	15	.003	1.875	.72	3.03

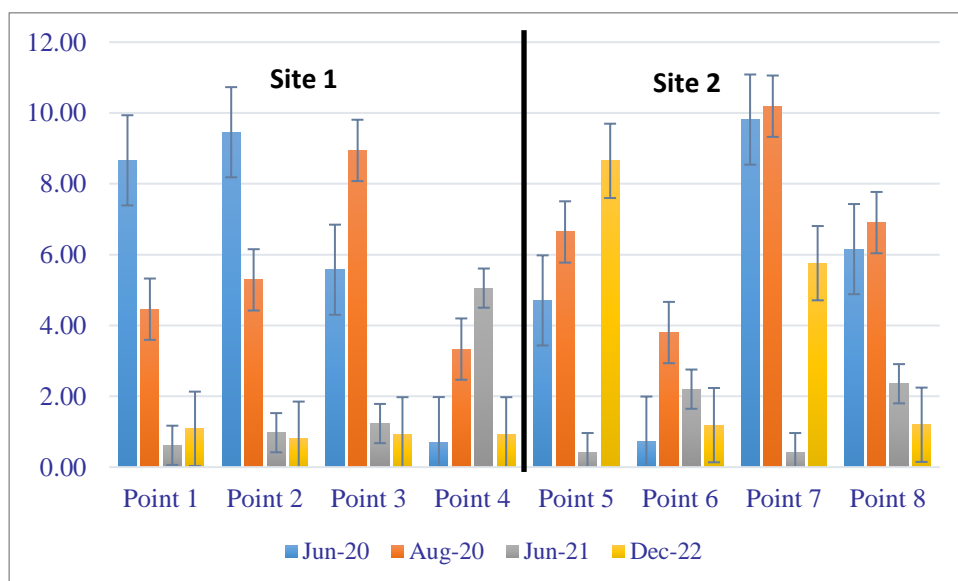


Figure 13. Calcium oxide (CaO) share percentage in the upper layer of sediments (0-5 cm), during the research period (2020-2022).

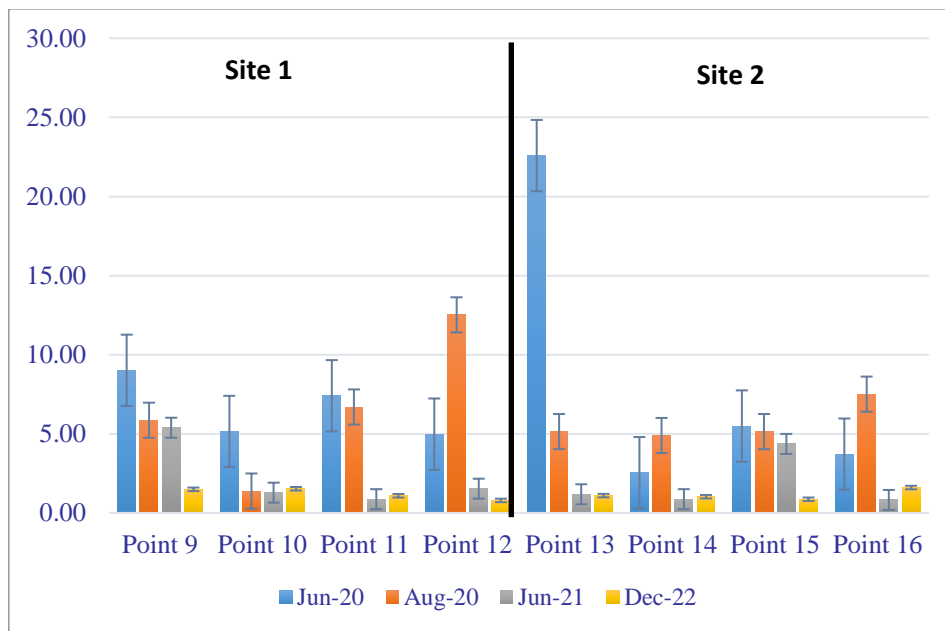


Figure 14. Calcium oxide (CaO) share percentage in the bottom layer of sediments (5-10 cm), during the research period (2020-2022).

### 8. Magnesium (Mg)

Table 15. Descriptive statistics of magnesium oxide (MgO) percentage in sediment.

	N	Mean	Std. Deviation	Std. Error
Jun-20	16	4.71	3.218	.804
Aug-20	16	5.66	3.866	.967
Jun-21	16	6.38	4.268	1.067
Dec-22	16	7.23	7.327	1.832

Table 16. T-test statistics of magnesium oxide (MgO) percentage in sediment for four-time intervals.

	t	df	Sig. (2-tailed)	Mean Difference	95% Confidence Interval of the Difference	
					Lower	Upper
Jun-20	5.852	15	.000	4.708	2.99	6.42
Aug-20	5.854	15	.000	5.658	3.60	7.72

Jun-21	5.981	15	.000	6.382	4.11	8.66
Dec-22	3.946	15	.001	7.228	3.32	11.13

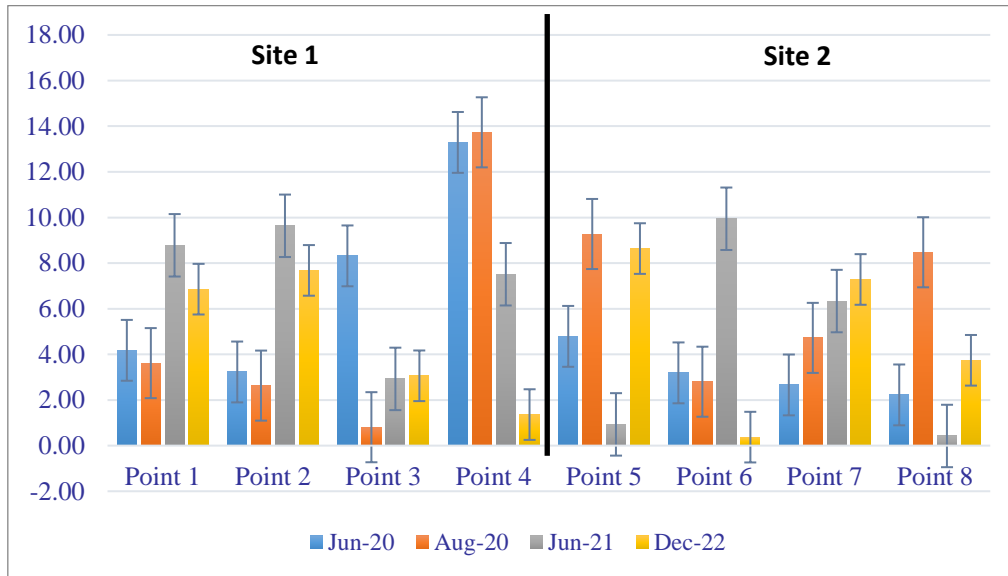


Figure 15. Magnesium oxide (MgO) share percentage in the upper layer of sediments (0-5 cm), during the research period (2020-2022).

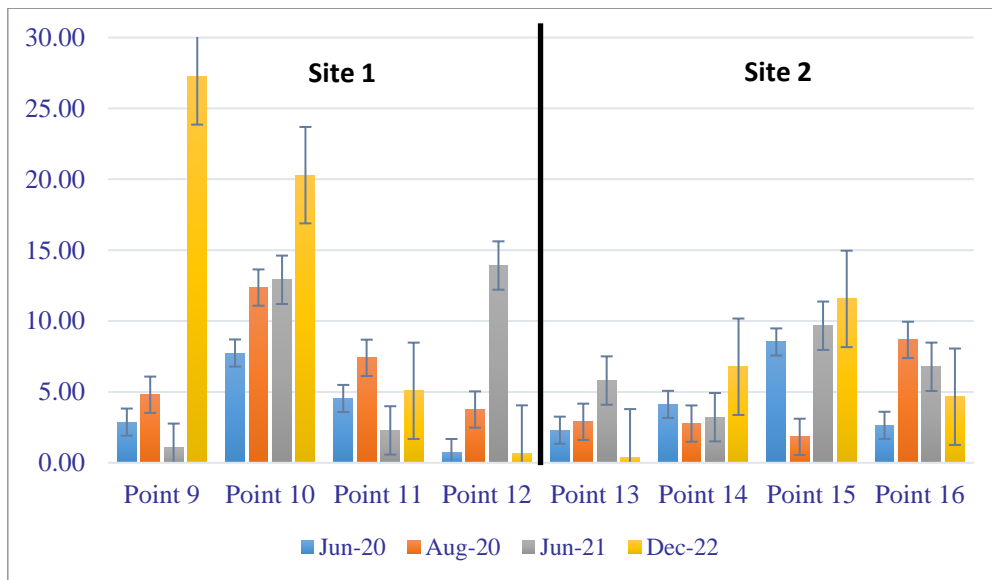


Figure 16. Magnesium oxide (MgO) share percentage in the bottom layer of sediments (5-10 cm), during the research period (2020-2022).

## 9. Total Nitrogen (TN)

Table 17. Descriptive statistics of total nitrogen (TN) percentage in sediment.

	N	Mean	Std. Deviation	Std. Error Mean
Jun-20	16	.95	.083	.021
Aug-20	16	.80	.342	.086
Jun-21	16	1.42	1.963	.491
Dec-22	16	.86	.171	.043

Table 18. T-test statistics of total nitrogen (TN) in sediments for four-time intervals.

	t	df	Sig. (2-tailed)	Mean Difference	95% Confidence Interval of the Difference	
					Lower	Upper
Jun-20	45.712	15	.000	.948	.90	.99
Aug-20	9.338	15	.000	.800	.62	.98
Jun-21	2.902	15	.011	1.424	.38	2.47
Dec-22	20.190	15	.000	.861	.77	.95

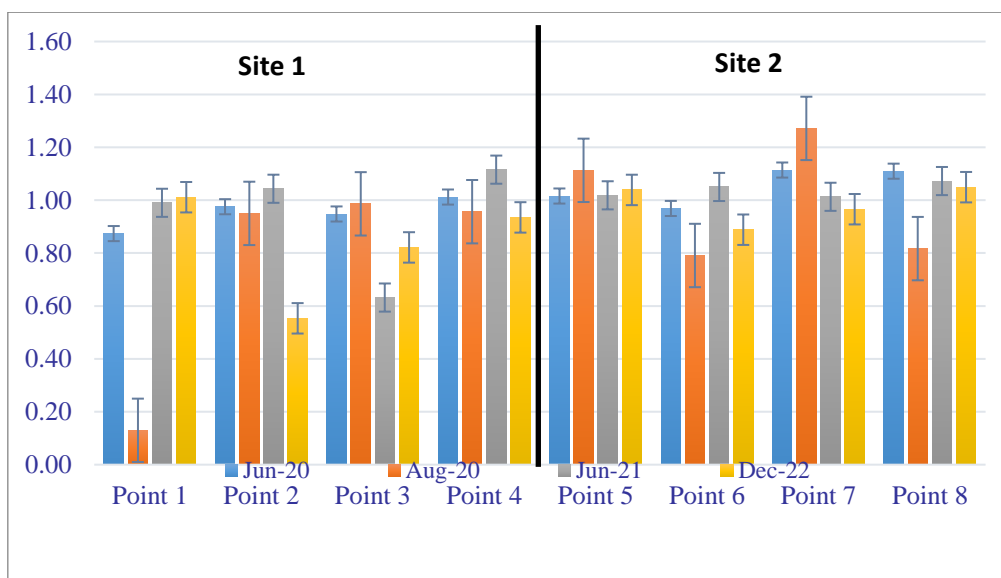


Figure 17. Total nitrogen (TN) share percentage in the upper layer of sediments (0-5 cm), during the research period (2020-2022).

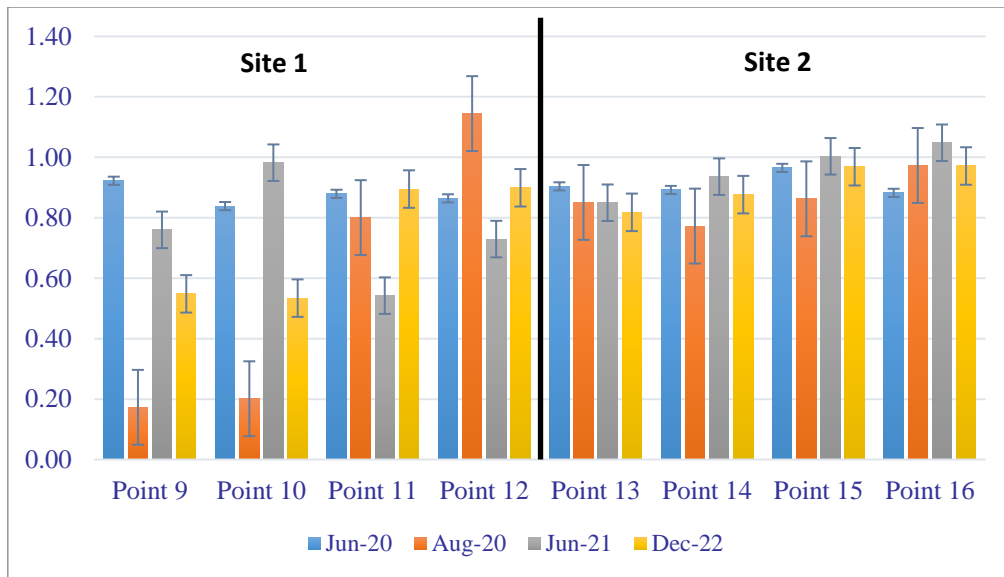


Figure 18. Total nitrogen (TN) share percentage in the bottom layer of sediments (5-10 cm), during the research period (2020-2022).

#### 10. Phosphorus (P)

Table 19. Descriptive statistics of diphosphorus pentoxide (P<sub>2</sub>O<sub>5</sub>) percentage in sediment.

	N	Mean	Std. Deviation	Std. Error Mean
Jun-20	16	.23	.141	.035
Aug-20	16	.21	.098	.025
Jun-21	16	.54	.029	.007
Dec-22	16	.56	.036	.009

Table 20. T-test statistics of diphosphorus pentoxide (P<sub>2</sub>O<sub>5</sub>) in sediments for four-time intervals.

	t	df	Sig. (2-tailed)	Mean Difference	95% Confidence Interval of the Difference	
					Lower	Upper
Jun-20	6.628	15	.000	.233	.16	.31
Aug-20	8.460	15	.000	.208	.16	.26
Jun-21	75.743	15	.000	.542	.53	.56
Dec-22	62.254	15	.000	.558	.54	.58

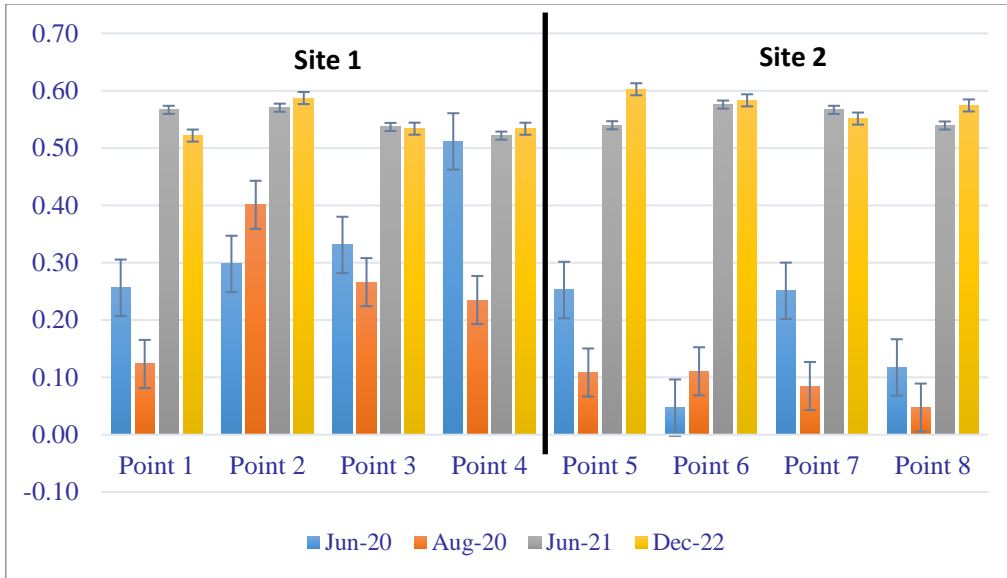


Figure 19. Diphosphorus pentoxide (P<sub>2</sub>O<sub>5</sub>) share percentage in the upper layer of sediments (0-5 cm), during the research period (2020-2022).

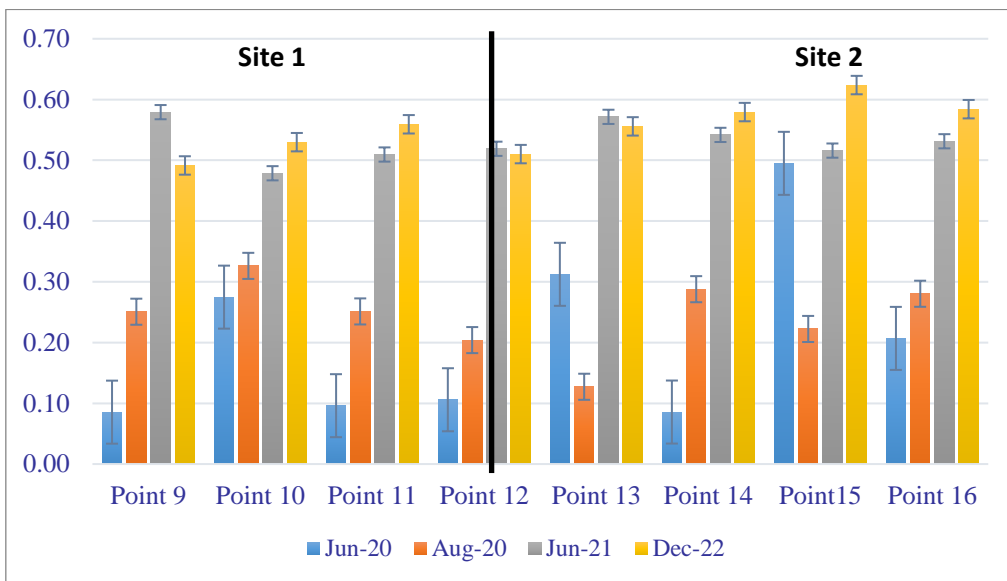


Figure 20. Diphosphorus pentoxide (P<sub>2</sub>O<sub>5</sub>) share percentage in the bottom layer of sediments (5-10 cm), during the research period (2020-2022).

## B. Sediment phosphorus fractions

### 1. NH<sub>4</sub>Cl-P fraction

Table 21. Descriptive statistics of (NH<sub>4</sub>Cl-P) fraction (mg P/g D.M.) in the sediment.

	N	Mean	Std. Deviation	Std. Error Mean
Jun-20	16	0.03	0.01	0.00
Aug-20	16	0.04	0.02	0.00
Jun-21	16	0.04	0.07	0.02
Dec-22	16	0.08	0.11	0.03

Table 22. T-test statistics of (NH<sub>4</sub>Cl-P) fraction (mg P/g D.M.) in sediments for four-time intervals.

	t	df	Sig. (2-tailed)	Mean Difference	95% Confidence Interval of the Difference	
					Lower	Upper
Jun-20	13.402	15	.000	0.03	0.03	0.04
Aug-20	10.109	15	.000	0.04	0.03	0.05
Jun-21	2.441	15	.028	0.04	0.01	0.08
Dec-22	3.046	15	.008	0.08	0.03	0.14

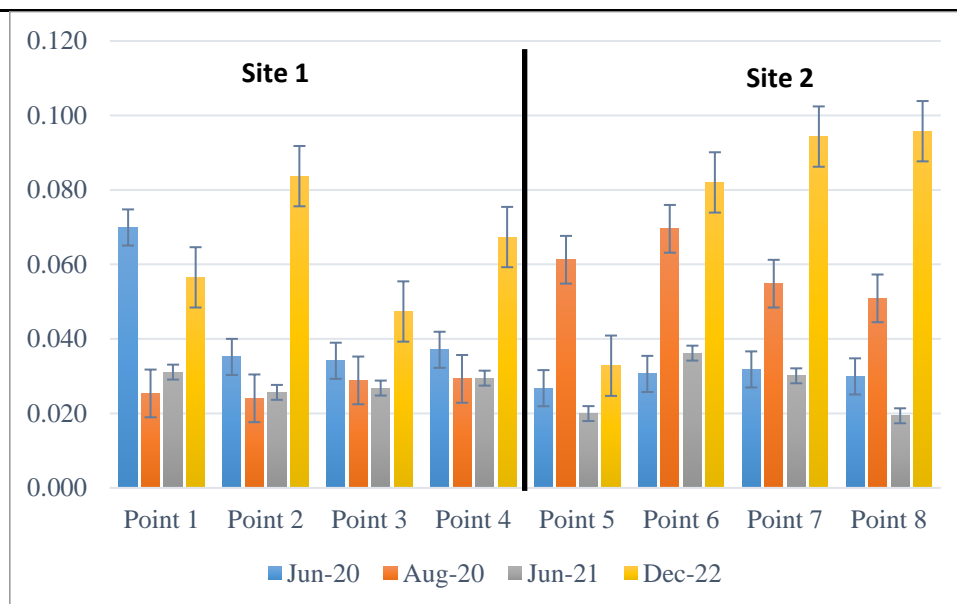


Figure 21. NH<sub>4</sub>Cl-P fraction (mg P/g D. M.) in the upper layer of sediments (0-5 cm), during the research period.



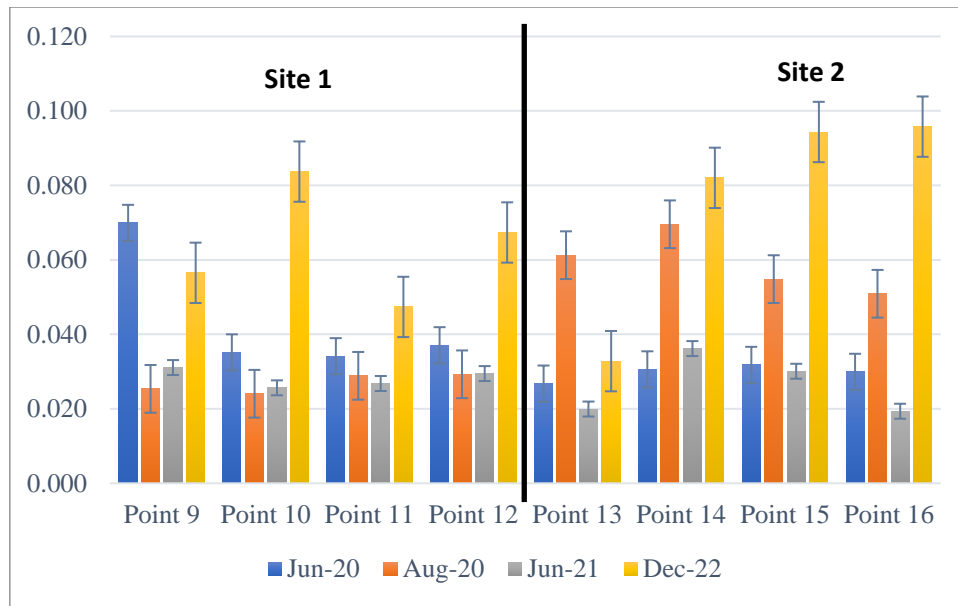


Figure 22. NH<sub>4</sub>Cl-P fraction (mg P/g D. M.) in the bottom layer of sediments (5-10 cm), during the research period.

## 2. BD-P fraction

Table 23. Descriptive statistics of (BD-P) fraction (mg P/g D.M.) in the sediment.

	N	Mean	Std. Deviation	Std. Error Mean
Jun-20	16	0.26	0.10	0.02
Aug-20	16	0.14	0.10	0.02
Jun-21	16	0.05	0.04	0.01
Dec-22	16	0.16	0.09	0.02

Table 24. T-test statistics of (BD-P) fraction (mg P/g D.M.) in sediments for four-time intervals.

	T	df	Sig. (2-tailed)	Mean Difference	95% Confidence Interval of the Difference	
					Lower	Upper
Jun-20	10.606	15	.000	0.26	0.21	0.31
Aug-20	5.636	15	.000	0.14	0.09	0.19
Jun-21	5.962	15	.000	0.05	0.03	0.07
Dec-22	7.441	15	.000	0.16	0.11	0.21

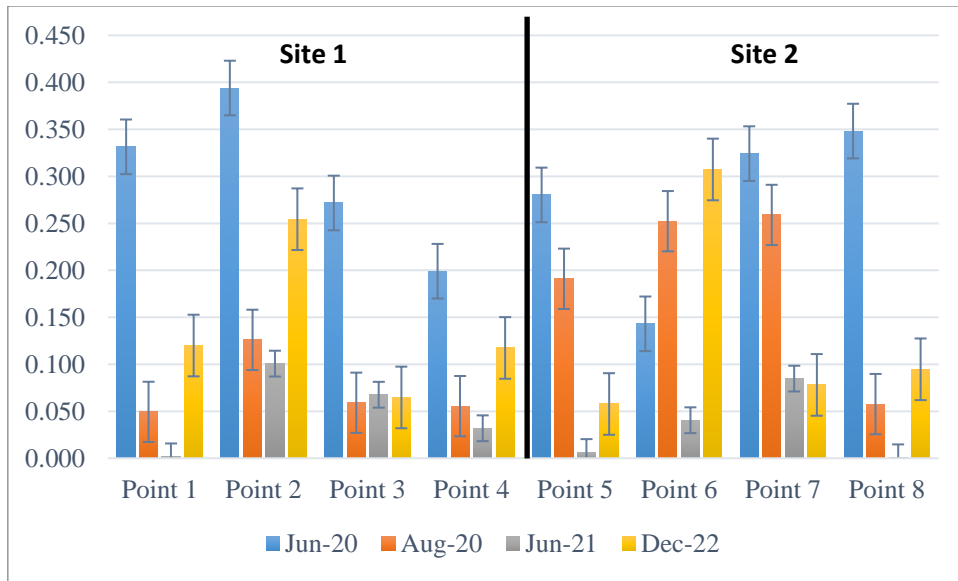


Figure 23. BD-P fraction (mg P/g D. M.) in the upper layer of sediments (0-5 cm), during the research period.

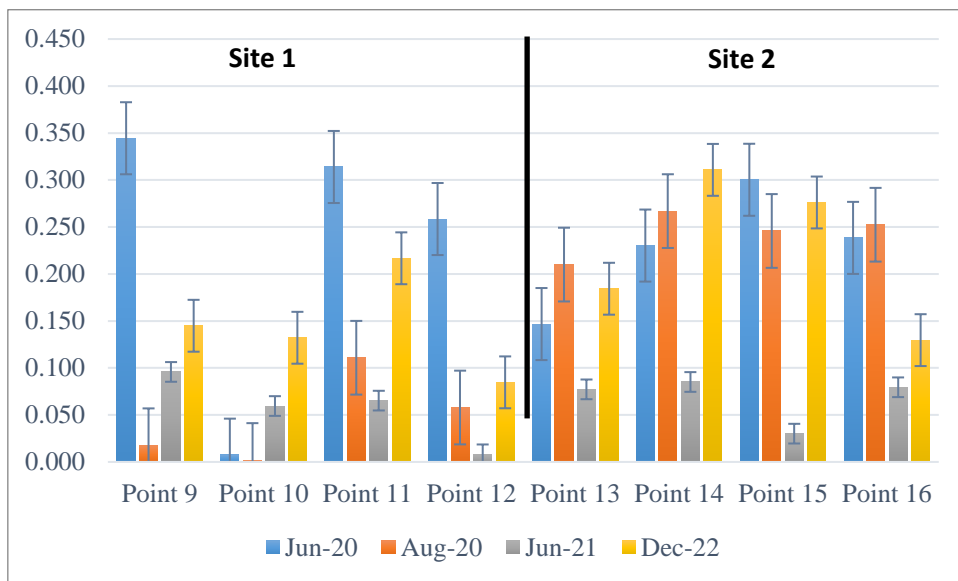


Figure 24. BD-P fraction (mg P/g D. M.) in the bottom layer of sediments (5-10 cm), during the research period.

3. NaOH-rP fraction:

Table 25. Descriptive statistics of (NaOH-rP) fraction (mg P/g D.M.) in the sediment.

	N	Mean	Std. Deviation	Std. Error Mean
Jun-20	16	0.03	0.00	0.00
Aug-20	16	0.13	0.11	0.03
Jun-21	16	0.03	0.01	0.00
Dec-22	16	0.29	0.03	0.01

Table 26. T-test statistics of (NaOH-rP) fraction (mg P/g D.M.) in sediments for four-time intervals.

	t	df	Sig. (2-tailed)	Mean Difference	95% Confidence Interval of the Difference	
					Lower	Upper
Jun-20	23.985	15	.000	0.028	0.026	0.031
Aug-20	4.824	15	.000	0.128	0.071	0.184
Jun-21	13.698	15	.000	0.033	0.028	0.038
Dec-22	35.046	15	.000	0.291	0.274	0.309

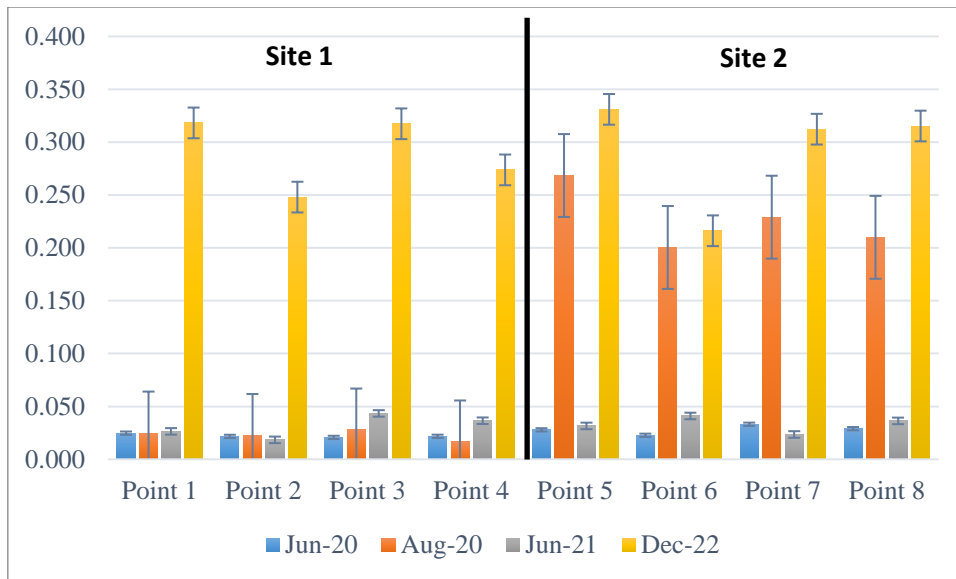


Figure 25. NaOH-rP fraction (mg P/g D. M.) in the upper layer of sediments (0-5 cm), during the research period.

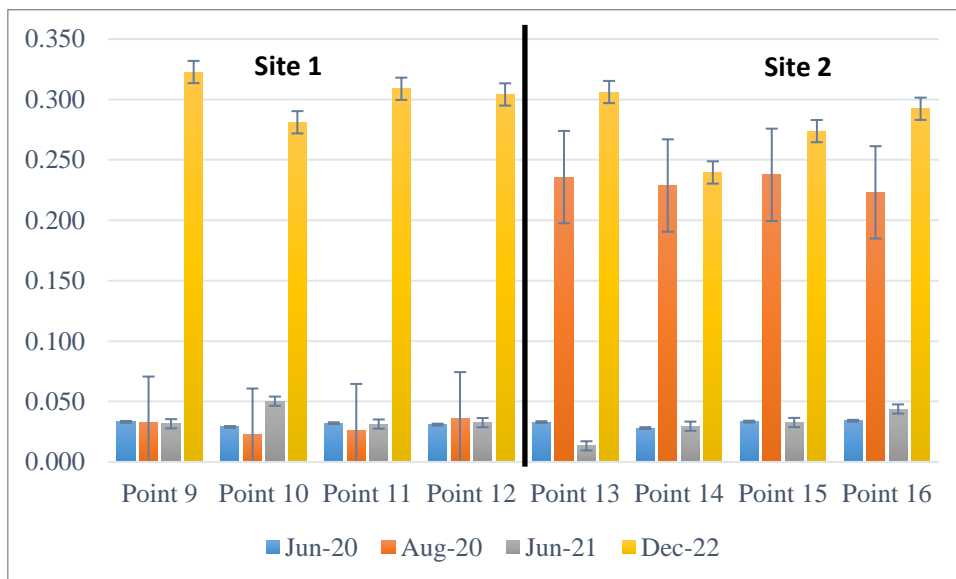


Figure 26. NaOH-rP fraction (mg P/g D. M.) in the bottom layer of sediments (5-10 cm), during the research period.

#### 4. NaOH-nrP fraction

Table 27. Descriptive statistics of (NaOH-nrP) fraction (mg P/g D.M.) in the sediment.

	N	Mean	Std. Deviation	Std. Error Mean
Jun-20	16	0.361	0.111	0.028
Aug-20	16	0.816	0.634	0.158
Jun-21	16	0.285	0.142	0.035
Dec-22	16	1.503	0.172	0.043

Table 28. T-test statistics of (NaOH-nrP) fraction (mg P/g D.M.) in sediments for four-time intervals.

	t	df	Sig. (2-tailed)	Mean Difference	95% Confidence Interval of the Difference	
					Lower	Upper
Jun-20	12.981	15	.000	0.361	0.302	0.421
Aug-20	5.150	15	.000	0.816	0.478	1.154
Jun-21	8.056	15	.000	0.285	0.210	0.361
Dec-22	34.913	15	.000	1.503	1.411	1.594

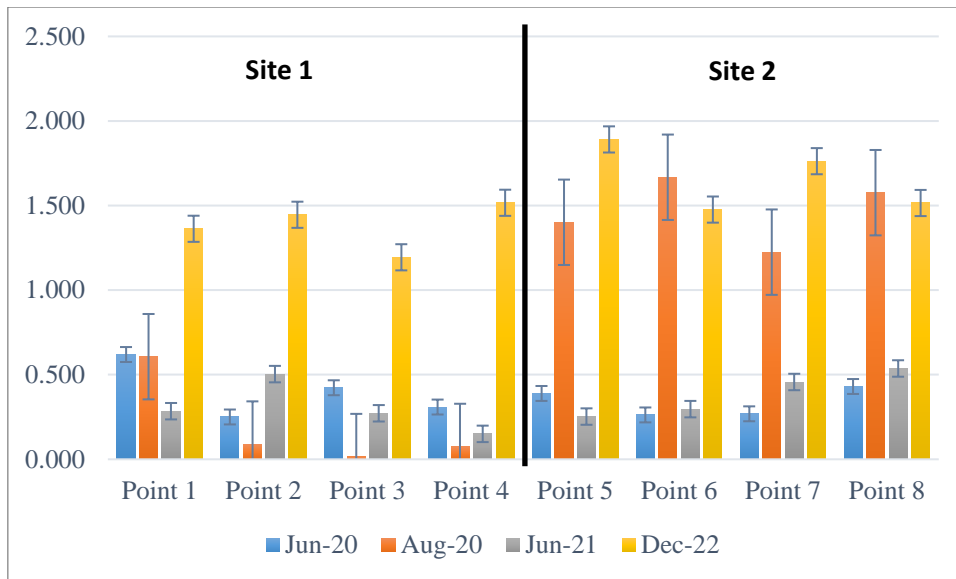


Figure 27. NaOH-nrP fraction (mg P/g D. M.) in the upper layer of sediments (0-5 cm), during the research period.

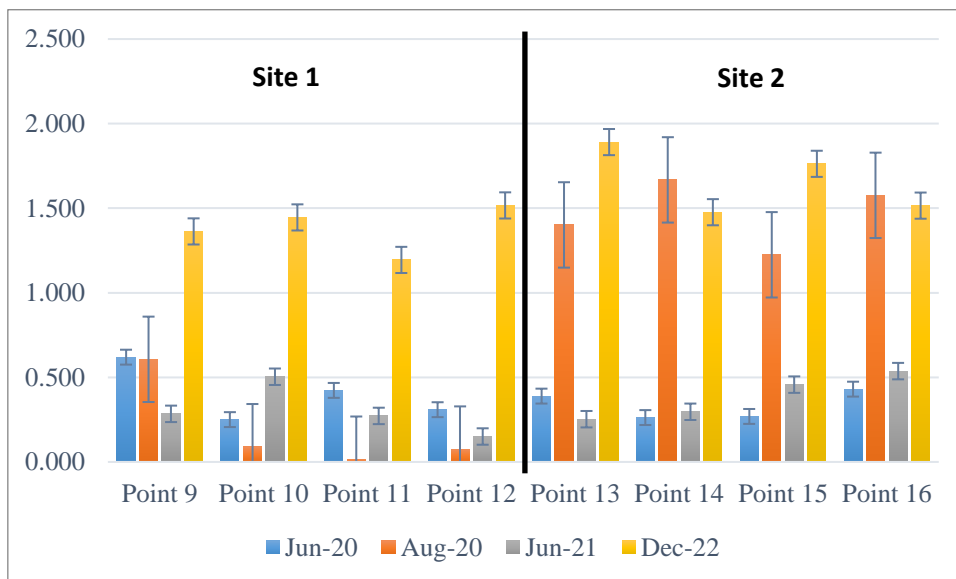


Figure 28. NaOH-nrP fraction (mg P/g D. M.) in the bottom layer of sediments (5-10 cm), during the research period.

7. NaOH-TP fraction

Table 29. Descriptive statistics of (NaOH-TP) fraction (mg P/g D.M.) in the sediment.

	N	Mean	Std. Deviation	Std. Error Mean
Jun-20	16	0.390	0.113	0.028
Aug-20	16	0.944	0.736	0.184
Jun-21	16	0.318	0.146	0.036
Dec-22	16	1.794	0.169	0.042

Table 30. T-test statistics of (NaOH-TP) fraction (mg P/g D.M.) in sediments for four-time intervals.

	t	df	Sig. (2-tailed)	Mean Difference	95% Confidence Interval of the Difference	
					Lower	Upper
Jun-20	13.823	15	.000	0.390	0.330	0.450
Aug-20	5.128	15	.000	0.944	0.551	1.336
Jun-21	8.717	15	.000	0.318	0.240	0.396
Dec-22	42.453	15	.000	1.794	1.704	1.884

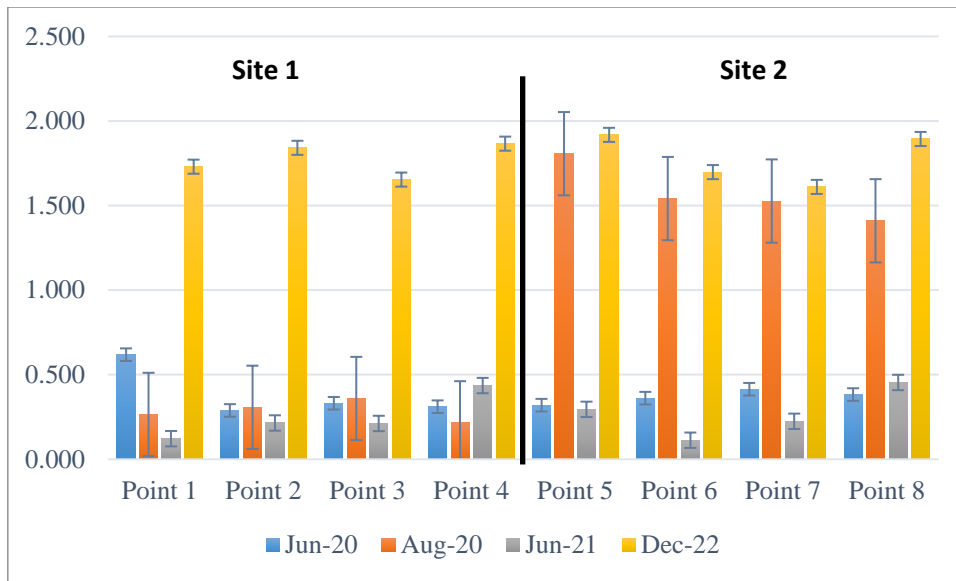


Figure 29. NaOH-TP fraction (mg P/g D. M.) in the upper layer of sediments (0-5 cm), during the research period.

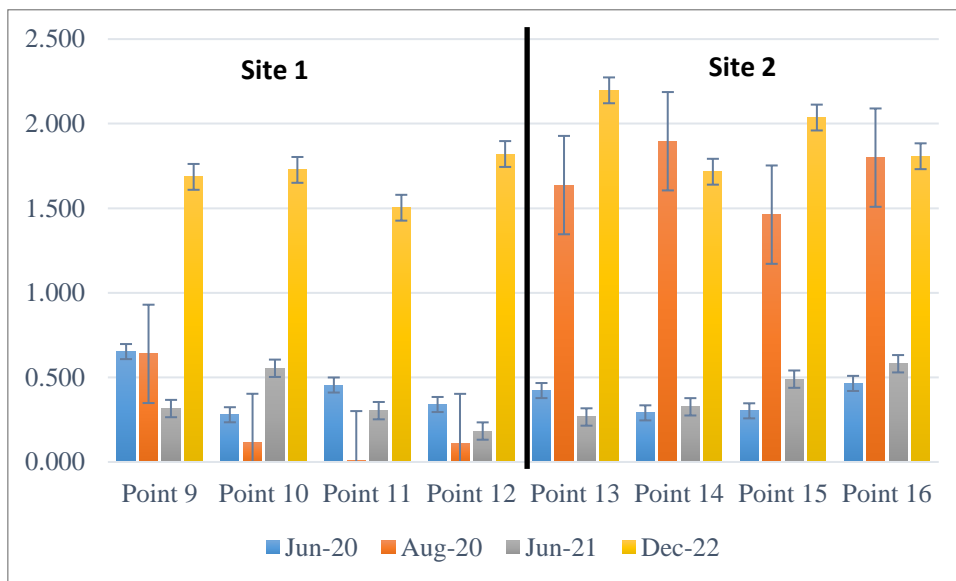


Figure 30. NaOH-TP fraction (mg P/g D. M.) in the bottom layer of sediments (5-10 cm), during the research period.



## 8. HCl-P fraction

Table 31. Descriptive statistics of (HCl-P) fraction (mg P/g D.M.) in the sediment.

	N	Mean	Std. Deviation	Std. Error
				Mean
Jun-20	16	0.330	0.069	0.017
Aug-20	16	0.118	0.157	0.039
Jun-21	16	0.020	0.055	0.014
Dec-22	16	0.436	0.156	0.039

Table 32. T-test statistics of (HCl-P) fraction (mg P/g D.M.) in sediments for four-time intervals.

	t	df	Sig. (2-tailed)	Mean Difference	95% Confidence Interval of the Difference	
					Lower	Upper
Jun-20	19.213	15	.000	0.330	0.293	0.366
Aug-20	3.021	15	.009	0.118	0.035	0.202
Jun-21	1.420	15	.006	0.020	0.010	0.049
Dec-22	11.201	15	.000	0.436	0.353	0.520

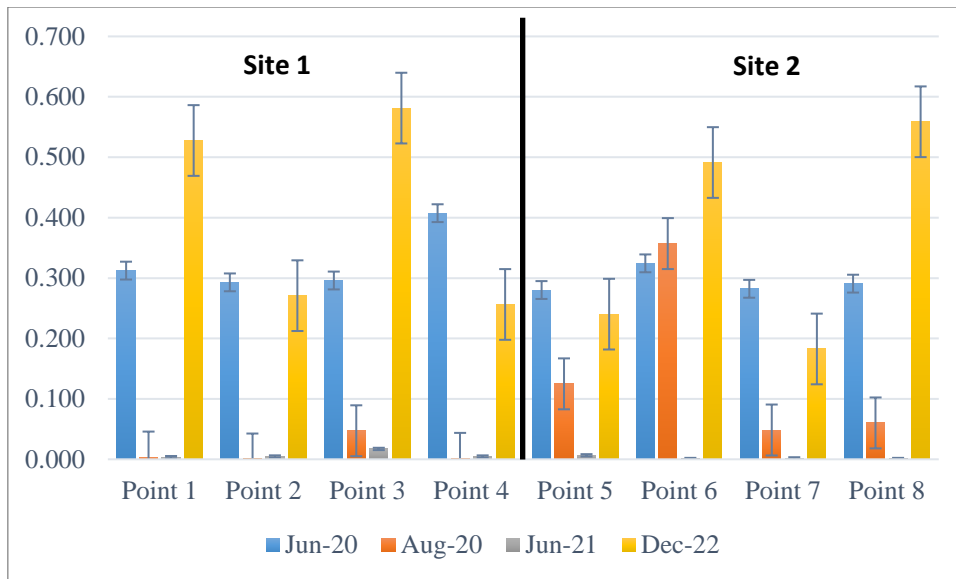


Figure 31. HCl-P fraction (mg P/g D. M.) in the upper layer of sediments (0-5 cm), during the research period.

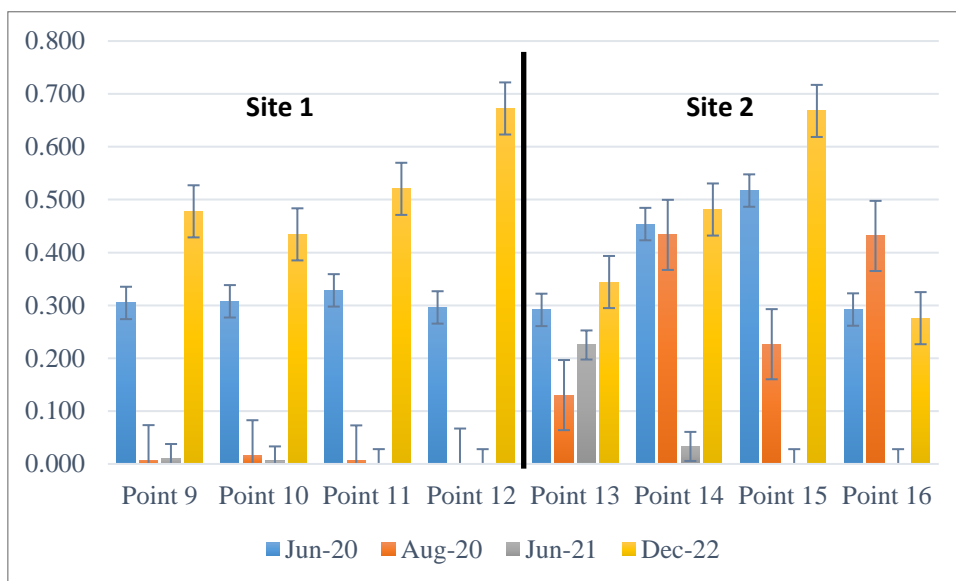


Figure 32. HCl-P fraction (mg P/g D. M.) in the bottom layer of sediments (5-10 cm), during the research period.

## 9. Res-P fraction

Table 33. Descriptive statistics of (res-P) fraction (mg P/g D.M.) in the sediment.

	N	Mean	Std. Deviation	Std. Error Mean
Jun-20	16	0.089	0.048	0.012
Aug-20	16	0.112	0.112	0.028
Jun-21	16	0.187	0.181	0.045
Dec-22	16	0.098	0.067	0.017

Table 34. T-test statistics of (res-p) fraction (mg P/g D.M.) in sediments for four-time intervals.

	t	df	Sig. (2-tailed)	Mean Difference	95% Confidence Interval of the Difference	
					Lower	Upper
Jun-20	7.331	15	.000	0.089	0.063	0.115
Aug-20	4.034	15	.001	0.112	0.053	0.172
Jun-21	4.137	15	.001	0.187	0.091	0.283
Dec-22	5.896	15	.000	0.098	0.063	0.134

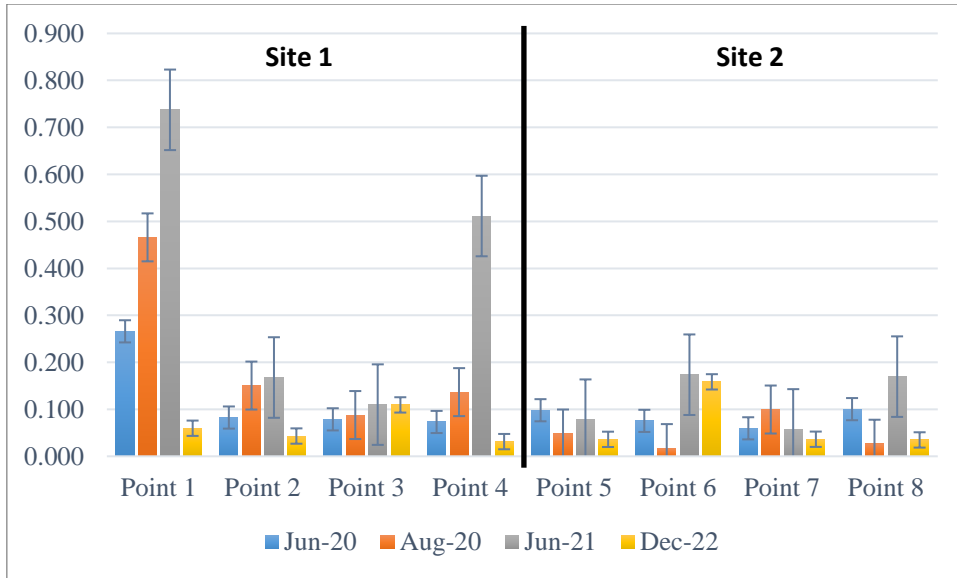


Figure 33. Res-P fraction (mg P/g D. M.) in the upper layer of sediments (0-5 cm), during the research period.

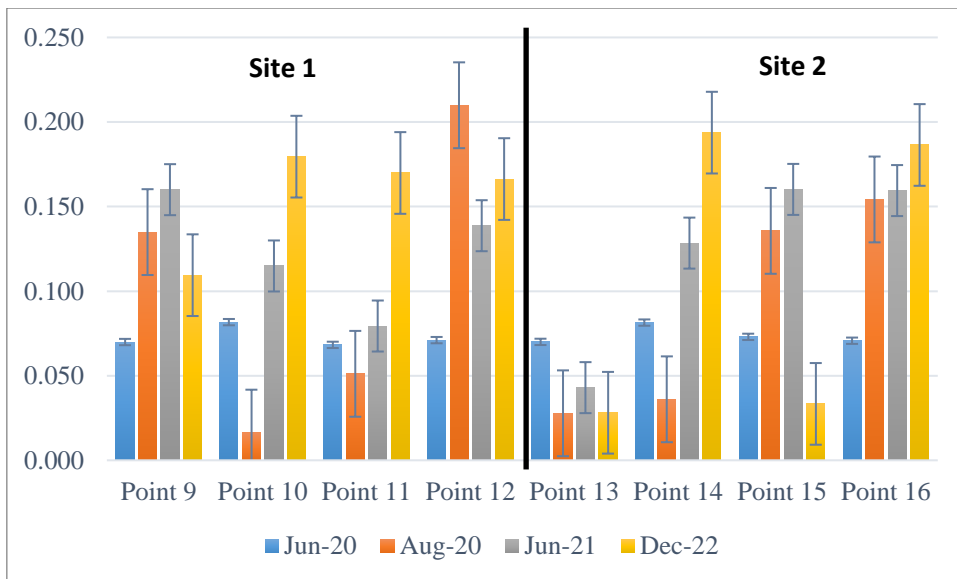


Figure 34. Res-P fraction (mg P/g D. M.) in the bottom layer of sediments (5-10 cm), during the research period.

### C. Full correlation of the sediment components

Table 35. Correlation between sediment components.

		Fe2O3	CaO	MgO	Al2O3	MnO	OM	SiO2	P2O5	N
		(%)	(%)	(%)	(%)	(%)	(%)	(%)	(%)	(%)
Fe2O3 (%)	Pearson	1								
	Correlation		-.271*	0.243	.545**	.648**	-	-0.117	.576**	0.195
	Sig. (2-tailed)		0.03	0.053	0	0	0.455	0.359	0	0.123
	N	64	64	64	64	64	64	64	64	64
CaO (%)	Pearson		1							
	Correlation	-.271*		-0.205	0.145	-.489**	.267*	-0.212	-	0.079
	Sig. (2-tailed)	0.03		0.104	0.252	0	0.033	0.092	.514**	0.534
	N	64	64	64	64	64	64	64	64	64
MgO (%)	Pearson			1						
	Correlation	0.243	0.205		0.002	.306*	-	-.271*	0.209	-
	Sig. (2-tailed)	0.053	0.104		0.987	0.014	0.376	0.031	0.098	0.165
	N	64	64	64	64	64	64	64	64	64
Al2O3 (%)	Pearson				1					
	Correlation	.545**	0.145	0.002		.353**	.261*	-0.022	.403**	0.09
	Sig. (2-tailed)	0	0.252	0.987		0.004	0.037	0.866	0.001	0.481
	N	64	64	64	64	64	64	64	64	64
MnO (%)	Pearson					1				
	Correlation	.648**	-.489**	.306*	.353**		-	-0.07	.656**	0.131
	Sig. (2-tailed)	0	0	0.014	0.004		0.626	0.584	0	0.301
	N	64	64	64	64	64	64	64	64	64

OM (%)	Pearson Correlation	-0.095	.267*	-0.113	.261*	-0.062	1	0.128	-	-
	Sig. (2-tailed)	0.455	0.033	0.376	0.037	0.626		0.315	0.228	0.862
	N	64	64	64	64	64	64	64	64	64
SiO2 (%)	Pearson Correlation	-0.117	-	-.271*	-	-0.07	0.128	1	-0.05	-
	Sig. (2-tailed)	0.359	0.092	0.031	0.866	0.584	0.315		0.695	0.422
	N	64	64	64	64	64	64	64	64	64
P2O5%	Pearson Correlation	.576**	-	0.209	.403**	.656**	-	-0.05	1	0.14
	Sig. (2-tailed)	0	.514**	0.098	0.001	0	0.228	0.695		0.27
	N	64	64	64	64	64	64	64	64	64
N (%)	Pearson Correlation	0.195	0.079	-0.165	0.09	0.131	-	-0.102	0.14	1
	Sig. (2-tailed)	0.123	0.534	0.194	0.481	0.301	0.862	0.422	0.27	
	N	64	64	64	64	64	64	64	64	64